IAEA-NDS-93
(Rev. 0)

INTERNATIONAL ATOMIC ENERGY AGENCY

NUCLEAR DATA SERVICES

DOCUMENTATION SERIES OF THE IAEA NUCLEAR DATA SECTION

92 pages

ALICE-87 (Livermore)

Precompound Nuclear Model Code
Version for Personal Computer IBM/AT

M. Blann
Lawrence Livermore National Laboratory, USA

Abstract: The precompound nuclear model code ALICE-87 from the Lawrence Livermore National Laboratory (USA) was implemented for use on personal computer. It is available on a set of high density diskettes from the Data Bank of Nuclear Energy Agency (Saclay) and the IAEA Nuclear Data Section.

Implemented on PC by
D.E. Cullen, V. Goulo

May 1988

IAEA NUCLEAR DATA SECTION, P.O. BOX 100, A-1400 VIENNA

sections for nucleon-induced reactions while either routine may be used for inverse cross sections.

The optical model routine in the earlier ALICE code used a pure surface

ALICE-87 (Livermore)

Precompound Nuclear Model Code
Version for Personal Computer IBM/AT

Introduction

Code ALICE [1] was presented by M. Blann at the International Centre of Theoretical Physics (Trieste) during the training course on Applied Nuclear Theory and Nuclear Model Calculations for Nuclear Technology Applications (15 February - 18 March 1988) with exercises on IBM compatible personal computer Olivetti M-380.

Due to the usefulness of the code for a number of applications in calculations and many requests for it for personal computers, several notes for users in the implementation of the code with DOS 3.2 and PROFORT 1.0 compiler are presented here.

1. Description of the program

ALICE-87 calculates particle and gamma-ray emission spectra induced with neutrons, protons, deuterons, alpha-particles, mesons and ions in the energy range till several hundred MeV. It uses precompound and compound decay models including fission competition. Pre-compound part of the code is presented by hybrid and geometry-dependent hybrid model.

Weiskopf-Ewing evaporation model with multiple particle emission or an S-wave approximation calculations for every partial wave in the entrance channel are used. Fission channel can be included in the Bohr-Wheeler approach.

2. Changes in the text of program made while implementing

a. Computer Olivetti M-380 is 32-bit machine and prescription for using *DOUBLE PRECISION* variables has been taken into account.

b. Long DATA operators were split and EQUIVALENCE operators were used for data representation.

c. Several FORMAT operators were corrected.

3. Compiling and linking were done in accordance with PROFORT compiler manual [2].

4. Due to large memory required to run the code it is very sensitive for the system configuration. CONFIG.SYS file should include the following lines:

```
files=30
buffers=20
```

expected from evaporation theory. This is a simple restatement of the adage that computational output is no better than the input, and points out the difficulties of getting good input in the near barrier region for charged

5. Example of batch file to run the code:

```
ALICE <ALICE.INP> ALICE.LST
```

6. Examples of input, output and data files used in the exercises are described in the proceedings of the Workshop and are available together with source file of the code.

   Running time of exercises: 8-10 minutes for 16 Mhz computer.

   In case of problems, please contact:

V. Goulo
IAEA Nuclear Data Section
P.O. Box 100
A-1400 Vienna, Austria

References

1. M. BLANN, Recent Progress and Current Status of Pre-equilibrium Reaction Theories and Computer Code ALICE, UCRL-Report, presented for the ICTP Workshop 1988, Trieste, SMR/284-1.

2. IBM Personal Computer Professional FORTRAN. Installation and use. Ryan McFarland Corporation, 1984.

Line 1

AP: Projectile mass number 1.000

INTERNATIONAL ATOMIC ENERGY AGENCY
UNITED NATIONS EDUCATIONAL, SCIENTIFIC AND CULTURAL ORGANIZATION

INTERNATIONAL CENTRE FOR THEORETICAL PHYSICS
34100 TRIESTE (ITALY) - P.O.B. 586 - MIRAMARE - STRADA COSTIERA 11 - TELEPHONE: 9240-1
CABLE: CENTRATOM - TELEX 460392-1

SMR/284 - 1

WORKSHOP ON

APPLIED NUCLEAR THEORY AND NUCLEAR MODEL CALCULATIONS

FOR NUCLEAR TECHNOLOGY APPLICATIONS

(15 February - 18 March 1988)

Recent progress and current status of preequilibrium reaction theories and computer code ALICE

presented by:

M. BLANN
Lawrence Livermore National Laboratory
P.O. Box 808
Livermore, CA 94550
U.S.A.

EX1: Blank

EX2: Blank

UCRL-
PREPRINT

Recent Progress and Current Status of Preequilibrium Reaction Theories and Computer Code ALICE

M. Blann

This paper was prepared for submittal to
the International Centre for Physics
Workshop on Applied Nuclear Theory
and Nuclear Model Calculations
for Nuclear Technology Application
Trieste, Italy

15 Feb - 18 March 1988

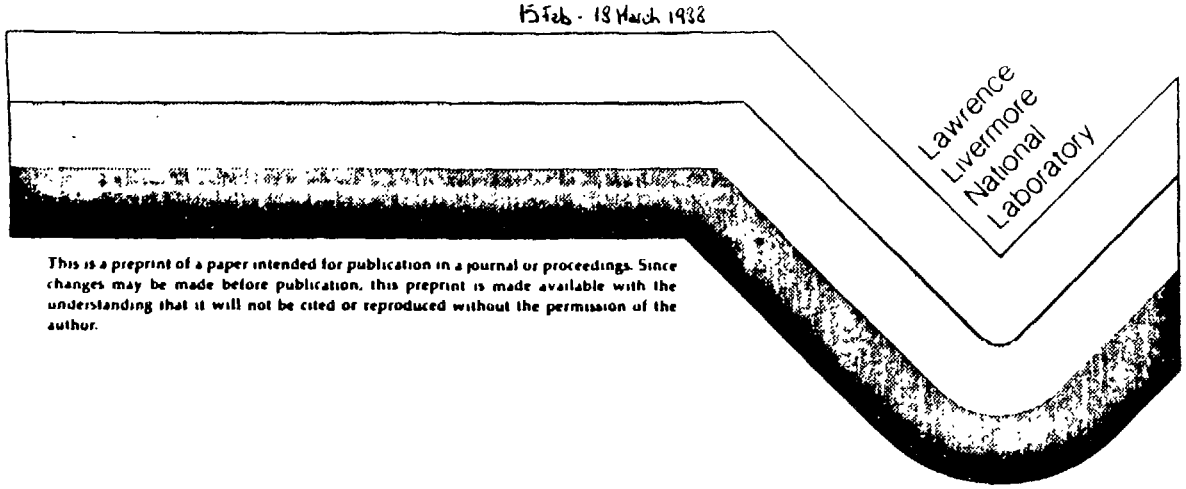

4.0 CALCULATION OF ANGULAR DISTRIBUTIONS

RECENT PROGRESS AND CURRENT STATUS OF PREEQUILIBRIUM REACTION THEORIES AND COMPUTER CODE ALICE

M. Blann
E-Division, Physics Department
Lawrence Livermore National Laboratory
Livermore, California, U.S.A.

Abstract

A review of the hybrid/geometry dependent hybrid models is given as implemented in the computer code ALICE. Discussion is given of evaluation of the relevant parameters. Exercises are given for executing different types of precompound plus compound decay processes in the code ALICE. Relevant supplementary literature is appended vis-a-vis parameter evaluation, calculations involving fission de-excitation.

1.0 INTRODUCTION

The purpose of these lectures is to give instruction in the use of the code ALICE[1] for a range of nuclear reaction problems, with emphasis on the direct reactions in the continuum, which are generally referred to by the equivalent terms "precompound" or "preequilibrium." The ALICE code has been designed and maintained to emphasize ease of use by non-experts, high speed, and versatility. It's predictive capabilities have been shown to be quite good, yet it has not been written to optimize accuracy when this goal conflicts with speed and ease of use. Other codes will be preferable when accuracy (better than ~80%) is more important than speed. Examples of such codes may, e.g., be the IDA code system of Reffo or the STAPRE code of Uhl.

The ALICE code can perform precompound decay calculations, followed by compound nucleus decay including fission competition. The equilibrium decay channels are calculated using a deterministic method. Nearly all input parameters may be generated internally, so that execution may take place with as little input as target and projectile charge and mass and projectile energy. On the other hand, possibilities exist to override internally determined input values and calculational parameters, if desired, making the code capabilities quite versatile; the user can grow into the codes.

Partial State Densities

The equilibrium reaction stages are treated via the Weiskopf evaporation model. Hauser-Feshbach versions exist under the names ALERT I and ALERT II;[2] however, we will not discuss these versions here.

To coordinate these lectures with code application exercises, I shall begin with a very cursory description of the hybrid[3-5] precompound decay model,[3] followed by a discussion of those elements of the code ALICE which are necessary to understanding the simplest PE (preequilibrium) plus evaporation calculation. Then, I will return to the subject of PE decay, covering treatment of gamma-ray emission, angular distributions and multiple PE decay. Precompound options including fission de-excitation will be described, as well as approximations for decay of systems at high angular momenta.

2.0 THE HYBRID PE DECAY MODEL

2.1 General Comments

Preequilibrium decay may be represented as a sequence of two body N-N (nucleon-nucleon) collisions - just as in the early intranuclear cascade calculations.[6] The difference is that PE decay models follow the reactions in energy space rather than in phase space; the geometric information is sacrificed.

The general concepts of the model are illustrated schematically in Fig. 1. It may be seen that in each scattering, some nucleons may be unbound. These nucleons may either be emitted into the continuum or may rescatter. Because the possibilities of rescattering are much greater than the possibilities for annihilation, the equilibration cascade may be formulated in a "never come back" approximation, i.e., in each step, each nucleon makes a two-body collision creating an additional particle-hole pair.

Several formulations of PE decay are in use; all are descendents of the pioneering paper of J. J. Griffin,[6] which allowed a qualitative description of the shape of PE spectra, though not of the absolute magnitude. All approaches rely on a quantity often called the "partial state density," which is the number (per MeV) of energy partitions available for a Fermi gas where every partition of p particles and h holes is assumed to occur with equal a-priori probability. The first expression for this partial state density was due to Ericson,[7]

---

where the 2! is added before the integral to correct for multiple counting

$$\rho_n(e) = g(gE)^{n-1}/(p!h!(n-1)!) \qquad (1)$$

where n, the exciton number equals the number of excited particles "p" plus holes "h," E is the excitation energy in MeV, and g is the (assumed constant) single particle level density (at the Fermi energy). PE decay models in use make the assumption that within each exciton hierarchy, all configurations are populated with equal a-priori probability. The correctness of this assumption has properly been challenged recently.[8] For the present, we will overlook this problem (which turns out to be not too important for our purposes[9]) but we will return to it later, time permitting.

2.2 Hybrid Model Formulation

The hybrid model[3] for precompound decay may be written as

$$\frac{d\sigma}{d\epsilon} = \sigma_R \sum_{n=n_0}^{\bar{n}} \left[\frac{X_\nu \rho_{n-1}(U)}{\rho_n(E)}\right]\left[\frac{\lambda_c(\epsilon)}{\lambda_c(\epsilon)+\lambda_+(\epsilon)}\right] D_n d\epsilon \qquad (2)$$

where the term in the first set of brackets uses terms similar to the Ericson partial state densities to calculate the number of excitons of type X_ν (ν=neutron or proton), which are available for emission in the energy range ϵ to $\epsilon+d\epsilon$, and $U=E-B_\nu-\epsilon$, where B_ν is the binding energy of particle type ν, neutron or proton). The term $\lambda_c(\epsilon)$ is the rate of nucleon emission into the continuum, and $\lambda_+(\epsilon)$ is the competing rate of two body collisions for the nucleons at energy ϵ. The factor D_n is a depletion factor which represents the fraction of the population surviving to the n exciton term in the summation over exciton number.

The nucleon-nucleon scattering rate is based on either the imaginary optical potential, where the mean free path is given by[10]

$$\lambda_+(E) = \frac{\hbar^2}{4m} \cdot \frac{1}{W^2} (E+V) + \sqrt{(E+V)^2+W^2}^{1/2} \qquad (3)$$

$$\rho(U) = \frac{1}{T} e^{-\epsilon/T} \qquad (21)$$

$$= \frac{\hbar^2}{2m\sigma_0 W} \sqrt{2m/\hbar^2(E+V)} \qquad (4)$$

or on Pauli corrected nucleon-nucleon scattering cross sections, where the mean free path is given by[10]

$$\lambda_+(\varepsilon) = \frac{1}{\rho \bar{\sigma}_0} \qquad (5) ,$$

where ρ is the density of nuclear matter and $\bar{\sigma}_0$ is the Pauli corrected nucleon-nucleon (N-N) scattering cross section, appropriately weighted for target neutron and proton number. The transition rate is the quotient of nucleon velocity (in the well) divided by the mean free path. A closed form expression valid for nuclear matter of average density was given as[11]

$$\lambda_+(\varepsilon) = 1.4\times10^{21}(\varepsilon+B_\nu) - 6\times10^{18}(\varepsilon+B_\nu)^2/\text{sec} \qquad (6)$$

where $\varepsilon+B_\nu$ is the energy of nucleon ν above the Fermi energy. The continuum emission rate, $\lambda_c(\varepsilon)$ is given by microscopic reversibility as

$$\lambda_c(\varepsilon) = (2s+1)\,\Omega\,\frac{4\pi p^2 dp}{h^3} \cdot \frac{\sigma v}{\Omega g} \qquad (7)$$

where s is the nucleon spin, Ω the laboratory volume, p the nucleon momentum, g the single particle level density in the nucleus, v the nucleon velocity in the laboratory, and σ the inverse cross section. With these last two equations and the Ericson density expression, we can calculate absolute PE spectra with Eq. 2. When we calculate N-N collision rates in the code ALICE, we have two options. One is to use the imaginary optical potential given by Becchetti and Greenlees;[12] the other is to use Eq. 5 calculating σ_0 based on expressions due to Kikuchi and Kawai[10] weighted for composite nucleus N and Z (rather than using the approximation of Eq. 6.

the liquid drop or finite range models as a general nuclear property. For heavier elements, shell corrections become increasingly important and care

2.4.2 Geometry Dependent Hybrid Model (GDH)

The nucleus has a density distribution which can affect PE decay in two ways. First, the nucleon mean free path is expected to be longer (on average about a factor of two) in the diffuse nuclear surface. Secondly, in a local density approximation, there is a limit to the hole depth: this will be expected to modify the Ericson state densities. These two changes were incorporated into the geometry dependent hybrid model.[4] We present next a description of these changes with specific reference to the code ALICE, taken from Ref. 13.

In order to provide a first order correction for the influence of nuclear density, the hybrid model may be reformulated as a sum of contributions, one term for each entrance channel impact parameter with parameters evaluated for the average local density of each impact parameter. In this way, the diffuse surface properties sampled by the higher impact parameters are crudely incorporated into the precompound decay formalism in the geometry dependent hybrid model (GDH). The differential emission spectrum is given in the GDH model cartoon figure as

$$\frac{d\sigma_\nu(\epsilon)}{d\epsilon} = \pi\lambda^2 \sum_{l=0}^{\infty} (2l+1)T_l P_\nu(l,\epsilon) \quad , \tag{8}$$

where the symbols are defined in Table I. When the approach is used for incident nucleons, the T_ℓ are provided by an optical model subroutine. Whereas the intranuclear transition rates entering (2) are evaluated for nuclear densities averaged over the entire nucleus, those appropriate to (8) are averaged over the densities corresponding to the entrance channel trajectories, at least for the contributions from the first projectile-target interaction.

The geometry dependent (surface) influences are manifested in two distinct manners in the formulation of the GDH model. The more obvious is the longer mean free path predicted for nucleons in the diffuse surface region. It has been shown[4] that this effect changes the predicted emission cross section about the same as would a factor of 2 increase in the mean free path in the formulation of the hybrid model (Eq. 2). (The evaluation of these parameters will be discussed further on in this section.)

Line 4: JCAL must now be zero.

ID is still 1., all other precompound parameters are zero. Other

The second effect is less physically secure, yet seems to be important in reproducing experimental spectral shapes. This is the assumption that the hole depth is limited to the value of the Fermi energy which is calculated for each trajectory in a local density approximation. The result of this is to effectively reduce the degrees of freedom, especially for the higher partial waves (for which a lower maximum hole depth is predicted), thereby hardening and enhancing the predicted emission spectra. The separate influences of these two surface (geometric) effects have been illustrated previously.[4] In our use of ALICE, we will use the option under which the restriction on hole depth in the GDH model applies only to the first collision, for which there is some knowledge of average density at the collision site, and only for nucleon induced reactions.

2.3 Parameter Evaluation and Modification

2.3.1 Nuclear Density Distribution

The original GDH model, and codes using this model, employed a Fermi density distribution function,

$$d(R_l)=d_s[\exp(R_l-C)/0.55\ \text{fm}+1]^{-1} \qquad (9)$$

with

$$C=1.07A^{1/3}\ \text{fm} \quad , \qquad (10)$$

taken from electron scattering results.[14] The radius for the lth partial wave was defined by

$$R_l=\bar{\lambda}(l+1/2) \quad . \qquad (11)$$

The charge radius C of Eq. 10 has been replaced in the present parameterization by a value characteristic of the matter (rather than charge) radius based on the droplet model work of Myers,[15] plus an ad hoc projectile range parameter $\bar{\lambda}$,

$$C=1.18A^{1/3}[1-1/(1.18A^{1/3})^2]+\bar{\lambda} \quad . \qquad (12)$$

Figure Captions

In the hybrid model, the average nuclear density is calculated by integration and averaging of Eq. 9 between R=0 and R=C+2.75 fm. Details of the integration have been given previously.[4,5] The single particle level densities are defined in the precompound and routine of ALICE by

$$g_n = \frac{N}{2B} \quad . \tag{13}$$

$$g_p = \frac{Z}{2B} \quad . \tag{14}$$

2.3.2 Intranuclear Transition Rates

The precompound decay models under discussion have employed intranuclear transition rates evaluated both from the imaginary optical potential (using parameters due to Becchetti and Greenless[12]) and from Pauli corrected nucleon-nucleon scattering cross sections.[10] Both methods gave similar results;[5] however, the optical model parameter set is valid only for projectile energies below 55 MeV. Because we wish to treat data sets considerably in excess of 55 MeV energy, we have adopted the Pauli corrected NN scattering evaluation as a standard default parameter.

For the reasons discussed above, the Pauli corrected λ_+ values from NN scattering have been used as default parameters for GOH calculations, and the λ_+ are reduced to one-half (mfp is multiplied twofold) when the hybrid model calculation is performed in order to approximate the effects of the diffuse surface. In the default version of GOH, we use the option whereby only the first collision is localized according to the impact parameter as implied by Eq. 11, with all higher order precompound terms being treated by the hybrid model - i.e., using nuclear densities averaged over the nucleus and independent of impact parameter. This is reasonable because the excitons can sample nearly the entire nuclear volume after a single scattering, since mfp values are ~4 fm.

2.3.3 Initial Exciton Numbers

The starting point in any nucleon induced reaction should be a 2p1h state. However, the selection of initial n and p particle exciton numbers within this 2p1h state seemed to cause the most confusion among users of the precompound routines of the OVERLAID ALICE code. This problem was alle-

viated by internal selection under the default option in the ALICE/LIVERMORE 82 code and in subsequent releases. The algorithm coded and used in results to be presented is as follows.

The free scattering n-p cross section σ_{np} is ~3 times the corresponding σ_{nn} or σ_{pp} over the energy range of interest for most precompound decay calculations. In a nucleon induced reaction, there will be a total of two initial particle excitons divided in some averaged manner between neutrons and protons. This should be crudely related to the relative free scattering cross sections, and to the neutron (N) and proton (Z) numbers of the target nucleus.

For an incident neutron, there should therefore be three np pairs for every nn pair if N=Z, or five neutron excitons to each three proton excitons, or $\frac{5}{8}$x2 neutron excitons and $\frac{3}{8}$x2 proton excitons to make the two particle excitons (remembering that we are interested only in the average particle exciton numbers, where the projectile is one of the two particle excitons). These results should be weighted further by the numbers of N and Z of the target, giving the default algorithms for neutron induced reactions,

$$ {}_3X_n = \frac{2(3Z+2N)}{(3Z+2N+3Z)} \qquad (15) $$

and

$$ {}_3X_p = 2-{}_3X_n \quad . \qquad (16) $$

and for proton induced reactions

$$ {}_3X_p = \frac{2(3N+2Z)}{(3N+2Z+3N)} \qquad (17) $$

and

$$ {}_3X_n = 2-{}_3X_p \quad . \qquad (18) $$

This is essentially the method used to determine initial exciton numbers in the past, which is now programmed as a default option for nucleon induced reactions. As in the past, the initial X_n and X_p numbers are each assumed to increase by 0.5 in successive values of n in Eq. 2, as the particle exciton number increase is by 1.0.

For reactions induced by α particles, the default initial exciton numbers are X_n, X_p=2; for other clusters we assume X_n=N+0.5, X_p=Z+0.5.

TABLE I. Definition of symbols.

$P_\nu(\epsilon)d\epsilon$	Number of particles of the type ν (neutrons or protons) emitted into the unbound continuum with channel energy between ϵ and $\epsilon+d\epsilon$ (MeV)
$P_\nu(l,\epsilon)d\epsilon$	As for $P_\nu(\epsilon)$, but evaluated for the lth partial wave

2.3.4 Pairing Options

Two choices of pairing are allowed in ALICE with the same choice used in both precompound and subsequent evaporation calculations. The value of the pairing correction is always defined by $\delta=11/A^{1/2}$, with either a backshift or standard pairing shift being applied. The standard shift uses true thermodynamic excitations for odd A nuclei, reduces the excitation by δ for doubly odd nuclei,and increases it by δ for doubly even nuclei. The back-shifted option uses true thermodynamic excitation for doubly even nuclei, and increases it by δ for odd A nuclei and 2δ for doubly odd nuclei. The pairing correction influences only the last few MeV of the precompound spectrum to a substantial degree, and we feel that the "best" mode of inclusion in precompound decay is still an open question.

2.3.5 Binding Energies

The binding energies and Q values used in ALICE are generally selected from experimental masses.[16] The ALICE code includes experimental masses in block data, so that a simple input parameter results in all Q values and binding energies being internally generated from experimental mass tables. When these are out of range of experimental masses, results are automatically taken from the Lysekil mass formula of Myers and Swiatecki.[17]

2.3.6 Reaction and Inverse Reaction Cross Sections

Comparisons between calculated and experimental spectra are no more meaningful than the uncertainties inherent in each. For example, the scattering distribution functions (partial state densities) used in Eq. 2 are shown to have an inherent error in assumptions for their derivation of the order of $\pm$20% at least. Another parameter which must be scrutinized is the value used for the reaction cross section in Eq. 2, and for the inverse reaction cross section for the $\lambda_c(\epsilon)$ in Eq. 7. Comparisons between calculated and experimental spectra cannot be interpreted beyond the "noise level" of these model uncertainties.

The present code has a classical sharp-cutoff routine for inverse reaction cross sections, and the earlier optical model routine. The optical model is the only internal source of entrance channel reaction cross

REFERENCES

1. M. Blann and F. Plasil, Univ. of Rochester Report No. COO-3494-10, 1973 (unpublished); M. Blann, Univ. of Rochester Report No. COO-3494-29 1975

sections for nucleon-induced reactions while either routine may be used for inverse cross sections.

The optical model routine in the earlier ALICE code used a pure surface form-factor parameter set of w for nucleon-induced reactions. While this should be adequate for energies consistent with compound nucleus evaporation, poor results were obtained at the higher energies required (up to 90 MeV) for the precompound studies of interest in the present work. Because we are interested only in generating reaction cross sections and transmission coefficients which are to be used in Eq. 2-7 from these subroutines, and not elastic scattering angular distributions, we have made ad hoc changes in the optical model parameters in the present ALICE code. The parameter set adopted and comparisons with data are summarized in Ref. 13.

At energies near and even somewhat above the Coulomb barrier, the global cross sections are in poor agreement with reported experimental results. The calculated low energy cross sections on Sn and Pb seriously underestimate experimental yields, whereas for the Ni targets, there is an overestimation of low energy yields. The test of agreement in the near barrier region really rests on very few experimental results. Comparison of calculated and experimental evaporation and precompound spectra in these regions must therefore be interpreted with extreme caution, as the quality of the input (reaction and/or inverse cross sections) may be uncertain.

While quite satisfactory agreement is shown between the calculated and experimental neutron cross sections for neutron energies above ~10 MeV, the values below ~3 MeV from the optical model subroutine-parameter set of the ALICE code are not reliable and are subject to large uncertainties (probably up to 50%). These uncertainties are not important in the precompound decay region, but could be very significant in attempts to fit low energy evaporation neutron spectra and especially in evaluating evaporation-fission competition in fissile nuclides.

The main point of this subsection may be summarized as follows. If one wishes good compound or precompound calculations involving reaction and inverse reaction cross sections in a near barrier region, input must be carefully selected based on experiments on the same (preferably) or nearly the same target nucleus. Conversely, if a global parameter set (such as the values specified in the ALICE codes) is used in a calculation, extreme care must be exercised before concluding, e.g., that the experimental evaporated protons or α particles are enriched in low kinetic energies over results

21. N. Bohr and J. A. Wheeler, Phys. Rev. 56, 426 (1939).

expected from evaporation theory. This is a simple restatement of the adage that computational output is no better than the input, and points out the difficulties of getting good input in the near barrier region for charged particles, and in the few MeV or lower region for neutrons.

3.0 CALCULATION OF PRECOMPOUND PLUS EVAPORATION SPECTRA

The ALICE code follows the PE emission by evaporation calculated according to the Weisskopf-Ewing theory. Calculations are done deterministically in a pointwise fashion over a nuclide array resembling a chart of the nuclides with the compound nucleus in the upper right corner. This is illustrated in Fig. 2 where the decay of the CN (IA=1, IZ=1) populates daughter nuclei following neutron emission (IA=2, IZ=1), proton emission (IA=1, IZ=2) and α emission (IA=3, IX=3). The same procedure is followed to treat the decay of each element populated by decay of the first neutron, the second neutron, etc., until all decay channels have been calculated and summed. Results then give particle spectra either from each nuclide or summed, and yields of all products (activation yields).

Example 1: Let us propose several example calculations for ALICE and describe the input. The first case will be 9.5, 14.2, and 18.5 MeV neutrons incident on $^{93}_{41}$Nb target nuclei. We wish the inclusive neutron spectra, γ-ray spectra and the product yields. A good energy meshsize is 0.5 MeV, and to save computational time, we will use the semi-classical sharp cutoff model for inverse reaction cross sections. We would like to use experimental masses and Q values, where available, and the standard pairing option. We would like to see all products formed by the emission of up to four neutrons and two units of charge. We would first like a result with the precompound hybrid model, followed by a calculation with the geometry dependent hybrid model at 14.2 MeV only.

In ALICE, the first input line gives most reaction parameters desired. The second line is a title card, and the third line gives the projectile energy and types of calculation desired. The third line may be repeated for different energies when there is no change necessary in quantities summarized on line 1.

The column numbers and input parameters are summarized in the comment cards preceding the source program. We will summarize the data necessary for the problem just posed.

Line 1

AP: Projectile mass number 1.000

AT: Target mass number 93.00

ZP: Projectile charge number 0.000

ZT: Target charge number 41.00

QVAL: Leave this blank and the value will be calculated internally from experimental masses

CLD: Blank-used for fission calculations

BARFAC: Blank-used for fission calculations

NA: For emission of four neutrons enter this value as 00005

NZ: For emission of two charges enter this value as 00003

INVER: For classical SCO inverse cross sections, use 2; check format for correct columns

ED: Enter as 0.5 for half MeV meshsize

IKE: Enter as 4 to get inclusive spectra in output

Leave other parameters on line 1 blank.

Line 2

Enter your name and the target, projectile and projectile energy in the first 80 columns.

Line 3

EQ: Enter the laboratory bombarding energy, e.g., 9.500

RCSS: Leave blank; the reaction cross section will be calculated internally via the optical model

IADST: Leave blank

IRFR: Leave blank

I3D: Leave blank

JCAL: We wish a standard (non-fission) evaporation calculation, so enter 1 for JCAL

DLT: Blank

JFRAC: Blank

JUPPER: Blank

JANG: Blank

TD: We wish to do a precompound calculation, and we wish all precompound parameters to be selected internally. We, therefore, enter any nonzero number here, e.g., 1.

EX1: Blank

EX2: Blank

TMX: We wish a hybrid model (no geometry dependence) result so leave this blank. For the geometry dependent hybrid model, enter any non-zero value, e.g., 1.

Leave all other entries on this line blank.

Line 3b

Repeat the above line 3, but modify input first to do 14.2 and 18.5 MeV energies, then to do a geometry dependent hybrid model calculation for 14.2 MeV incident energy.

Lines 4,5

Place two blank cards to terminate the calculation.

Note that two blank lines at the end of a data set is the standard exit from ALICE. It results in the line "DAS IST ALICE DAS IST ALICE..." being printed across the bottom of the page. If one wishes to follow with a new calculation requiring changes in the first input line (e.g., a new target or projectile, change of level density parameter, etc.) then the last data set should be followed by a single blank line, and then the next problem should be entered beginning with line one as described above.

As an exercise, do this for the reaction of 90 MeV protons with a $^{58}_{28}$Ni target, doing a geometry dependent hybrid model calculation.

Plot neutron spectra versus experimental results on the figures (14.2 MeV n+Nb, 90 MeV p+Ni) provided. For ^{58}Ni(p,p') also plot the proton spectra.

For the hybrid model results on ^{93}Nb, plot the γ-ray spectra versus the experimental results. The physics involved in the computation of "compound" gamma-rays is described in UCRL-95374 (Sept. 1986) which is in press in Nuclear Instruments and Methods.

4.0 CALCULATION OF ANGULAR DISTRIBUTIONS

ALICE may be used to calculate emitted nucleon angular distributions for nucleon induced reactions.[18] The physics assumed is based on the angular distribution of a nucleon scattering with nucleons having a Fermi gas momentum distribution. Simple considerations show that the angular distributions should, however, be sensitive to quantal effects, refractive and diffractive. When this is the case, a quantal calculation is probably required for a good description of the data. Nonetheless, the code allows additional folding estimates in the entrance and exit channels for enhancing the calculated back angle yields. The physics involved, and the options of the code, are described in Phys. Rev. C 30, 1493 (1984). This publication is appended to these notes and we refer to this reference for further discussion.

Exercise

Calculate the angular distribution of emitted neutrons for the reaction ^{90}Zr (p,n) with 25 MeV incident neutrons. Calculate results for no refraction, entrance channel refraction and entrance plus exit channel refraction. Calculate angular distributions at 2.0 MeV intervals. Use the GDH model. To save computational time, use the sharp cutoff inverse cross sections and two dimensional folding of the angular distributions. Plot your results on the figure which includes the experimental data.

The new input parameters which you must use are all on input line 3; IADST (=1)(calculate angular distributions for neutrons in the exit channel), IRFR (choice of estimates of refraction (diffraction), I3D (choice of 2D (fast) or 3D (slow) folding of kernels), DLT (the separation between energies for which the angular distributions will be calculated.

Plot the results of these exercises versus the experimental data.

Multiple PE Decay

The ALICE code includes certain estimates of multiple PE decay. Versions exist with more sophisticated treatments. This subject was reviewed by the author in February 1988 at the NEANDC meeting in Semmerling, Austria.[19] These notes are appended to these lecture notes and will be used for discussion of this topic.

Partial State Densities

Earlier we stated that most PE decay models use partial state densities of the type given by Ericson,[7] or in some cases, by permitting shell model single particle levels, but still with the assumption that every energy partition within a hierarchy specified by exciton number should be populated with equal a-priori probability. Here, we wish to address the question in more detail.

Let us address the question of the validity of the exciton distribution function [$\rho_n(E)$ or $N_n(E)$] as giving the population versus excitation which would result from multiple two-body scattering following the kinematics of free nucleon-nucleon scattering, modified by the Pauli exclusion principle. This dynamic justification of the distribution function is necessary since the relative scattering rates expected within a given exciton hierarchy are very much less than those resulting in creation of a p-h pair. With this in mind, we reproduce below a derivation of the distribution function based on the dynamics of nucleon-nucleon scattering.[13] We begin with a hypothesis, derive the distribution function, and then check the degree of accuracy of the hypothesis.

Hypothesis: For the process of nucleon-nucleon scattering in nuclear matter, as initiated by an incident nucleon, the differential cross section $d\sigma/d\epsilon$ for all final energies is constant, independent of the nucleon energy of the partner to be scattered.

Let us consider a nucleon entering a nuclear well, as shown in Fig. 3. The particle can scatter with nucleons having an energy within one unit of the Fermi energy, giving a 2p1h distribution. There are E' equally likely ways this can be done where E'=gE, and 1/g is the natural unit of energy. The "equally likely" statement is a consequence of the kinematic hypothesis made above.

The particle could also scatter with nucleons having energies between one and two units below E_f; there would be E'-1 equally likely ways this could happen rather than E' ways, since one possibility is now excluded by the Pauli principle. And it may be seen that the total number of allowed arrangements due to scattering with the hypothesis above is given by

$$N_{2p1h}(E) = \frac{1}{2!}\int_0^{E'}(E'-x)dx = \frac{g^2E^2}{2!2!} \quad , \tag{19}$$

where the 2! is added before the integral to correct for multiple counting of the two indistinguishable particles.

Given that an incident nucleon of energy ε, giving excitation energy E can populate a 2p1h configuration approximately, as given by the Ericson distribution, we can ask about population of higher order terms. The higher order terms should, as shown by Bisplinghoff, be populated as a sum of cascades initiated by each exciton of the initial 2p1h configuration according to the transition rates of either the hybrid or Exciton models; each of these mini-cascades should give a 2p1h configuration given by the Ericson distribution function, and the integral over all contributions should give the higher order exciton populations. Bisplinghoff showed that neither approach yields the Ericson 5 (or higher) exciton density result.[8]

The consistent method of following the exciton distribution derived by Bisplinghoff has been followed for several cases using a modified hybrid model routine.[9] Results are shown in Ref. 9. The consequences may be seen not to be too serious for particle spectra. A larger influence would be expected for calculation of angular distributions, and for reactions such as those of stopped pions.

5.0 CALCULATIONS INCLUDING FISSION

We should now specify more details about the particle evaporation and fission physics of the ALICE code. Then we will present an exercise to calculate excitation functions for (α,xn) yields from actinide targets.

The evaporation physics of ALICE is that of Weisskopf and Ewing,[20]

$$P_\nu(\varepsilon)d\varepsilon \propto (2s_\nu+1)\mu\sigma_\nu(\varepsilon)\varepsilon\rho(U)d\varepsilon, \qquad (20)$$

where $P_\nu(\varepsilon)d\varepsilon$ is the probability of emitting particle ν(=n,pα,d) with channel energy between ε and ε+dε, s_ν is the spin of particle ν, μ_ν is the reduced mass, $\sigma_\nu(\varepsilon)$ the inverse reaction cross section, and $\rho(U)$ the level density of the residual nucleus following emission of particle ν.

The level density used in ALICE is the constant temperature form up to the average of the binding energies of the first two neutrons which might be emitted from the compound nucleus, B_{12}:

$$\rho(U) = \frac{1}{c} e^{-\epsilon/T} \qquad (21)$$

where $T=\sqrt{E/a}$ and by default a=A/9.

For excitations above B_{12}, the Fermi gas level density is joined to the constant temperature form,

$$\rho(U) \propto (U^{-5/4}+1).) \exp 2\sqrt{a(U-\delta)} \qquad (22)$$

where the usual pre-exponential has had a "one" added to maintain civilized mathematical properties.

The level densities are stored in four tables each of 3000 words as POW (4,3000). They are calculated and stored in intervals of 100 keV, centered in the middle of each bin (i.e., at energies of (50, 150, 250, etc. keV). This table should be run in double precision on 32 bit wordlength computers. The masses used for the tables in calculating a=A/9 are the compound nucleus mass less one for products following n and p emission, less two for deuteron emission, and less four for α emission. For reasonably energetic reactions of light elements it would be wise to move the table computation inside the loop on mass change (IA=) so that the table would be recomputed for each emitting nucleus mass. The present construction is a compromise on computing time. Note that the default value of a=A/9 may be changed in input line one via the parameter PLD (F5.0) beginning in column 71.

Fission is treated via the Bohr-Wheeler[21] transition state theory, where one calculates the rate at which the excited nucleus may pass over the fission barrier or saddle point. Because nuclei are deformed at the saddle point relative to the more spherical shapes, the level density parameter a_f tends to be different from that for nuclei in their equilibrium shapes.

The fission rate is proportional to

$$P_f \propto \int_0^{E-\epsilon_{sp}} \rho_f\,(E-\epsilon_{sp}-K)dk \qquad (23)$$

where the saddle point energy enters the integration over level density. For elements lighter than, e.g., mercury, fission barriers may be given by

the liquid drop or finite range models as a general nuclear property. For heavier elements, shell corrections become increasingly important and care is necessary in selecting fission barriers. Similarly, for elements where liquid drop barriers dominate, $a_f/a_\nu \sim 1.02$ is a good parameter in theory and in practice; in actinide nuclei a_f/a_ν ratios include shell effects, and care must again be shown in selecting these parameters.

An application of the code ALICE to calculation of excitation functions with actinide targets is in Phys. Rev. C29, 1678 (1984). Use the values of a_f/a_ν (parameter CLD in input line 1) and the experimental barriers given for Pu isotopes to calculate yields of 235-238 Pu from ^{4}He bombardment of ^{235}U targets. Use incident α energies of 25 and 35 MeV. Always use the hybrid model for incident particles other than nucleons. Plot your results on Fig. 7 of Phys. Rev. C29, 1678 (1984).

ALICE may also be used to calculate fission decay of nuclei at high angular momenta using internal routines to provide fission barriers versus angular momentum from the rotating liquid drop[22] or finite range routines.[23] In this case, the evaporation calculation is run in what has been called the s-wave approximation. No discussion of this physics in intended here, but some discussion has been given in the report UCID-19614 "Code ALICE/LIVERMORE 82," LLNL Lab Report (1982) by M. Blann and J. Bisplinghoff.

Additional Input for the Fission Problem Given Above:

Line 1: CLD, ratio a_f/a_ν to be read in after choosing
IFIS - ignore
BARFAC - ignore
IPCH - enter as 1

Line 2: Enter fission barriers as per comment cards, using values given in Phys. Rev.

Note that NZ must be 1 on line 1 if only 1 line of B_f is entered.

Line 3: is now title card

Line 4: JCAL must now be zero.
TD is still 1., all other precompound parameters are zero. Other parameters on lines 1 and 4 should be obvious. Recommend ED=1.0, which may be achieved by default by leaving this entry blank.

Code ALISO

A separate version of ALICE is being maintained for the present. It differs from the standard version only in that it will do calculations for natural isotopic targets, giving weighted results at the end. It is maintained as a separate code because it required significant additional memory space for the single option of isotopic weighting.

Consider the special problem of calculating the particle spectra and activation yields following the bombardment of bromine with 20 and 25 MeV protons. The natural abundance of bromine is 50.5% $^{79}_{25}Br$ and 49.5% $^{81}_{35}Br$.

The ALICE code will run the separate isotopes as two separate problems; the results will then be combined with proper isotopic weighting and published as a table at the end of the output. The code needs two additional parameters on line 1 to implement this option: the parameter isot, which is nonzero advises that an isotopic weighting is to be performed, and the isotopic abundance (expressed as a fraction) is now entered in place of the parameter CLD.

Figure Captions

Figure 1 Pictorial representation of the ideas inherent in the exciton model. The series of two-body interactions leading toward an equilibrium distribution is illustrated, as well as the concept of some fraction of each configuration having some fraction of the particles unbound.

Figure 2 Representation of the storage sequence, element by element, in the decay cascade of the ALICE code. A description may be found in Section 3.

Figure 3 Angle averaged spectra for nucleon-nucleon scattering. Spectra are averaged over all initial and final scattering angles using anisotropic free scattering angular distributions (upper figures) or isotropic free scattering angular distributions (lower curves). Particle 1 energies of 1 and 17 MeV are shown versus particle 2 energies of 50 and 80 MeV relative to the well bottoms. The upper and lower Pauli exclusion cutoffs are indicated for scattering within a nucleus for which the Fermi energy is 20 MeV. The small drawings above each set of differential cross sections represents the energy relationships of the two nucleons and the nuclear potential.

Appendix I

Listing of comment lines from code ALISO; these may be used for guidance in providing input for the code ALICE 87.

Appendix II

These figures may be used for comparisons of results of computer exercises.

(1) ^{93}Nb (n,xn) differential spectra for 14.2 MeV incident neutrons.
(2) γ-rays from 9.5 MeV n+^{93}Nb.
(3) γ-rays from 14.2 MeV n+^{93}Nb.
(4) γ-rays from 18.5 MeV n+^{93}Nb.
(5) Angular distributions for the reaction ^{90}Zr(p,n) with 25 MeV incident protons and 9 and 14 MeV neutrons.
(6) Excitation functions for the ^{235}U(α,xn) reactions.

Appendix III

Relevant Literature. The following should be considered as part of the lecture material:

M. Blann, "Multiple Preequilibrium Decay Processes," Lawrence Livermore National Laboratory Report UCRL-97778, (1987) unpublished.

M. Blann, G. Reffo and F. Fabbri, "Calculation of γ-ray Cascades in Code ALICE," Lawrence Livermore National Laboratory Preprint UCRL-95374 (1986) in press, Nucl. Inst. and Methods.

M. Blann, W. Scobel and E. Plechaty, Phys. Rev. C30, 1493 (1984).

G. Reffo, M. Blann and B. A. Remington, "On the Origin of Medium Energy Gamma Rays in Nuclear Reactions," Lawrence Livermore National Laboratory Report UCRL-97866 (1987) unpublished.

M. Blann and T. T. Komoto, Phys. Rev. C29, 1678, (1984).

TABLE I. Definition of symbols.

$P_\nu(\epsilon)d\epsilon$	Number of particles of the type ν (neutrons or protons) emitted into the unbound continuum with channel energy between ϵ and $\epsilon+d\epsilon$ (MeV)
$P_\nu(l,\epsilon)d\epsilon$	As for $P_\nu(\epsilon)$, but evaluated for the lth partial wave
$\bar{n}$	Equilibrium (most probable) particle plus hole (exciton) number
n_0	Initial exciton number
${}_nX_\nu$	Number of particles of type ν (proton or neutron) in an n exciton hierarchy
E	Composite system excitation
U	Residual nucleus excitation
$N_n(\epsilon,U)$	Number of ways that n excitons may be combined such that one, if emitted, would have channel energy ϵ and the remaining $n-1$ excitons would share excitation $U=E-B_\nu-\epsilon$, where B_ν is the particle binding energy
$N_n(E)$	Number of combinations with which n excitons may share excitation energy E
$\lambda_c(\epsilon)$	Emission rate of a particle into the continuum with channel energy ϵ
$\lambda_+(\epsilon)$	Intranuclear transition rate of a particle which would have channel energy ϵ if it were emitted into the continuum
D_n	Fraction of the initial population which has survived to an n-exciton hierarchy
σ_R	Reaction cross section
l	Orbital angular momentum in units $\hbar$
T_l	Transmission coefficient for lth partial wave
$d(R_l)$	Nuclear density at radius R_l, where l denotes the entrance channel orbital angular momentum
d_s	Saturation density of nuclear matter
$\lambda\!\!\!^{-}$	Reduced de Broglie wavelength
σ_l	Partial reaction cross section for the incident lth partial wave
g_ν	Single particle level density for particle type ν
N	Target neutron number
Z	Target proton number
ϵ_f	Fermi energy
B_ν	Binding energy of particle type ν
ϵ	Channel energy
C_n	Cross section for emitting one and only one neutron summed over exciton number
C_p	As for C_n, but proton only cross section.
C_{np}	Cross section summed over exciton number for which one neutron and one proton are estimated to have been emitted from a single nucleus in the same exciton number configuration
C_{nn} (C_{pp})	Cross section summed over exciton number for which it is estimated that two neutrons (protons) are emitted from the same nucleus and exciton number

REFERENCES

1. M. Blann and F. Plasil, Univ. of Rochester Report No. COO-3494-10, 1973 (unpublished); M. Blann, Univ. of Rochester Report No. COO-3494-29 1975 (unpublished); M. Blann and J. Bisplinghoff, LLNL Report No. UCID-19614, 1983 (unpublished);M. Blann, LLNL Report UCID-20169, 1984 (unpublished).

2. M. Blann and T. T. Komoto, UCID-19390 1982 (unpublished).

3. M. Blann, Phys. Rev. Lett. 27, 337 (1971); 27, 700(E)(1971); 27, 1550(E)(1971).

4. M. Blann, Phys. Rev. Lett. 28, 757 (1972).

5. M. Blann, Nucl. Phys. A213, 570 (1973).

6. J. J. Griffin, Phys. Rev. Lett. 17, 478 (1966); J. J. Griffin, In "Intermediate Structure in Nuclear Reactions," edited by H. P. Kennedy and R. Schrils (Univ. of Kentucky Press, Lexington, 1968); J. J. Griffin, in "Nuclear Physics: An International Conference," edited by L. Becker, C. D. Goodman, P. H. Stelson, and A. Zucker (Academic, New York, 1967), p. 778; J. J. Griffin, Phys. Lett. 24B, 5 (1967).

7. F. C. Williams, Jr., Nucl. Phys. A166 , 231 (1971); T. Ericson, Adv. Phys. 9, 423 (1960).

8. J. Bisplinghoff, Phys. Rev. C33, 1569 (1986).

9. M. Blann and J. Bisplinghoff, Zeit. f. Physik A326, 429 (1987).

10. K. Kikuchi and M. Kawai, "Nuclear Matter and Nuclear Interactions (North-Holland, Amsterdam, 1968).

11. M. Blann and A. Mignerey, Nucl. Phys. A186, 245 (1972).

12. F. D. Becchetti and Greenlees, Phys. Rev. 182, 1190 (1969).

13. M. Blann and H. K. Vonach, Phys. Rev. 28, 1475 (1983).

14. R. Hofstadter, Ann. Rev. Nucl. Sci. 7, 295 (1957).

15. R. D. Myers, Droplet Model of Atomic Nuclei (Plenum, New York, 1977).

16. A. H. Wapstra and N. B. Gove, Nucl. Data Tables 9, 265 (1971).

17. W. D. Myers and W. J. Swiatecki, Ark. Fys. 36, 343 (1967).

18. M. Blann, W. Scobel and E. Plechaty, Phys. Rev. C30, 1493 (1984).

19. M. Blann, "Multiple Preequilibrium Decay Processes," LLNL Report UCRL-97778 (1987)(unpublished).

20. V. F. Weisskopf and D. H. Ewing, Phys. Rev. 57, 472 (1940).

21. N. Bohr and J. A. Wheeler, Phys. Rev. 56, 426 (1939).

22. S. Cohen, F. Plasil and W. J. Swiatecki, Ann. Phys. (N.Y.) 82, 557 (1974).

23. A. J. Sierk, private communication (1984); M. Blann and T. T. Komoto, Phys. Rev. C26, 472 (1982).

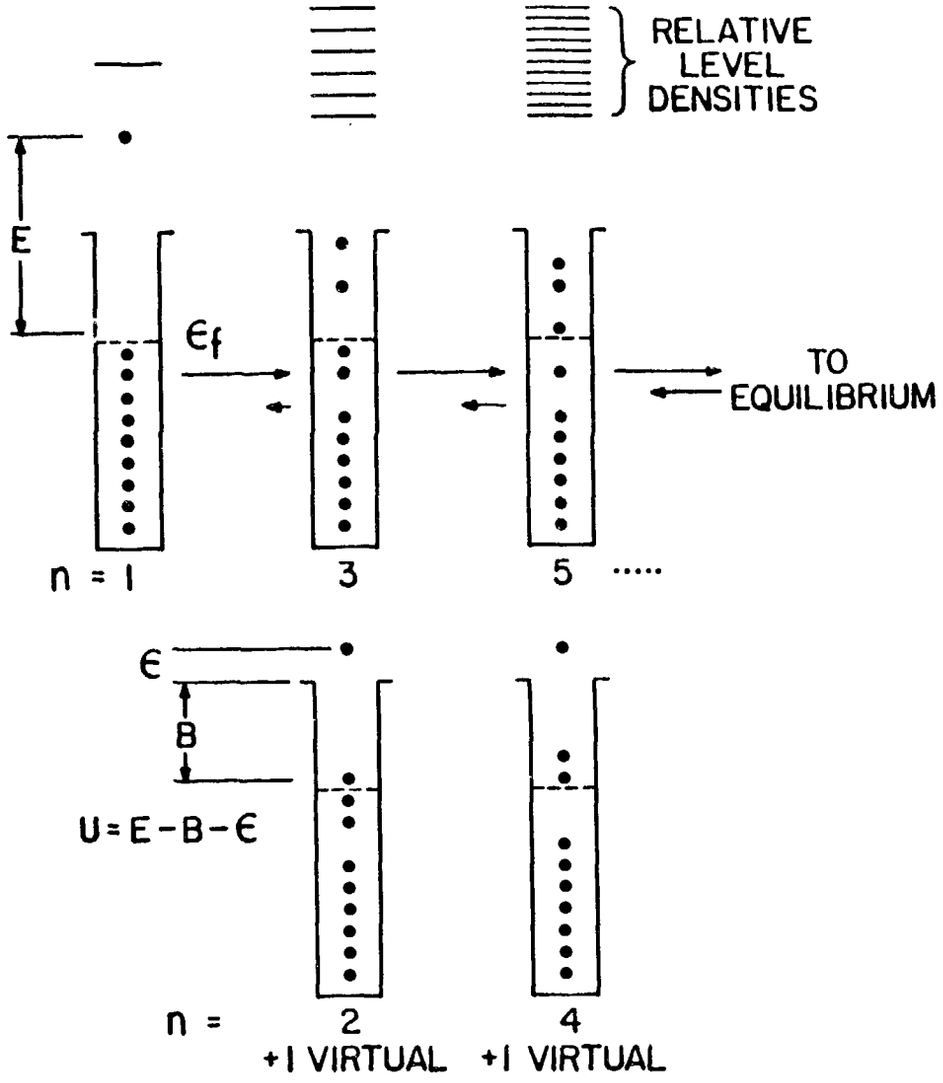
RELATIVE
LEVEL
DENSITIES
E
ϵ_f
TO
EQUILIBRIUM
n = 1
3
5
.....
ϵ
B
U=E-B-ϵ
n =
2
4
+1 VIRTUAL
+1 VIRTUAL

Figure 1

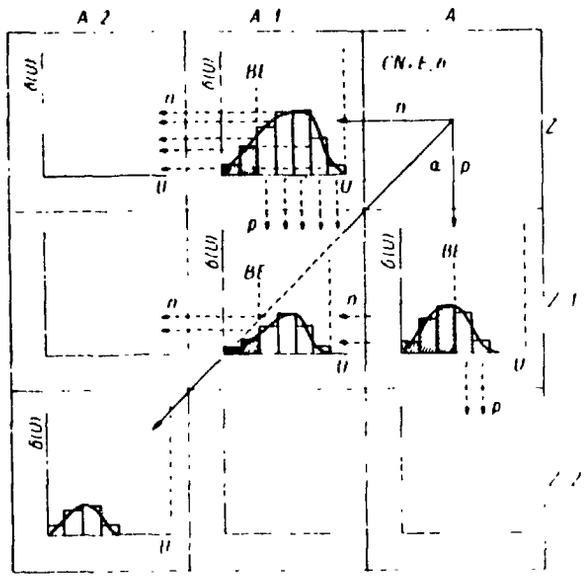

dσ/dε (mb/MeV)

Figure 2

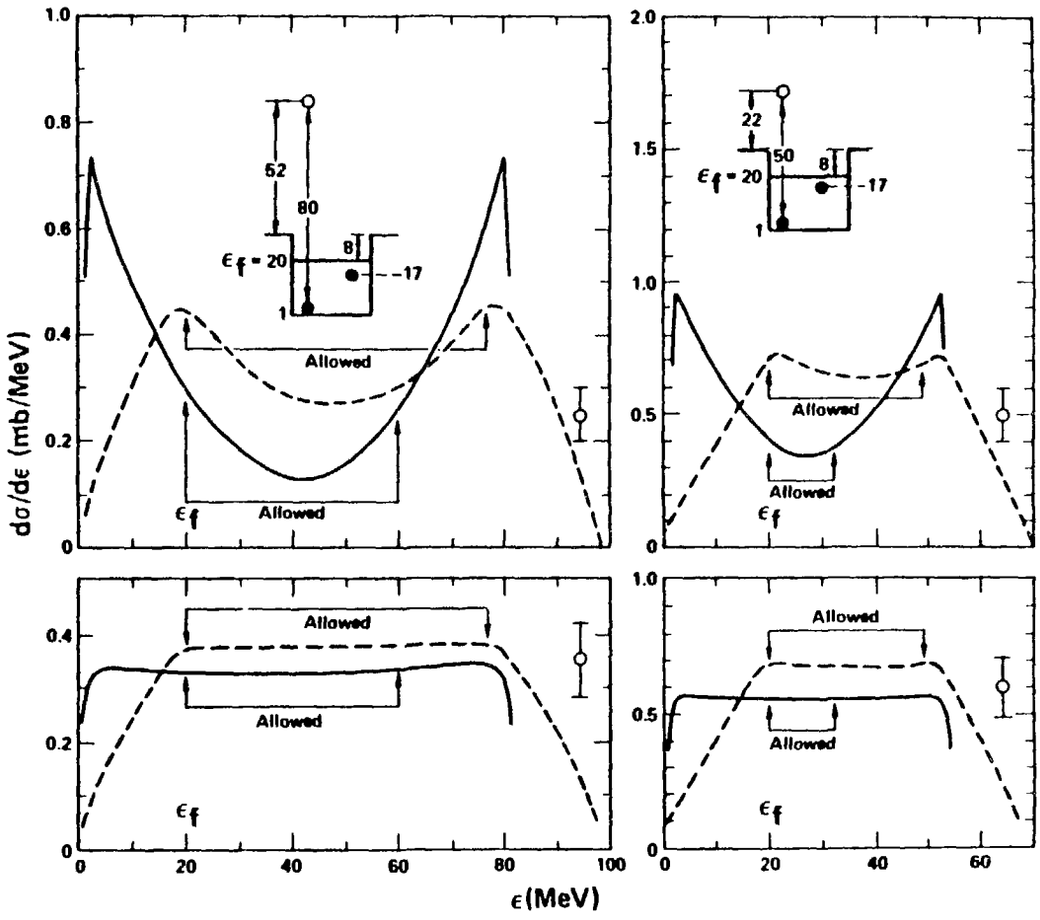
dσ/dε (mb/MeV)
ε(MeV)
Allowed
Allowed
Allowed
Allowed
Allowed
Allowed
Allowed
Allowed
52
80
8
-17
1
22
50
8
-17
1
ε_f = 20
ε_f

Figure 3

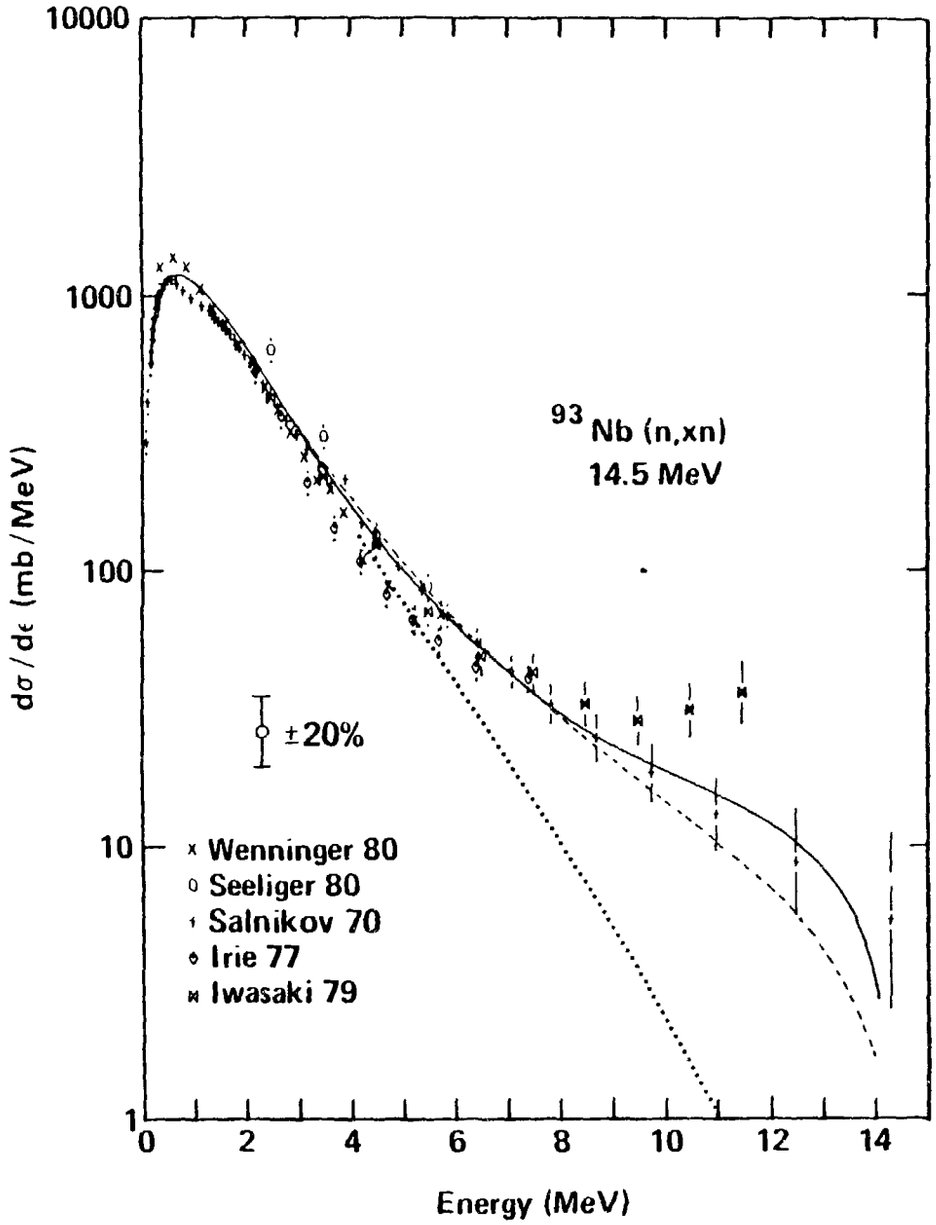
10000
1000
100
10
1
0
2
4
6
8
10
12
14
dσ/dε (mb/MeV)
Energy (MeV)
93 Nb (n,xn)
14.5 MeV
±20%
x Wenninger 80
o Seeliger 80
Salnikov 70
Irie 77
Iwasaki 79

dσ/dε (b/MeV)

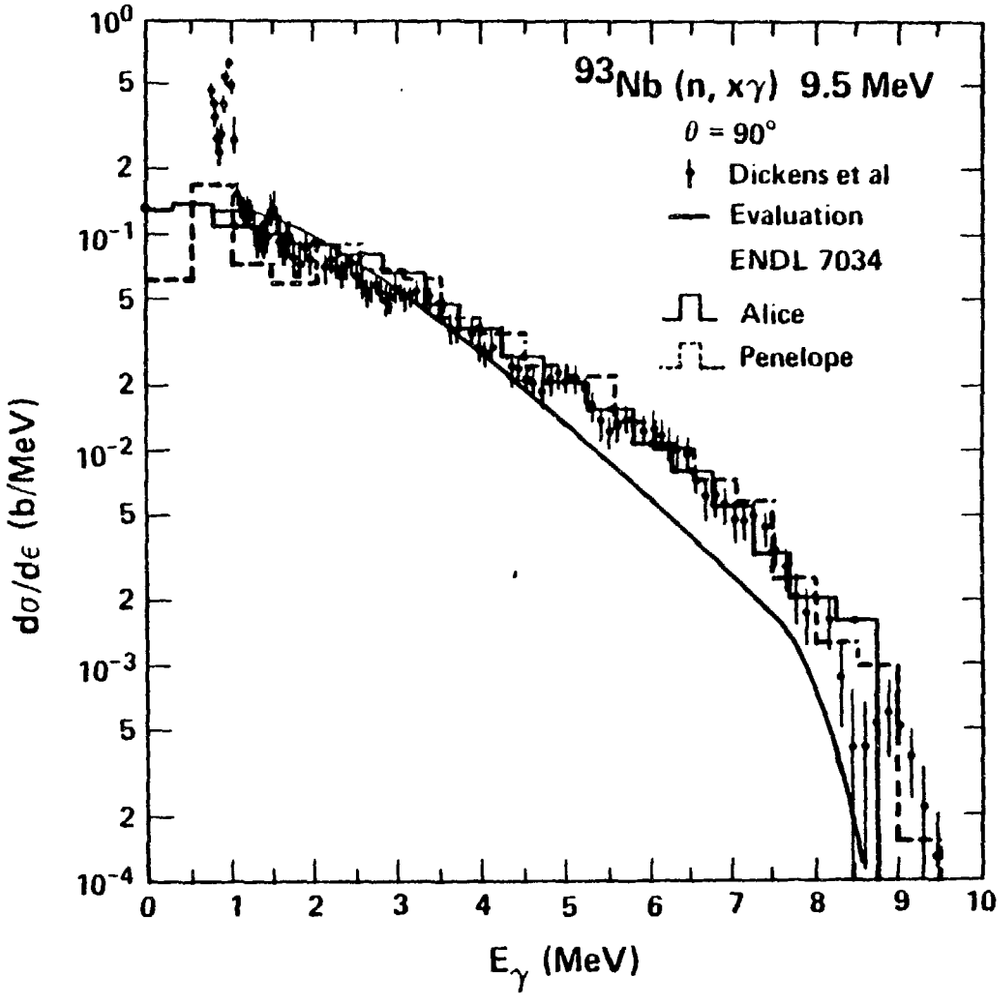
^{93}Nb (n, xγ) 9.5 MeV
θ = 90°
Dickens et al
Evaluation
ENDL 7034
Alice
Penelope
dσ/dε (b/MeV)
E$_\gamma$ (MeV)
10^0
5
2
10^{-1}
5
2
10^{-2}
5
2
10^{-3}
5
2
10^{-4}
0 1 2 3 4 5 6 7 8 9 10

dσ/dε (b/MeV)

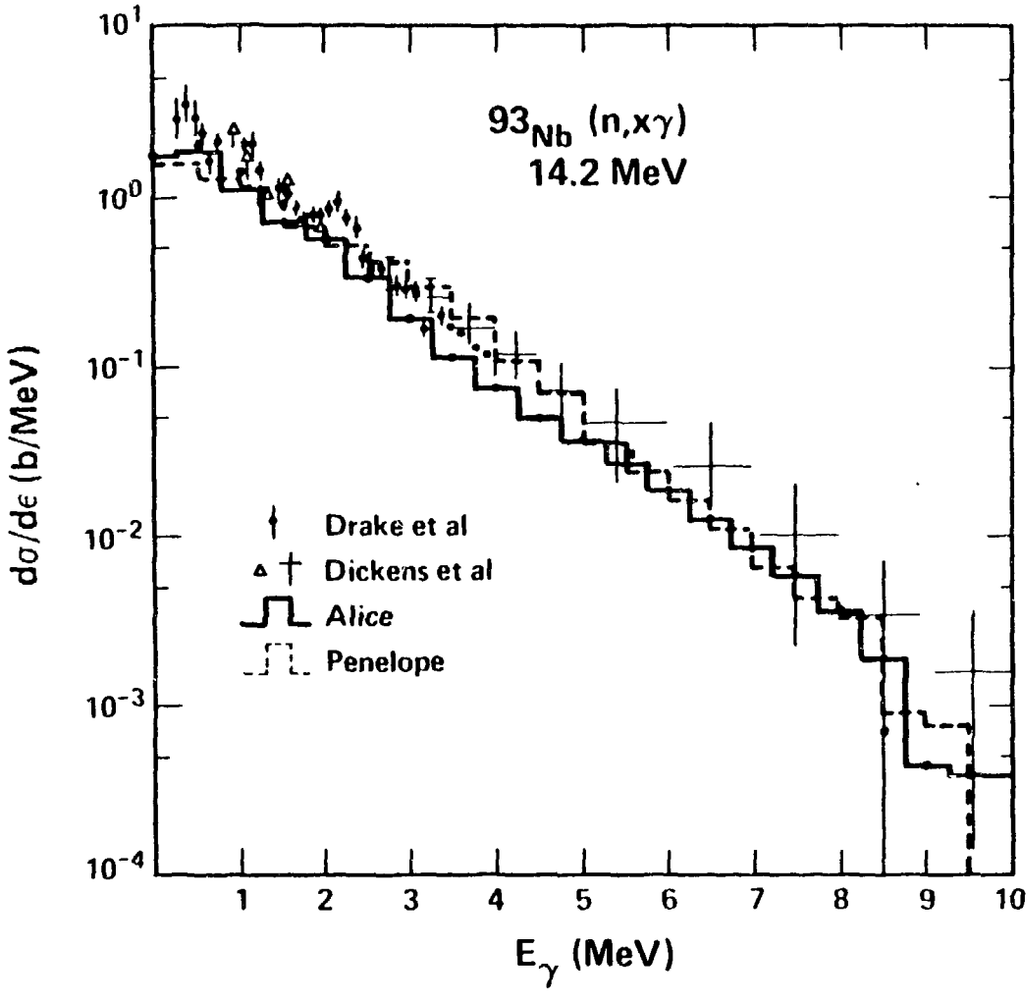

distribution of excitation energies U corresponding to the initial excita-

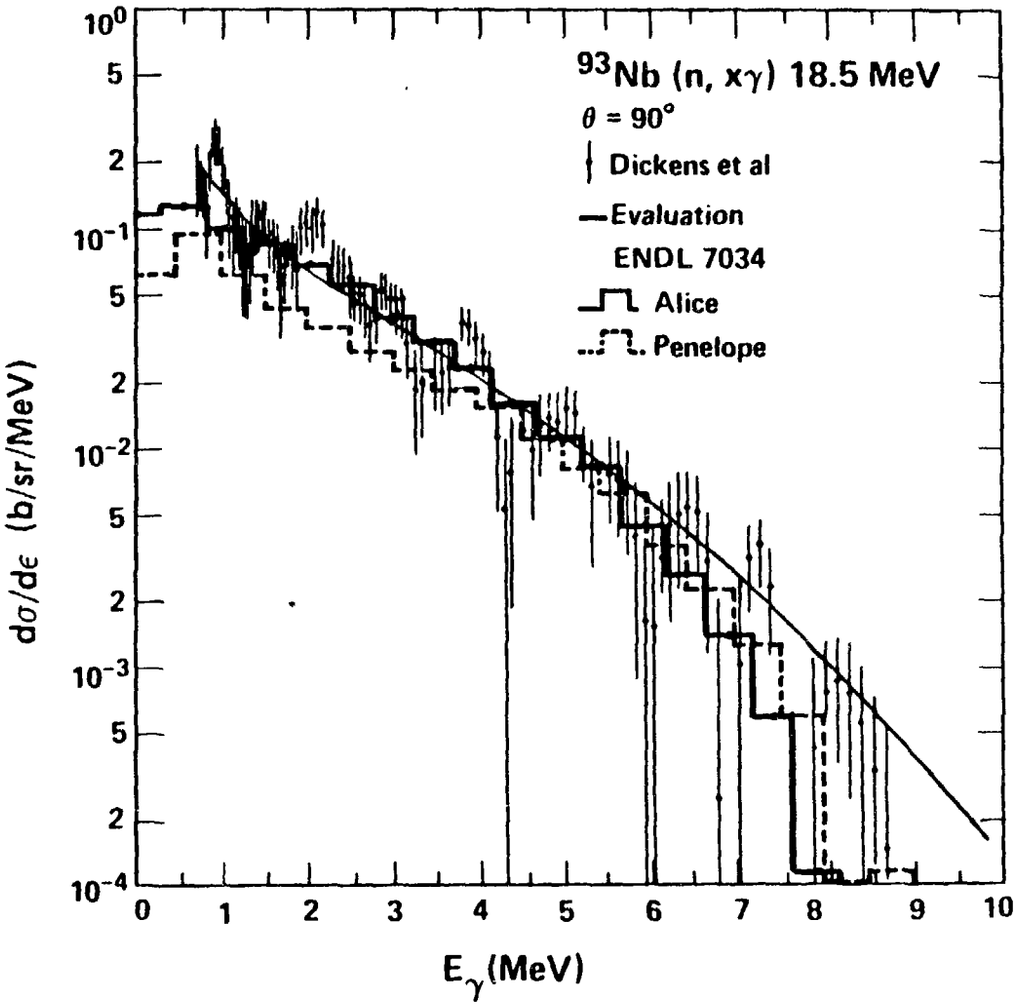
^{93}Nb (n, xγ) 18.5 MeV
θ = 90°
Dickens et al
Evaluation
ENDL 7034
Alice
Penelope
dσ/dε (b/sr/MeV)
E$_\gamma$(MeV)
10^0
5
2
10^{-1}
5
2
10^{-2}
5
2
10^{-3}
5
2
10^{-4}
0 1 2 3 4 5 6 7 8 9 10

dσ/dε (b/sr/MeV)

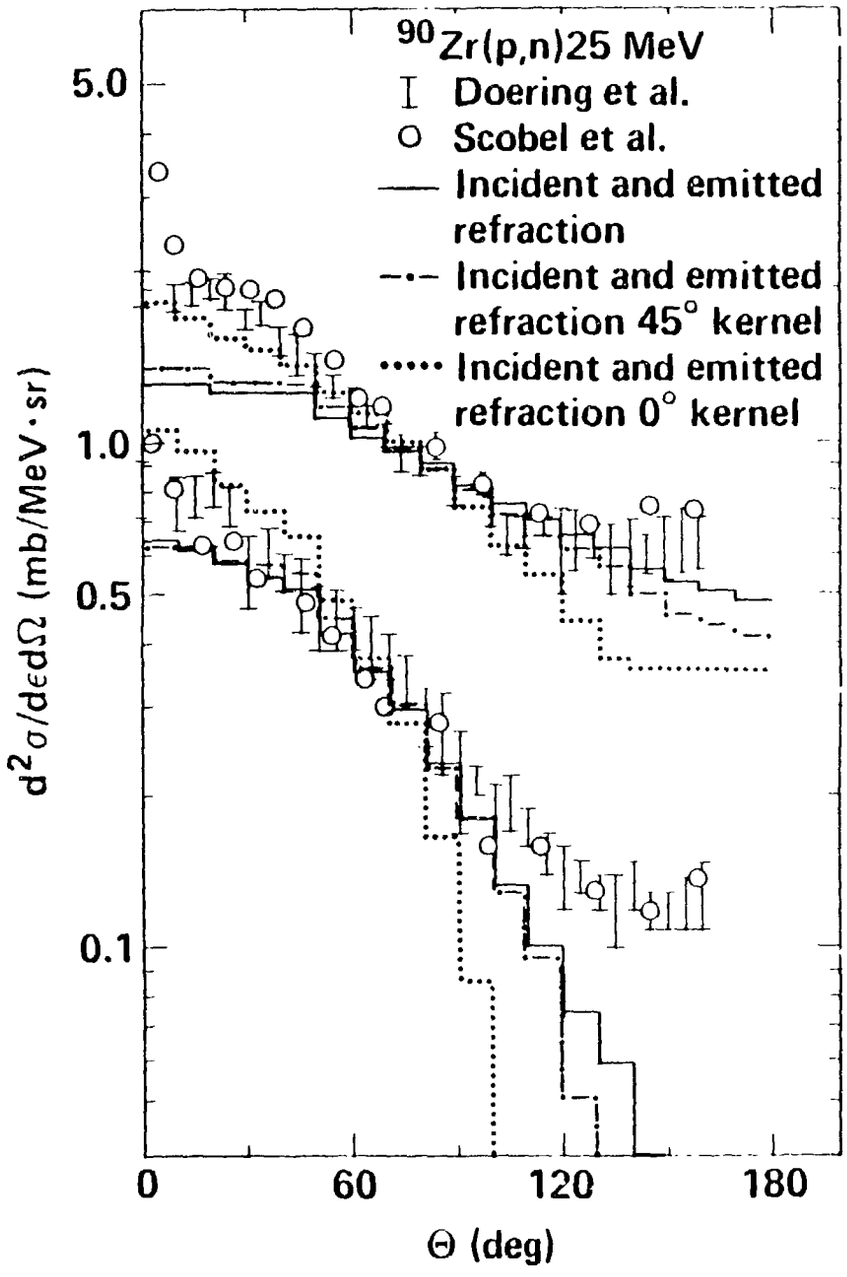
^{90}Zr(p,n)25 MeV
Doering et al.
Scobel et al.
Incident and emitted refraction
Incident and emitted refraction 45° kernel
Incident and emitted refraction 0° kernel
5.0
1.0
0.5
0.1
0
60
120
180
Θ (deg)
d²σ/dεdΩ (mb/MeV·sr)

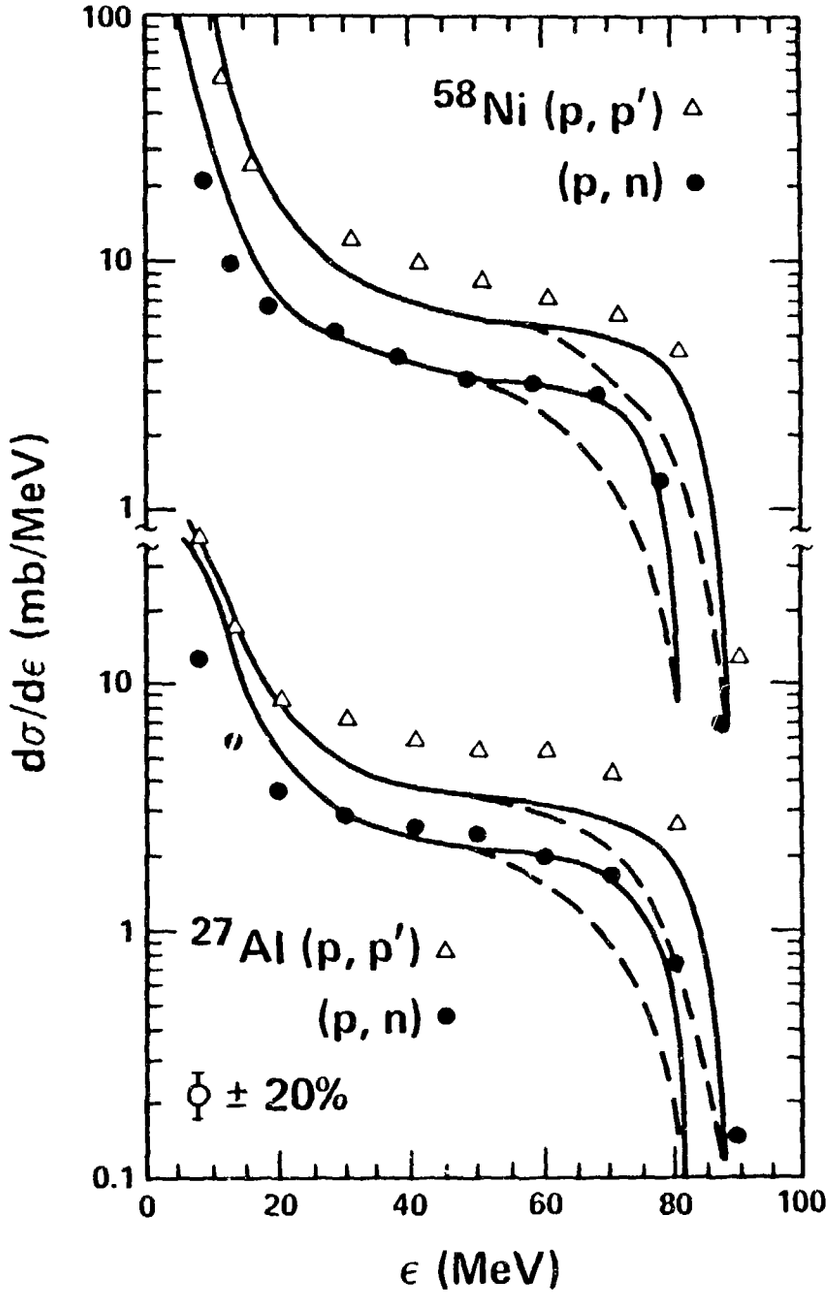
100
10
1
10
1
0.1
^{58}Ni (p, p′) △
(p, n) ●
^{27}Al (p, p′) △
(p, n) ●
Φ ± 20%
0
20
40
60
80
100
dσ/dε (mb/MeV)
ε (MeV)

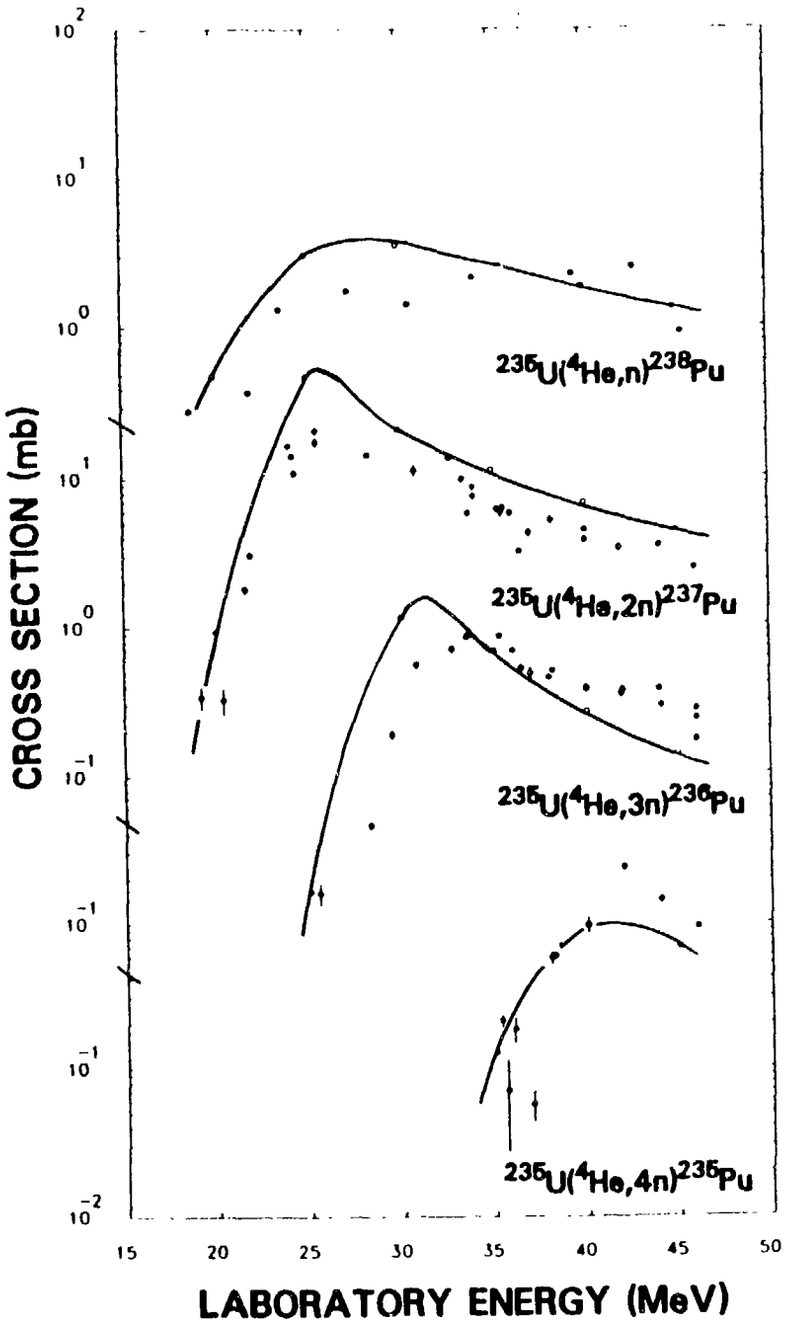


```
      program a'   o(input,output,tape5=input,tape6=ou   ut)
cccccccccccccccccccccccccccccccccccccccccccccccccccccccccccccc
c           alice/livermore/85/300 version aliso to give isotopically weighted res
c                 ults
```

```
      program a'   o(input,output,tape5=input,tape6=ou   ut)
ccccccccccccccc  :ccccccccccccccccccccccccccccccccccccccccccccccccccccc
c          alice/livermore/85/300 version aliso to give isotopically weighted res
c          ults
c          has ultimate input default options, changes per s.perlstein
c          march 10,1987
c          ==============
c          minor modifications make Nov 1987
c*************************************************************************
c
c       this version has gamma rays per ucrl report
c      this version of alice was tentatively released march 1984
c      it differs from alice/livermore82 as follows*
c        the fixed 1 mev bin size is now variable(input variable 'ed')
c        the na dimension has been increased from 11 to 22
c        the maximum excitation has been increased from 200 to 300 mev
c        level densities differ according to ejectile mass
c        precompound angular distributions may be calculated for nucleon
c        induced reactions (input variables 'iadst,irfr,imxx')
c        some inconsistancies in pairing treatment have been corrected
c        constructions which could cause errors on pre-1977 compilers
c        have been modified
c        rotating finite range barriers due to a.j.sierk may be chosen.
c
c*************************************************************************
c
c        some discussion of codn physics may be found in phys. rev.28,
c        1475(1983),and in llnl report no. ucid 19614(1982),and in
c        references therein.
c
c*************************************************************************
c
c
c ************************************************************************
c          corrected up to april 24,1983, changed sept 1980
c          to include gove mass table and provide backshifted
c          pairing in level densities.
c          errors concerning zero barrier fission competition,
c          exciton precompound option and renormalisation for
c          gt.1 precompound emission probability corrected,
c          classical (sharp cutoff) inverse cross section option
c          included.
c          s-wave condition removed from preequilibrium.
c          exciton lifetime option ij eliminated.
c          punch of inverse cross sections eliminated.
c          minor errors corrected, some formats changed for clarity.
c          comments updated, some statement positions and numbers
c          changed for clarity, meaning of tmx and rcss changed.
c
c          some effort was made to make the various precompound
c          options compatible with any evaporation/fission option
c          (jcal). there is no substitute, however, for carefully
c          checking any output for consistency.
c          new option to read in fission barriers also added to this opus.
c          multiple precompound decay algorithms added
c          this version has all changes up to sept.8,1982
c          optical model parameters for n and p are changed from earlier
c          overlaid alice code.
c
c
```

```
c  this is code alice/livermore/82 described in report
c  alice/livermore/82/llnl 1982,and in a newer alice85 report to be issued.
c  input is briefly described below.
c
c  'd' means default option.
c
c cardl format(6f5.1,i1,f4.1,i1,i4,4i5,f4.1,i1,i5,f5.1,i1,i4)
c
c    s     f   s c
c    y     o   t o
c    m     r   a l
c    b     m   r u
c    o     a   t m
c    l     t     n
c    !     !   !
c
c ap    f5.1   1 projectile mass number
c at    f5.1   6 target mass number
c zp    f5.1  11 projectile charge
c zt    f5.1  16 target charge
c qval  f5.1  21 reaction q value=ap+at-acn. d=calculated from msl mass formula.
c cld   f5.1  26 ratio of single particle level densities 'af/an. d=1.00
c                if parameter isot is nonzero,cld is isotopic abundance input
c
c ifis   i1   31 if=0,use rotating finite range fission barriers due to a.j.
c                 sierk(note double precision comments in subroutine asierk);
c                 if ifis is greater than 0,rotating liquid drop barriers will
c                 be used.
c
c barfac f4. 32 scales liquid drop or finite range fission barrier;d=1.
c
c isot   i1   36 if isot is non zero,cld will be isotopic abundance;
c                the different isotopes must be entered with the highest
c                mass number first; other isotopes (of the same atomic
c                number) may be entered in any order; in this mode the
c                isotopic abundances input must sum to 1.00
c
c
c
c                if input parms na,nz,mc,mp are all entered as blank or zero
c                then default will set na=11,nz=9,mc=10,mp=3,and on card(s) 3,
c                jcal=1(weisskopf calculation), and geometry dependent hybrid
c                precompound decay.these are suggested for beginners.in this
c                mode,ike=4 and inver=2 are also selected.
c
c na     i4   37 number of nuclides  of each z to be included in calculation.
c nz     i5   41 number of z to be calculated in the emission process.
c                both na and nz may be left blank;default is 11,9
c                 suggest values mc=10,mp=1,and inver=2 (all right adjusted)
c mc     i5   46 mass option, for separation enrgies and level density ground
c                state shifts (ldgs) (together with mp)
c                mc=0, myers swiatecki lysekil (msl) masses incl. shell corr.
c                mc=1, msl masses without shell correction term (with mp=0 only)
c                mc=2, msl masses incl. shell corr, but separation energies
c                      and/or ldgs at least partly provided by user (see below)
c                if mc increased by 10, alice will substitute 1971 gove mass
c                table masses for msl masses where available and (if so selected
c                by mc=11 or mp=0) subtract pairing or shell correction from the
c                be
c mp     i5   51 pairing option. mp=0, no pairing term in masses
```

```
c                mp=1, pairing term in masses, ldgs calculated
c                      from msl formula and applied backshifted
c                mp=2, as mp=1, but shell corr. also included in ldgs
c
c                mp=3 normal pairing shift,zero for odd-even nuclei,
c                delta added to excitation for odd-odd nnuclei,etc.
```

```
c                mp=1, pairing term in masses, ldgs calculated
c                   from msl formula and applied backshifted
c                mp=2, as mp=1, but shell corr. also included in ldgs
c
c                mp=3 normal pairing shift,zero for odd-even nuclei,
c                delta added to excitation for odd-odd nnuclei,etc.
c
c                 recommend values mc=10,mp=3
c
c inver i5  56 inverse cross section param. =0,results supplied by o.m. sub-
c                routine, =1, user supplies;if=2,sharp cutoff values each z.
c
c                 option inver=2 greatly reduces total cpu time
c
c ed   f4.1 61  energy bin mesh size in mev(f4.1).
c
c
c ike   i1  65 if=0,no particle spectra will be printed; if=1,equilibrium
c                spectra for each nuclide will be printed; if=2,only pre-
c                compound spectra printed; if=3,as 1+2; if=4,precompound
c                spectra will be printed as well as the sum (over all
c                emitting nuclides and all partial waves) of precompound
c                plus equilibrium spectra.
c ipch  i5  66 if ipch=1 or =2,fission barriers may be read in after card #1
c                as bexp(ia,iz),one card for each z(11f5.1).barriers are indep-
c                endent of ang. momentum for ipch=1,and are scaled as rldm
c                barriers for ipch=2.
c                this option should be used with care as abuses are not dissalowed
c pld  f5.1 71 level density parameter 'a',a=acn/pld, d=acn/9.
c kplt  i1  76 if kplt is 1 excitation functions will be plotted on line
c                printer. note that kplt and m3 are not in five column format.
c m3    i4  77 number and type of particles to be emitted from each nuclide.
c                if=1,n only,=2,n&p,=3 or 0,n,p,&alpha,=4,n,p,alpha&deuteron.
c
c                 recommend pld=0.,kplt=0,m3=0 (blank=0)
c
c card2 title card-80 columns
c
c
c       if mc=2 or 12 on card 1,read user supplied n,p,alpha,deuteron
c       binding energies and/or ldgs here, format(5f10.5),
c       one line per nuclide, order ((ia=1,na+2),iz=1,nz+2)
c       whenever non zero n binding energy is detected, alice will
c       use user provided binding energies for this nuclide, same
c       convention for ldgs.
c       if inver=1 on card1,read n,p,alpha,deut inverse cross sections
c       here, format(6e10.5), in ascending channel energy,
c       1st value for 0.1 mev channel energy, then up in 1 mev
c       steps, 48 values for each particle type, sequence n,p,
c       alpha, deuteron
c
c card3 energy/options card. this card (and card(s)4 if selected)
c       is repeated for each energy for a given target+projectile
c       format(2f5.1,3i1,i2,f3.0,i2,2i5,8f5.1,i5)
c
c   s    f  s c
c   y    o  t o
c   m    r  a l
c   b    m  r u
c   o    a  t m
```

```
c eq   f5.1  1 projectile kinetic energy in the laboratory system.
c              if=0.,a new problem will begin at card1.
c              if=-1.,previously calculated excitation functions will be
```

```
c eq    f5.1   1 projectile kinetic energy in the laboratory system.
c                if=0.,a new problem will begin at card1.
c                if=-1.,previously calculated excitation functions will be
c                       plotted, if kplt=1 was selected and if eq values
c                       were run in ascending order
c                if eq=0. on two successive cards,a normal exit will occur.
c rcss f5.1   6 reaction cross section.if left blank,the reaction cross
c                section will be internally generated by the optical
c                model subroutine for incident n or p,and by the par
c                abolic model routine for all other projectiles.if
c                rcss is  read in,this value entered for rcss will
c                be used.if a geometry dependent hybrid model and/or
c                fission calculation is selected,and if one wishes to
c                enter transmission coef. for entrance channel,then
c                the negative of the no. of t(l) to be read must be
c                entered for rcss.the t(l) will then be read on card(s)4
c
c
c iadst i1   11 if=0,no angular distribution,if=1,yes-for neutrons;
c                =2,yes for protons
c
c
c irfr  i1   12 choice for refraction with angular distributions
c
c
c                if irefr=0, no refraction
c                if irefr=1 or 2,entrance channel refraction
c                if irefr=3, heisenberg entrance and exit refraction
c                if irefr=2,std entrance refraction and heisenberg exit channel
c
c
c i3d   i1   13 if=0,three dimensional folding for angular dist.,else 2d
c
c
c jcal  i2   14 type of calculation option.
c                jcal=1, weisskopf-ewing evaporation calculation
c                jcal=2, s-wave approximation, liquid drop moment of inertia
c                jcal=3, s-wave approximation, rigid body moment of inertia
c                        (only if entrance channel cross sections calculated
c                        by parap, i.e. zp.gt1..and.rcss.eq.0.)
c                jcal=0, evaporation-fission competition, partial
c                        wave by partial wave
c                if fission is to be calculated using zero barrier for all
c                j.gt.jcrit, increase jcal by 10.
c
c
c dlt   f3.0 16 energy increment for calculating angular distributions (f3.0)
c                if adist =1. default value is 5 mev.
c
c
c jfrac i2   19 if a fission calc is to be only in a specified angular momentum
c                range, this is the lower limit.
c jupperi5   21  upper limit of angular momentum,if the range is to be
c                restricted
c jang  i5   26 option of emitted particles decreasing ang. mom.if=1,yes;=0,no.
c                if jang is greater than 100 (less than 200) loop over angular
c                momenta will be for increments of jang-100 and 'no' option on
c                removal of angular momentum holds.  if jang is greater than
```

```
c                delta 1 'yes' option holds, and loop is incremented by
```

```
c                200, delta 1 'yes' option holds, and loop is incremented by
c                jang-200.  -- use jang.gt.100 with jcal=0 and td=0. only --
c
c                all additional parameters on this card are for precompound
c                option, leave remaining columns blank if no precompound
c                calculation selected
c
c                if td is positive and ex1 and ex2 are blank,default parameters
c                will be selected.the gdo option may still be selected.
c                 for default precompound hybrid model,use td=1.,
c                 remaining variables zero.for gdh calculation,enter
c                 td=1.,tmx=1.,and leave all other variables after td blank.
c
c
c td    f5.1  31 initial exciton number=p+h.
c ex1   f5.1  36 initial excited neutron number.
c ex2   f5.1  41 initial excited proton number.
c tmx   f5.1  46 if=0. hybrid model. if eq.1., gdh.
c av    f5.1  51 if av=0, optical model transition rates;
c                these values should not be used above 55 mev.
c                if av=1,nucleon-nucleon mean free paths are used.
c gav   f5.1  56 no longer used
c
c cost  f5.1  61 mean free paths are multiplied by cost+1.
c gdo   f5.1  66 if =1, gdh calculation (if any) restricted to initial
c                exciton number, hybrid calc. for higher exciton numbers
c
c ij     i5   71  if ij=1,isospin precompound option is selected.
c                 if so,the next card'3a' will be format(3f10.2),
c                 containing (p,n)q values qpn(1),qpn(2),and qpnc.
c                 qpnc is (p,n) q value for making compound
c                 nucleus by a (p,n) reaction;qpn(i) is for nucleus
c                 populated by emission of particle i,1=n,2=p.
c
c                 qpnc=bp(at+ap+1,zt+zp)-bn(same),and qpn(1)=(bp-bn)
c                 of (at+ap,zt+zp),and qpn(2)=(bp-bn)of(at+ap,zt+zp-1)
c
c card4          entrance channel transmission coefficients t(l),
c                needed only, if rcss.lt.0, alice will try to read as many
c                t(l) as indicated by the absolute value of rcss (i.e. it
c                may expect several cards here). format(10f5.3)
c
c                for overlay mode use same entry point for all subroutines.
c                enter following subroutine sequences=
c                overlay alpha
c                insert hybrid,mfp,nucmfp
c                overlay alpha
c                insert over,tlj
c                overlay alpha
c                insert shaft,fisrot,pnch,plt,plexc,sigi
c                overlay alpha
c                insert parap,lymass,binden,mass
c
c************** caution  revised code not tested in overlayed mode
c
c
c
```

UCRL- 97778
PREPRINT

Multiple Preequilibrium Decay Processes

Marshall Blann

This paper was prepared for submittal to
the Nuclear Energy Agency
Nuclear Data Committee (NEANDC)
Specialists' Meeting on
Preequilibrium Nuclear Reactions
Semmerling, Austria
February 10-12, 1988

November 1987

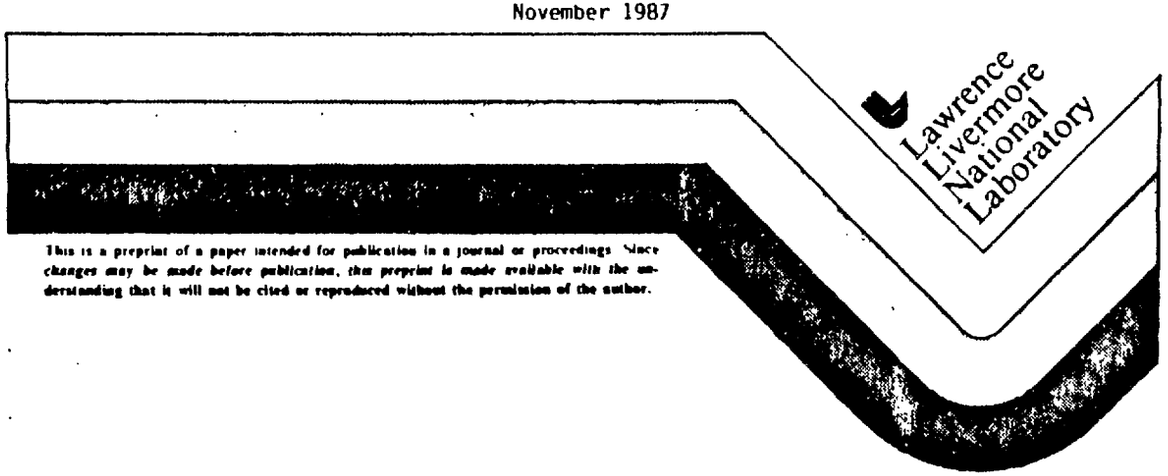

MULTIPLE PREEQUILIBRIUM DECAY PROCESSES

Marshall Blann
E-Division, Physics Department
University of California
Lawrence Livermore National Laboratory
Livermore, California, U.S.A. 94550

ABSTRACT

Several treatments of multiple preequilibrium decay are reviewed with emphasis on the exciton and hybrid models. We show the expected behavior of this decay mode as a function of incident nucleon energy. The algorithms used in the hybrid model treatment are reviewed, and comparisons are made between predictions of the hybrid model and a broad range of experimental results.

This work was performed under the auspices of the U.S. Department of Energy by the Lawrence Livermore National Laboratory under contract number W-7405-ENG-48.

1. Introduction

This presentation is intended first, to compare different treatments of precompound (PE) decay, secondly, to show the importance of multiple decay versus energy, and finally, to compare calculated and experimental results where multiple PE decay is an important component of the calculated yield.

In Section II, we will describe the INC approach [1-3] to the multiple PE decay problem, and then two different exciton model [4] approaches: the Exciton [5,6] and Hybrid models [7,8]. In Section III, we will compare predictions of the latter two approaches versus incident neutron energy, and we will present comparisons of hybrid model calculations with a range of experimental results. Conclusions will be presented in Section IV.

2. Models for Multiple Preequilibrium Decay

2.1 Intranuclear Cascade Model

Although we are primarily concerned with exciton model formulations for multiple PE decay, it is worth remembering that the first treatment was the intranuclear cascade model [1-3]. In Fig. 1, we show three cascade processes in which one and only one, two and only two, and three and only three, PE particles are emitted. By following the history of each reaction separately (rather than by an average ensemble) the distribution of PE multiplicities naturally follows. Here the treatment of multiple PE decay is very clear; the calculation, however, is teoious, so we wish to consider exciton model approaches.

2.2 The Exciton Model

The Exciton model may be expressed in the following familiar form: [5,6]

$$\frac{d\sigma}{d\varepsilon} = \sigma_R \sum_{n=n_0}^{\bar{n}} \left[\frac{X_\gamma \rho_{n-1}(U)}{\rho_n(E)} \right] \cdot \left[\frac{\lambda_c(\varepsilon)}{W_c(E)+W_+(E)} \right] D_n \qquad \text{(Eq. 1)}$$

where the first set of square brackets represents the number of excitons of type γ which could be emitted with channel energy ε, and the second set represents the probability that the particle will be emitted before <u>any</u> n exciton configuration either emits a particle or undergoes an intranuclear (two body) interaction. Here the decay normalization is based on <u>any</u> action of all members of the n-exciton configuration ensemble, a two-body interaction or particle emission. One can calculate precisely the fraction of the ensemble which will emit a particle, and the fraction which will make a two-body transition, and these two fractions sum to unity for the n exciton ensemble. This mode is shown pictorially in Fig. 2. In this work we use Exciton model with a capital "E" to refer to formulations which may be used to predict absolute cross sections; we use the lower case to refer to any models using exciton densities.

Under this proper and civilized normalization, the ensemble at excitation E will either (in the never-come-back approximation) go to an n+2 exciton configuration, or emit an exciton at energy ε leaving the residual nucleus with a residual excitation and one particle exciton fewer. Multiple emission is then treated in a completely straightforward fashion by following the decay of the daughter nuclei with p-1 particles and h holes, and

distribution of excitation energies U corresponding to the initial excitation E, reduced by the particle binding energy B_γ and distribution of channel energies ϵ. This formulation of PE decay has been elegantly formulated and exploited by Gadioli and his collaborators [5,9] for single PE decay. Akkermans and Gruppelaar have explored the importance of the multiple precompound decay mode at incident energies up to 50 MeV, and their results will be presented shortly [10,11]; first, it is instructive to describe the much more convoluted approach to this problem which is taken in the hybrid model.

2.3 Hybrid Model

The hybrid model is a semi-classical approach analogous to the INC, where each particle interacts independently of all others. A consequence of this is a different normalization than that of the Exciton model, with:

$$\frac{d\sigma}{d\epsilon} = \sigma_R \sum_{n=n_0}^{\bar{n}} \left[\frac{X_\gamma \rho_{n-1}(U)}{\rho_{n(E)}} \right] \cdot \left[\frac{\lambda_c(\epsilon)}{\lambda_c(\epsilon)+\lambda_+(\epsilon)} \right] D_n \qquad \text{(Eq. 2)}$$

where the second set of square brackets has a denominator consisting of the two-body transition rate and continuum emission rate of the exciton under consideration, rather than integrated over all excitons as in Eq. 1. The consequence of this difference for decay normalization is great, for now, e.g., a 2p1h configuration could decay by both parcicles (and the hole) making a two-body transition (which would give a 3p exciton final configuration), or by one and only one exciton being emitted, or by two and only two excitons being emitted [12,13]. With two types of excitons (neutrons and protons) the number of exclusive possibilities increases. The choices for a one exciton gas are illustrated in Fig. 3.

The distribution of these many inclusive channels is not clear and exact as it is in the Exciton model formulation. Rather, the differentiation is made on statistical arguments, which is a euphemistic manner of stating that we make an educated guess, and hope that intuitive arguments will not leave us too far from the truth. We will present a discussion of the algorithms used which will be quoted almost completely from Ref. 12, without explicitly indicating quotation.

Multiple precompound decay processes must be considered at higher excitations since they are important in determining the cross section surviving to the (equilibrium) compound nucleus, and in determining yields of products which require multiple precompound emission for population, e.g., a (p,2p) reaction on a heavy element target. There are two types of multiple precompound decay which might be considered. Type I results when a nucleus emits more than one exciton from a single exciton hierarchy (see Fig. 3). It may be seen that, e.g., in a two-particle-one-hole configuration, up to two particles could be emitted; in a three-particle-two-hole configuration up to three particles could be emitted, etc. The particle density distribution of these excitons, as given in the first set of brackets in Eq. 1, may be seen to be governed by the total composite system excitation. For illustrative purposes, we show the number of excitons expected at excitations above 8 MeV (taken as an estimate of average particle binding energy) versus composite nucleus excitation in Fig. 4. The importance of considering this "type I" multiple decay mode at excitations above 50 MeV is evident from Fig. 4.

The second type of multiple precompound decay (type II) would be described by the sequence "particle emission, one or more two body intranuclear transitions in daughter nucleus, particle emission." If the intervening two-body transitions are omitted from this sequence, it becomes type I multiple emission.

In the type II sequence for nucleon induced reactions, the leading term would be two-particle-two-hole. The particle density for this hierarchy for nucleons above 8 MeV is shown as a function of residual nucleus excitation energy in Fig. 4. It should be recognized that the relevant residual excitation of this population curve should be reduced by the nucleon binding energy and by the kinetic energy of the first emitted nucleon before comparing with the type I curve. Then it may be seen that at excitations below ~50 MeV for the residual nucleus following one particle emission, type II multiple precompound decay should rapidly become small compared with type I decay. We have investigated type II decay quantitatively in unpublished work. Results confirm the speculation that type I multiple precompound decay is far more important than type II for most reactions at moderate excitations. Because the first particle emission leaves a range of residual excitations and exciton numbers, a calculation of type II emission becomes more complex and time consuming than for type I emission. Nonetheless, one version of the ALICE code has been written to compute both type I and type II PE emission.

To extend Eq. 2 to higher energies and maintain its simplicity, we have made some arbitrary assumptions to estimate type I multiple particle emission branches. We define these assumptions based on simple probability arguments.

If P_n and P_p represent the total numbers of neutron and proton excitons emitted from a particular exciton number configuration, we assume that

$$P_{np} = P_n P_p \qquad \text{(Eq. 3)}$$

is the number of either type of particle emitted in coincidence with the other from the same nucleus and exciton hierarchy. This definition covers P_{pn} since in an emission from the same exciton number there is no distinction to be made.

We assume that the number of neutrons which are emitted in coincidence with another neutron from a particular exciton number configuration is given by

$$P_{nn} = 2\frac{P_n}{2}\frac{P_n}{2} \qquad \text{(Eq. 4)}$$

with the fraction of the reaction cross section decaying by the emission of two coincident neutrons being $P_{nn}/2$. The value of P_{nn} is restricted to be $\leq P_n - P_{np}$. Similar expressions are used for proton-proton coincident emissions.

The number of neutrons (protons) emitted from the n-exciton configuration, which were not in coincidence with another particle, would be given by

$$P_n \text{ (n only)} = P_n - P_{nn} - P_{np}, \qquad \text{(Eq. 5a)}$$

$$P_p \text{ (p only)} = P_p - P_{pp} - P_{np}, \qquad \text{(Eq. 5b)}$$

and the fraction of the population f_n which had survived decay of the exciton number in question would be

$$f_n = 1. - P_n(\text{n only}) - P_p \text{ (p only)} - P_{pp}/2 - P_{nn}/2 - P_{np}. \qquad \text{(Eq. 6)}$$

This fraction would multiply the fractional population which had survived to the n exciton state, i.e., is the depletion factor multiplier.

The treatment of multiple emission is completed by storing spectra of excited nuclei into the appropriate daughter nucleus buffers following the emission of one neutron only, one proton only, one neutron and one proton, two neutrons only, and two protons only. The sum of these cross sections plus the cross section predicted to survive to the original parent compound state, must equal the reaction cross section. This aspect of the calculation will have very little effect on the predicted emission spectra (none on the precompound spectra) but will have major impact on the predicted excitation functions for products for which one or two neutrons or protons, or one n and one p are emitted in the precompound mode. We describe next the method used for this last step of the precompound calculation, following which the evaporation calculation is performed within the code.

Within each exciton hierarchy, we calculate the number of neutrons (protons) emitted in singles, in coincidence with protons, or in coincidence with neutrons, as the product of the nucleon numbers from Eqs. 3-5 multiplied by the surviving population cross sections and the reaction cross sections. These cross sections ([$C_n(C_p)$, C_{np}, C_{nn}, etc.] are defined in Table I.

From the calculated total precompound neutron emission spectrum $d\sigma_n(\varepsilon)/d\varepsilon$, the cross section which could be involved in the emission of two neutrons is calculated as

$$\sigma_{2n} = \int_{U=0}^{E-B_{2n}} \frac{d\sigma_n(\varepsilon)}{d\varepsilon}\, d\varepsilon \quad , \qquad \text{(Eq. 7)}$$

where B_{2n} represents the sum of first and second neutron binding energies.

Similarly the neutron cross section which could be emitted in coincidence with protons is given by

$$\sigma_{np} = \int_{U=0}^{E-B_n-B_p} \frac{d\sigma_n(\varepsilon)}{d\varepsilon}\, d\varepsilon \quad , \qquad \text{(Eq. 8)}$$

where B_n is the first neutron out binding energy and B_p is the proton binding energy of the daughter nucleus following neutron emission. Similar integrals are made for the proton emission cross section which could consist of two coincident protons, σ_{pp}, and of a proton in coincidence with a neutron σ_{pn}. The cross section available for the emission of a single nucleon $\sigma_{n(p)}$ is, of course, the sum of all $d\sigma(\varepsilon)/d\varepsilon$ (the integrals are replaced by sums since the code computes spectra at fixed energy intervals).

For the daughter nucleus following emission of one and only one precompound neutron, we store

$$\sigma^{A-1,Z}(U) = \frac{d\sigma_n(\varepsilon)}{d\varepsilon}\ \frac{C_n}{\sigma_n} \quad , \qquad \text{(Eq. 9)}$$

where $U=E-B_n-\varepsilon$; for the daughter nucleus following the coincident emission of two neutrons, we store

$$\sigma^{A-2,Z}(U) = \frac{d\sigma_n(\varepsilon)}{d\varepsilon}\ \frac{C_{nn/2}}{\sigma_{nn}} \quad , \qquad \text{(Eq. 10)}$$

where $U=E-B_{2n}-\epsilon-\bar{\epsilon}_n$.

where $\bar{\epsilon}_n$ is the average kinetic energy of the second neutron for a given energy ϵ of the first neutron. For the case of the daughter nucleus produced by the coincident emission of a neutron and a proton,

$$\sigma^{A-2,Z-1}(U) = \frac{C_{np}}{2\sigma_{np}} \left[\frac{d\sigma_n(\epsilon)}{d\epsilon}\right] + \frac{C_{np}}{2\sigma_{pn}} \left[\frac{d\sigma_p(\epsilon)}{d\epsilon}\right] , \qquad \text{(Eq. 11)}$$

where $U=E-B_n-B_p-\epsilon-\bar{\epsilon}_{p(n)}$ as previously defined, and where $\bar{\epsilon}_{p(n)}$ is the average kinetic energy of the proton (neutron) emitted in coincidence with a neutron (proton) of kinetic energy ϵ. An expression analogous to Eq. 10 is used for the case of two proton emission.

3. Comparisons of Different Approaches with Data

The algorithms presented limit multiple precompound decay to two particle emission. For nucleon induced reactions at energies below 200 MeV does not provide a serious shortcoming. The types of algorithms employed could be extended beyond the two particle limit, if necessary, by someone with greater energy.

The calculated contributions to single vs. multiple PE decay are shown versus neutron energy for the system $n+^{127}I$ for neutrons up to 300 MeV in the hybrid model approach (in the geometry dependent form) [8] and for neutrons up to 50 MeV in the Exciton model formulation of Ref. 10 in Fig. 5. There is a quite reasonable agreement between these two approaches for the energy range of overlap. These comparisons are for a one Fermion gas, and for type I multiple PE decay in the hybrid model approach; type II decay is relatively less important. Results for a two Fermion system are summarized in Fig. 6.

Tests of the algorithms for multiple PE decay must ultimately be made by reference to experimental data. One set of comparisons is presented in Fig. 7, where we have made comparisons for the reactions $^{202}Hg(p,2p)$ and $^{202}Hg(p,2pn)$ using the new multiple emission algorithms versus the older single precompound particle emission decay code [14]. These excitation functions should provide a fairly rigorous test of the multiple decay assumptions, as proton evaporation is very highly inhibited in nuclei of high atomic numbers. The proton emission yields should therefore result primarily from the precompound process. The earlier GDH-evaporation calculation may be seen to give poor shapes for the excitation functions, and more signicantly to underestimate yields of the (p,2pn) and (p,2p) products by 3 and 5 orders of magnitude, respectively. The new algorithm gives cross sections to the correct order of magnitude, and of quite satisfactory shapes over nearly the entire energy range. It should be emphasized that these cross sections are only around 0.3% of the total reaction cross section, so that the fraction of the reaction cross section calculated to populate these yields is given surprisingly well.

In Fig. 8, we present calculated (p,pxn) and (p,2pxn) yields from ^{62}Ni targets for incident proton energies of 80 to 164 MeV [15]. The relatively good agreement of the (p,p) and (p,2p) yields indicates that the algorithms used are quite successful in estimating the multiple yields. Similar comparisons are shown in Fig. 9 for the $^{64}Ni(p,xpyn)$ reactions [15]; again the multiple decay algorithms work quite well.

A very interesting test of multiple PE decay is the case of reactions following the capture of stopped negative pions. For these reactions, both

mass yields and nucleon spectra are available. An unusual aspect of these reactions is that the neutron spectra result primarily from the initial exciton distribution, whereas the proton spectra result primarily from decay of configurations following an intranuclear two-body transition. Then we have a good test of the contribution of higher order (than n_0) terms to the PE decay; in terms of the hybrid model this also means a large contribution from type II PE decay.

The reason for this result is the quasi-deuteron merhanism for stopped pion capture; the pion may be captured either by a pn or by a pp pair

$$\pi^- + p + n \rightarrow n + n \qquad \pi^- + p + p \rightarrow n + p \quad . \qquad \text{(Eq. 12)}$$

The ratio of these reactions becomes a parameter to determine from the emitted nucleon spectra; results indicate that the first reaction dominates, consistent with the observation that the np interaction is stronger than the pp interaction.

In Fig. 10-12, we show calculated and experimental neutron spectra following stopped pion capture [16,17], and in Figs. 13-15 [18-21], we show proton spectra. In Figs. 16 and 17, we show the neutron and proton spectra from a ^{12}C target divided into type I and type II precompound decay. We see that the different slopes of the neutron and proton spectra are given quite nicely by the hybrid model, reflecting the contributions of first vs. higher order (for protons) contributions. We see also that the type II contributions are important to the total proton spectrum, and that the multiple decay (I+II) contributions dominate the proton spectra. The success in reproducing these proton data so well is strong evidence in support of the algorithms adopted for treating multiple PE decay in the framework of the hybrid model. Detailed results for the division of single and multiple PE decay for nine targets between ^{12}C and ^{208}Pb (following π^- capture) are tabulated in Ref. 22.

In Figs. 18-20, we show calculated and experimental yields following stopped π^- capture by ^{209}Bi, ^{197}Au and ^{181}Ta [23,24]. The generally good agreement in both the xn and pxn channels, once more supports the validity of the algorithms adopted, testing both type I (xn channels) and type II decay (pxn channels).

4. Conclusions

The Exciton PE model offers a precise normalization for considering multiple PE decay processes. There are, however, unanswered questions about the consistency of rates and partial state densities used in some formulations. It is important to compare results of exciton model codes with experimental results for which multiple PE decay is important. To the authors knowledge, this has not yet been done.

The hybrid model is decidedly less satisfactory for treating multiple PE decay than is possible in principle using the Exciton model normalization. Intuitive statistical arguments were made to estimate the contributions of exclusive reactions involving multiple PE decay. These algorithms have been tested against a very broad range of experimental results which are sensitive to the correctness of these algorithms, with quite satisfactory results. Similar comparisons are needed for Exciton formulations before reaching conclusions on that approach, which could offer a preferable alternative if the same predictive power were shown to be present.

References

1. R. Serber, Phys. Rev. 72, 1114 (1947).
2. M. L. Goldberger, Phys. Rev. 74, 1269 (1948).
3. N. Metropolis et al., Phys. Rev. 110, 185 (1958); 110, 204 (1958).
4. J. J. Griffin, Phys. Rev. Lett. 17, 478 (1966); J. J. Griffin, in "Intermediate Structure in Nuclear Reactions," edited by H. P. Kennedy and R. Schrils (University of Kentucky Press, Lexington, 1968); J. J. Griffin, in "Nuclear Physics: An International Conference," edited by L. Becker, C. D. Goodman, P. H. Stelson, and A. Zucker (Academic, New York, 1967), p.778; J. J. Griffin, Phys. Rev. Lett. 24B, 5 (1967).
5. M. Blann and A. Mignerey, Nucl. Phys. A186, 245 (1972).
6. E. Gadioli, E. Gadioli-Erba, and P. G. Sona, Nucl. Phys. A217, 589 (1973); C. Birattari et al., Nucl Phys. A166, 605 (1971); C. Birattari et al., Nucl. Phys. A166, 605 (1973); C. Birattari, E. Gadioli, A. M. Grassi Strini, G. Strini, and G. Tagliaferri, Lett. Nuovo Cimento 7, 101 (1973); E. Gadioli, A. M. Grassi Strini, G. LoBianco, G. Strini, and G. Tagliaferri, Nuovo Cimento 22, 547 (1974); G. M. BragaMarcazzan, E. Gadioli-Erba, L. Milazzo-Colli, and P. G. Sona, Phys. Rev. C6, 1398 (1972); E. Gadioli and L. Milazzo-Colli, in "Proceedings of the Europhysics Study Conference on Intermediate Processes in Nuclear Reactions, Yugoslavia, 1973," edited by N. Cindro, P. Kulisic, and T. Mayer-Kuckuk (Springer, Heidelberg, 1973); E. Gadioli and E. Gadioli-Erba, Acta Phys. Slovaca 25, 126 (1975).
7. M. Blann, Phys. Rev. Lett. 27, 337 (1971); 27, 700(E) (1971); 27, 1550(E) (1971).
8. M. Blann, Phys. Rev. Lett. 28, 757 (1972).
9. E. Gadioli and E. Gadioli-Erba, Nucl. Instrum. Methods 146, 265 (1977).
10. J. M. Akkermans and H. Gruppelaar, Z. Phys. A300, 345 (1981).
11. J. M. Akkermans, Radiat. Effects 95, 103 (1986).
12. M. Blann and H. K. Vonach, Phys. Rev. C28, 1475 (1983).
13. J. Bisplinghoff, Phys. Rev. C33, 1569 (1986).
14. M. V. Kantelo and J. J. Hogan, Phys. Rev. C13, 1095 (1976).
15. M. E. Sadler, P. P. Singh, J. Jastrzebski, L. L. Rutledge, Jr., and R. E. Segal, Phys. Rev. C21, 2303 (1980).
16. R. Madey et al., Phys. Rev. C25, 3050 (1982).
17. R. Hartmann et al., Nucl. Phys. A308, 345 (1978).
18. G. Mechtersheimer et al., Phys. Lett. 73B, 115 (1978).
19. H. S. Pruys et al., Nucl. Phys. A352, 388 (1981).
20. F. W. Schleputz, J. C. Comiso, T. C. Meyer, and K. O. H. Ziock, Phys. Rev. C19, 135 (1979).
21. H. Randall et al., Nucl. Phys. A381, 317 (1982).
22. M. Blann, Phys. Rev. C28, 1648 (1983).
23. C. J. Orth et al., Phys. Rev. C21, 2524 (1980).
24. H. S. Pruys et al., Nucl. Phys. A316, 365 (1979).

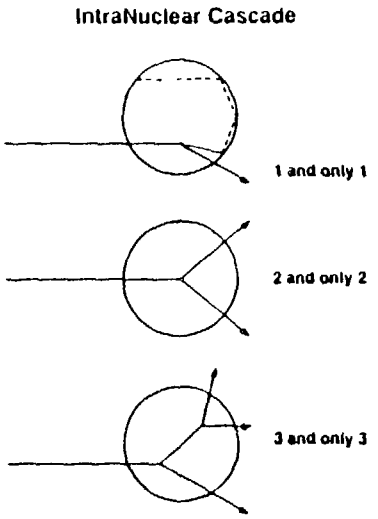

Figure 1 Diagrammatic representation of the intranuclear cascade calculation. Each projectile-target interaction is individually followed so that each reaction is treated on an exclusive basis.

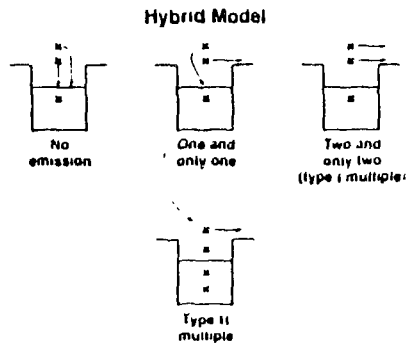

Figure 3 Diagrammatic representation of type I and type II multiple precompound decay processes. This figure is supplemented by the discussion in the text.

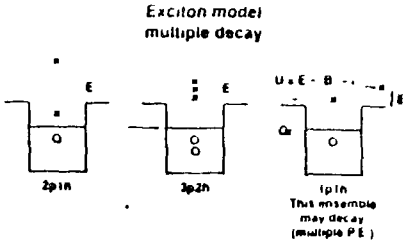

Figure 2 Diagrammatic representation of the Exciton model. A change in exciton configuration occurs when any member of the hierarchy either emits a particle or makes a two body transition. If a nucleon of energy ϵ is emitted, the daughter nucleus of one fewer particle at excitation U may be put into an ensemble to treat secondary PE decay.

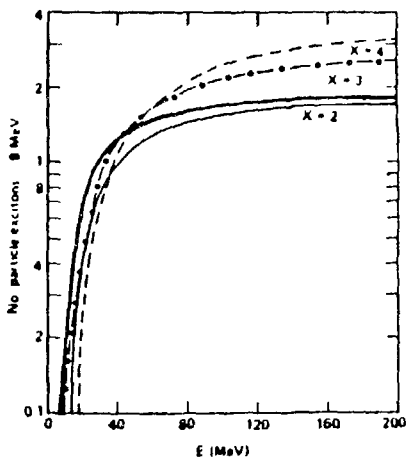

Figure 4 Number of particle excitons at excitations greater than 8 MeV above the Fermi energy versus composite nucleus excitation and particle exciton number. The heavy solid curve is for a 2p1h configuration, the dotted-dashed curve is for 3p2h, and the dashed curve is for 4p3h. The thin solid curve is for a 2p2h configuration which would be relevant for type II multiple precompound decay as discussed in the text.

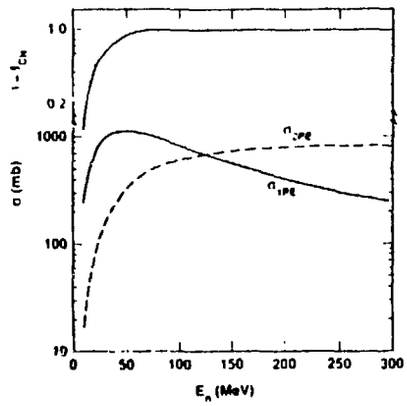

Figure 5 Calculated PE emission for one and only one, two and only two particles, vs. incident neutron energy for n+^{127}I. These results are for a one component Fermi gas. The upper scale gives one minus the fraction of the reaction cross section surviving to the compound nucleus. The solid line is the result of the GDH model calculation. The open circles represent one minus the sum of first plus second chance PE emission from the Exciton model as reported in Ref. 10. The lower scale gives one particle emission (solid line) and two particle emission (dashed) in mb as predicted by the hybrid model.

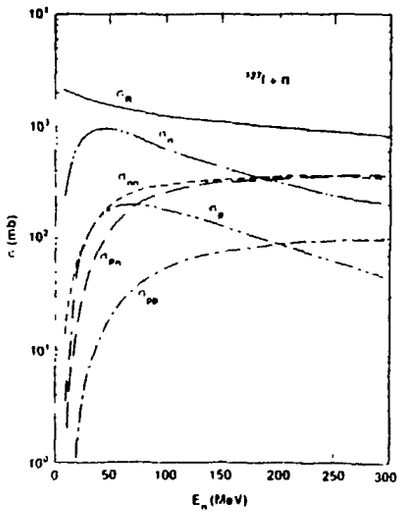

Figure 6 As in Fig 5, for a two component Fermi gas. The solid curve gives the reaction cross section versus incident neutron energy (abscissa). Other curves give the excitation functions for emission of one neutron only, two neutrons only, etc.

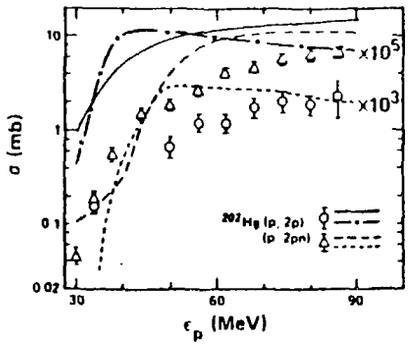

Figure 7 Calculated and experimental ^{202}Hg(p,2p) and (p,2pn) excitation functions. The points represent experimental yields from Ref. 14. The long dashed curve is the (p,2pn) prediction of this work, and the solid line the (p,2p) result. Multiple precompound decay algorithms are used in these results. The dotted-dashed curve is the GDH result (x10^4) for (p,2p) from the precompound formulation without multiple precompound decay, and the short dashed curve is the same (x10^2) for the (p,2pn) reaction.

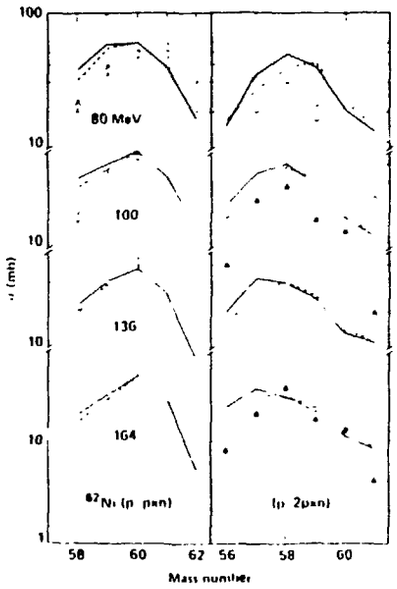

Figure 8 Calculated and experimental yields from 100 and 136 MeV proton bombardment of ^{62}Ni. Experimental points are from Ref. 15. The calculated GDH model results have been connected by solid line segments. The dashed line is the result when the equilibrium level density parameter is varied from A/9 to A/12.

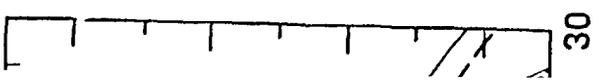

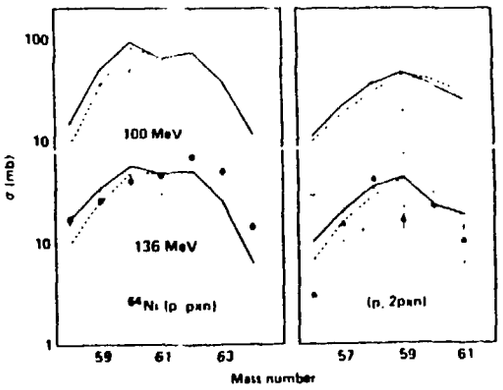

Figure 9 Experimental and calculated product yields from 80-136 MeV proton bombardment of ^{64}Ni. Points and lines are as in Fig 8

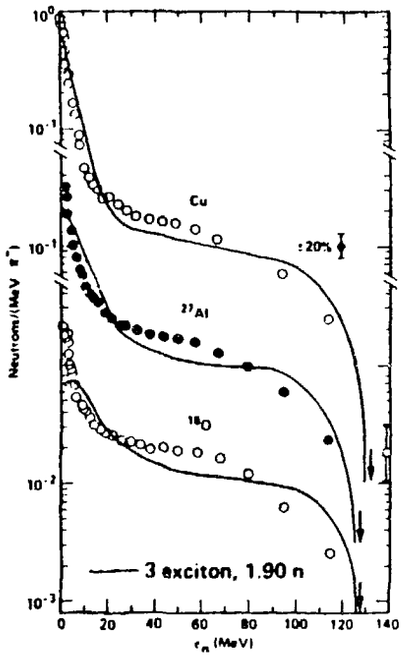

Figure 10 Calculated and experimental (π⁻,xn) spectra following the capture of stopped pions on Cu, ^{27}Al, and ^{16}O Data are from Ref 16 The calculated result is for the hybrid model with 1 90 primary neutron excitons and 0 10 proton excitons Other details of the calculation are given in the text. The arrows indicate the thermodynamic end points for the spectra.

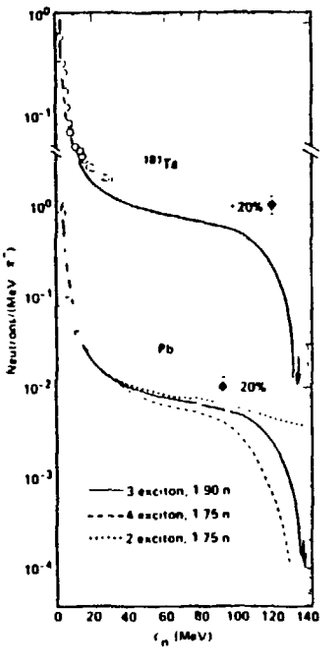

Figure 11 Calculated and experimental (π⁻,xn) spectra for ^{181}Ta and Pb targets. Data are from Ref 16, solid curve as in Fig 10 The dotted curve is the predicted hybrid model spectrum if a 2p0h primary excitation is assumed (with 1.75 neutron excitons); the dashed curve results if a 2p2h primary excitation is assumed.

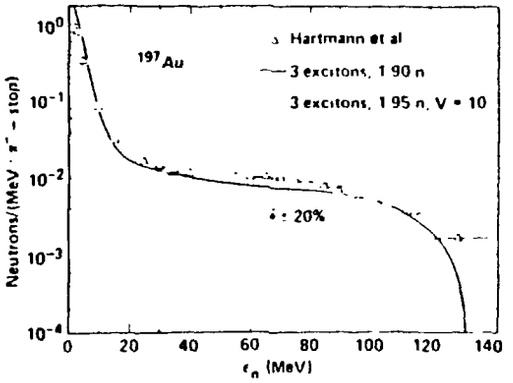

Figure 12 Calculated and experimental ^{197}Au(π⁻,xn) spectra Experimental results are from Ref 17 The solid curve is as in Fig. 10 The dotted curve is calculated for capture in nuclear matter for which maximum energy per hole is 10 MeV, assuming 1 95 neutron and 0 05 proton excitons following π⁻ capture

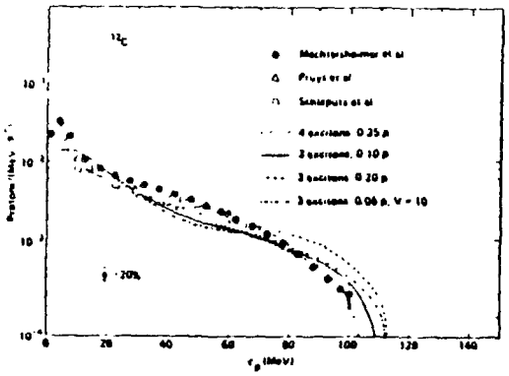

Figure 13 Calculated and experimental $^{12}C(e^-,xp)$ spectra. Experimental results are from Refs 18-20. Results of the hybrid model calculation (with maximum hole depth of 30 MeV) due to different initial proton exciton numbers are shown. A result with maximum hole depth of 10 MeV is also shown.

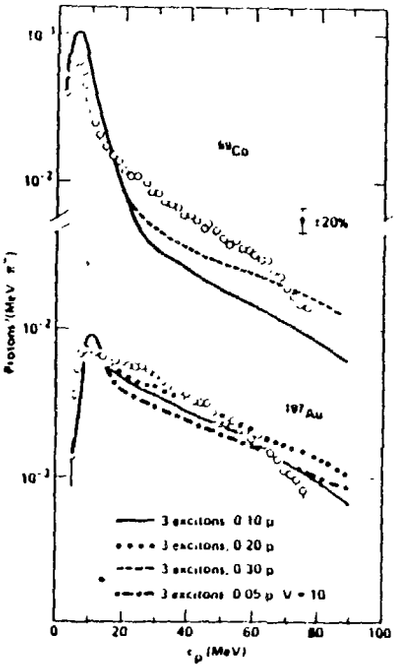

Figure 15 Calculated and experimental $^{59}Co(e^-,xp)$ and $^{197}Au(e^-,xp)$ spectra. Experimental results are from Ref. 19. The solid line is the result of the calculation described in Fig. 10. Different initial proton exciton numbers are used for the dotted and dashed curves, maintaining the 30 MeV maximum hole depth. The dotted-dashed curve assumes 0.05 initial proton excitons, and a maximum hole depth of 10 MeV.

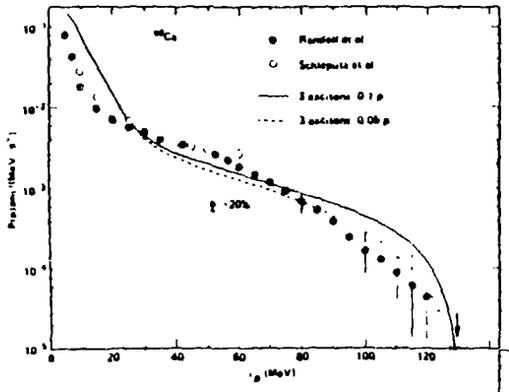

Figure 14 Experimental and calculated $^{40}Ca(e^-,xp)$ spectra. Experimental results are from Refs. 20 and 21. Calculations are as in Fig. 10, plus a result in which the initial proton exciton number is reduced to 0.05.

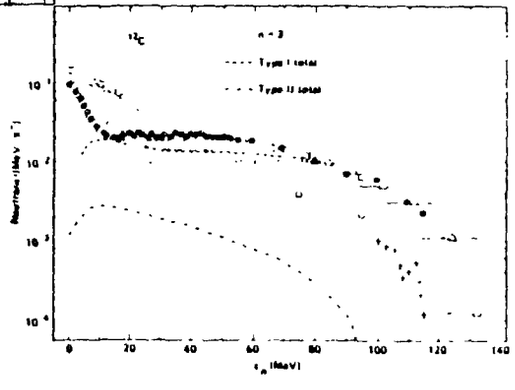

Figure 16 Contributions to the calculated $^{12}C(e^-,xn)$ spectrum from several components. Results are as described for Fig. 17.

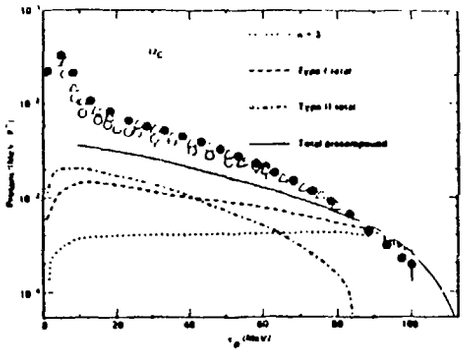

Figure 17 Contributions to calculated $^{12}C(\pi^-,xp)$ spectrum due to several components. The dotted line represents the primary (n=1) proton spectrum, including type I multiple precompound decay. The dashed line represents contributions from all precompound decay terms (n=1 to n) including type I multiple decay. The dotted-dashed curve represents only the contribution of type II multiple precompound decay. The solid line gives the sum of type I (total) plus type II precompound decay. No equilibrium component has been added to these spectra. Calculations were performed for the parameters used in Fig. 10.

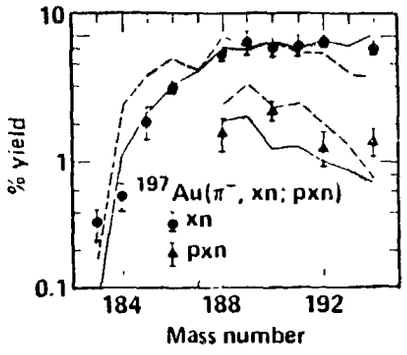

Figure 19 Calculated and experimental (π^-,xn) and (π^-,pxn) yields for stopped pions on ^{197}Au. Experimental yields are from Ref. 24. Calculated results given by the dotted and dashed lines are as in Fig. 18. The solid line represents a calculation with 1.95n and 0.05p (primary) and with the maximum hole depth of 5 MeV (10 MeV maximum for the hole pair assumed in the 2pln primary excitation).

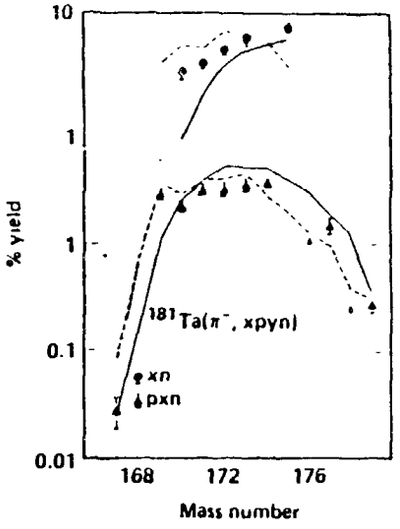

Figure 18 Calculated and experimental (π^-,xn) and (π^-,pxn) yields for stopped pions on ^{181}Ta. Experimental results are from Ref. 23. The solid line is the intranuclear cascade result reported in Ref. 23. The dashed lines is for an emission spectrum multiplied by $2.4 \times \exp - [(\sqrt{2}-5.5)^2/16]$. The dotted curve is for ε_f=10 MeV, 1.95n, 0.05p.

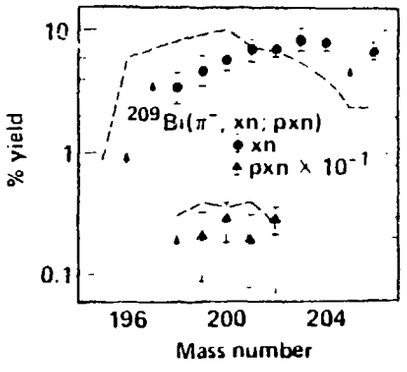

Figure 20 Calculated and experimental (π^-,xn) and (π^-,pxn) yields for stopped pions on ^{209}Bi. Experimental results (points with error bars) are from Ref. 24. Calculated points have been connected by line segments. The dotted line results from the parameters (E_f=10, 1.95n, 0.05p). The dashed line results from the parameters giving the dashed line yields in Fig. 18.

On the Origin of Medium Energy γ-rays in Nuclear Reactions

G. Reffo
M. Blann
B. A. Remington

This paper was prepared for submittal to
Physical Review C

December 1987

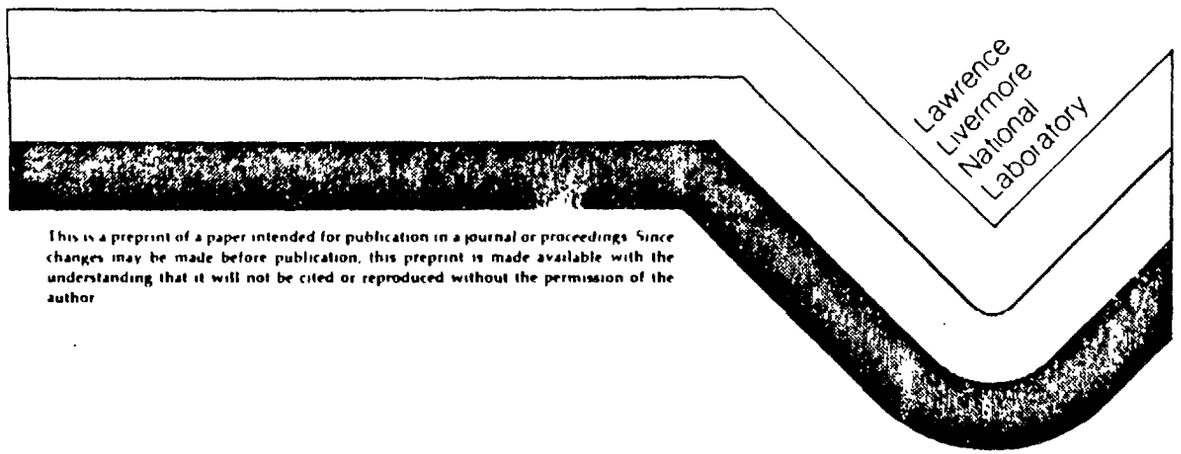

competition. If this is so, we may sum populations of all residual nuclei

On the Origin of Medium Energy γ-rays in Nuclear Reactions

G. Reffo,* M. Blann and B. A. Remington

Physics Department, E-Division
Lawrence Livermore National Laboratory
Livermore, California

1. Introduction

A recent review by Snover[1] reported γ-ray spectra at energies up to 30 MeV following α and ^{3}He induced reactions on samarium targets. The spectra at energies up to ~12 MeV were easily reproduced by a calculation based on the giant dipole resonance for statistical decay. The higher energy γ-rays were not readily reproducible by known nuclear models or theories.[1,2] In this work, we wish to explore two possible mechanisms for these high energy γ-rays: an n-p bremsstrahlung mechanism, which has been successful in reproducing high energy γ-rays in heavy ion reactions,[3-5] and a one body radiative nucleon transition model to be applied via the hybrid precompound decay model.[6]

2. n-p Bremsstrahlung

In Figures 1-3, we show experimental γ-ray spectra resulting from the 14.1 MeV n + ^{59}Co, ^{93}Nb reactions,[7] and from 27 MeV α + ^{154}Sm and 27 MeV ^{3}He + ^{148}Sm reactions.[1] We show results calculated for compound nucleus γ-rays based on a giant dipole resonance by Snover[1] for the Sm targets. It may be seen that a large discrepancy remains above 10-15 MeV γ-ray energy.

In the case of γ-rays of ~30-150 MeV from heavy ion reactions, it was found that the spectra for most systems reported could be reproduced by following the transport of excited nucleons by the Boltzmann Master Equation (BME) or by the Vlasov-Uehling-Uhlenbeck equation, with allowance for

inelastic (n,pγ) collision processes producing γ-rays from a bremsstrahlung process. Details of these calculations may be found in the literature and are not reproduced here.[3-5] In Figures 1-3, we show the contributions to the γ-ray spectra calculated from this source. It may be seen that this approach fails to reproduce γ-rays in the 10-30 MeV regime by one to several orders of magnitude.

3. Precompound γ-ray Emission

There should be a contribution to high energy γ-rays from one-body processes during the initial target-projectile interaction and the subsequent precompound cascade. This would consist of the individual excitons making a transition between two energy levels with the emission of a γ-ray. In the hybrid precompound decay model, one needs an expression for the absolute rate of emission of γ-rays of energy ε_γ by an exciton of energy ε in the potential well. This will be in competition with the absolute rates of nucleon-nucleon collisions, and of emission into the continuum for unbound nucleons. Our approach will have some similarities to earlier work by Plyuiko et al.[8] and other groups,[9] but will differ in details and because it is applied to the hybrid model.

Based on the Breit-Wigner expression and the hypothesis of Brink and Axel, we will assume that the rate of dipole γ-ray emission for γ-rays of energy ε_γ by a nucleon of energy ε above the Fermi energy is given by

$$R(\varepsilon,\varepsilon_\gamma,n) = \frac{\langle q\rangle}{2\pi\hbar}_{eff} \frac{1}{(\pi\hbar c)^2} \varepsilon_\gamma^2 \sigma(\varepsilon_\gamma) \cdot \frac{\rho(\varepsilon-\varepsilon_\gamma,n)}{\rho(E,n)} d\varepsilon_\gamma \qquad (1)$$

with $\sigma(\varepsilon_\gamma)$ given by the Lorentzian line shape

$$\sigma(\varepsilon_\gamma) = \Sigma_R \sigma_R \frac{\varepsilon^2\Gamma_R^2}{(\varepsilon^2-E_R^2)^2+\varepsilon^2\Gamma_R^2} \qquad (2)$$

where σ_R, E_R, Γ_R are fit parameters corresponding to the peak cross section, peak energy and half maximum width respectively. Numerical values

of these parameters have been given elsewhere.[10] These transition rates are transformed for effective neutron charge (by multiplication by (-Z/A) and effective proton charge (-N/A)[11] by the multiplier $\langle q \rangle_{eff}$ in Eq. 2.

In the case of a reaction initiated by an incident nucleon, the first term calculated for γ-ray emission is due to radiative one body transitions of the projectile ("direct capture"), followed by contributions from 3 and higher exciton configuration (semi-direct processes). In the case of ^{3}He and α projectiles, it is assumed that the projectile "dissolves" in the nuclear mean field, giving in each case a four exciton configuration with all energy partitions occuring with equal a-priori probability. This is the usual assumption in treating cluster induced reactions in precompound decay, justified a-posteriori by good success in reproducing a broad range of experimental results.[6] The use of four excitons for a ^{3}He projectile is again empirical based on earlier analyses of (^{3}He, n) and (^{3}He, p) spectra.[12] The assumption of three excitons would produce better agreement with the experimental γ-ray spectra, but is not supported empirically by the results of Ref. 12.

The hybrid model for nucleon emission[1] may be written as

$$\frac{d\sigma(\varepsilon)}{d\varepsilon} = \sigma_R \sum_{n=n_0}^{\bar{n}} \left[\frac{p\rho_{n-1}(U)}{\rho_n(E)}\right]\left[\frac{\lambda_c(\varepsilon)}{\lambda_c(\varepsilon)+\lambda_+(\varepsilon)}\right] D_n \qquad (3)$$

where σ_R is the reaction cross section; the first set of square brackets uses partial state densities to calculate the number of excitons in a given energy range, and $\lambda_c(\varepsilon)$, $\lambda_+(\varepsilon)$ are respectively the rate at which those excitons are emitted into the continuum or undergo nucleon-nucleon collision processes. The D_n represents population depletion due to decay of simpler configurations. Calculation of γ-ray spectra during the precompound cascade is accomplished by substituting $R(\varepsilon,\varepsilon_\gamma)$ for $\lambda_c(\varepsilon)$ in Eq. (3); we do not use $R(\varepsilon,\varepsilon_\gamma)$ in the denominator of Eq. 3 since $R(\varepsilon,\varepsilon_\gamma) \ll \lambda_+(\varepsilon)$ for all cases considered. The partial state densities used are those due to Ericson as modified by Williams.

References

In Figures 1 and 2, we show the precompound γ-ray component calculated as described above versus the γ-ray spectra from 14.1 MeV neutron bombardment of ^{59}Co and ^{93}Nb. The major contribution comes from the n-l (direct capture) term. This gives a reasonable estimate of the highest energy γ-ray yields. The missing lower energy γ-rays may well be due to compound nucleus γ-rays, as is the case in Fig. 3. In general, the calculated (n,γ) precompound spectra are about one half the experimental results. This very crude approach certainly gives a reasonable "ballpark" estimate of the γ-rays above ~16 MeV. The discrepancy allows for additional contributions from enhanced one body transitions to collective states.

In Figure 3, we show results of the calculation for the ^{3}He and α induced reactions. Here, the agreement with experimental spectra above ~12 MeV is excellent. The addition of the statistical γ-ray spectra due to compound nucleus decay (as calculated by Snover et al.) to the precompound components gives agreement over the entire spectral range. This agreement suggests that we may now have one viable model to explain this medium energy γ-ray domain. It would be valuable to have a broader range of experimental results with which to test the model proposed herein.

The authors wish to acknowledge helpful discussions with Profs. H. A. Weidenmuller, G. F. Bertsch and with Dr. F. S. Dietrich.

*permanent address, ENEA, Bologna, Italy

1270A-12/1/87

This work was performed under the auspices of the U.S. Department of Energy by the Lawrence Livermore National Laboratory under contract number W-7405-ENG-48.

Figure Captions

References

1. K. Snover, Ann. Rev. Nucl. Part. Sci. 36, 599 (1986).

2. K. Nakayama and G. F. Bertsch, Phys. Rev. C36, 1848 (1987).

3. B. A. Remington, M. Blann, G. F. Bertsch, Phys. Rev. 35, 1720 (1987).

4. T. S. Biron, K. Niita, A. L. DePaoli, W. Bauer, W. Cassing, U. Mosel, Univ. of Giessen Preprint (1987); P. Grimm, Doctoral Thesis and G.S.I. Report #GSI-87-2, ISSN 0171-4546 (1987).

5. K. Nakayama and G. Bertsch, Phys. Rev. C 34, 2190 (1986); W. Bauer, W. Cassing, U. Mosel and M. Tokyama, Nucl. Phys. A456, 159 (1986); W. Bauer, G. F. Bertsch, W. Cassing and U. Mosel, Phys. Rev. C34, 2127 (1986); R. Heuer, B. Müller, H. Stöcker and W. Greiner, Institut für Theoretische Physik, Johann Wolfgang Goeth Universität Preprint No. UFTP 204/1987 (1987).

6. M. Blann, Phys. Rev. Lett 27, 337, 700E (1971), M. Blann, Ann. Rev. Nucl. Sci. 25, 123 (1975).

7. F. Rigaud, G. Longo and F. Saporetti, Nucl. Phys. A173, 551 (1971).

8. V. A. Plyuiko and G. A. Prokopets, Phys. Lett. 76B, 253 (1978).

9. P. Oblozinsky, Phys. Rev. C35, 407 (1987); J. M. Akkermans and H. Gruppelaar, Phys. Lett. 157B, 95 (1985); E. Betak and J. Dobes, Phys. Lett. B48, 368 (1979).

10. G. Reffo, IAEA(UNESCO) Winter Courses in Nuclear Physics and Reactors, Trieste, 17 January - 10 March 1978, published by IAEA as IAEA-SMR-43 (1980).

11. J. Eisenberg and W. Greiner, Nuclear Theory, Vol. 2: Excitation Mechanisms of the Nucleus, North Holland Publishing Co., London, p. 93, (1970).

12. A. Chavarier et al., Nucl. Phys. A231, 64 (1984).

Figure Captions

Figure 1 Experimental and calculated γ-ray spectra for the reaction $^{59}Co + n(14.1\ MeV)$. Closed circles represent experimental results from Ref. 7. The dotted curve is the calculated npγ (bremsstrahlung) yield described in Ref. 3. The dashed curve is the result of the assumed one body transition competition described in the text. The arrow indicates the thermodynamic end point energy.

Figure 2 As in Fig. 1 for the reaction $^{93}Nb + n$.

Figure 3 Calculated and experimental γ-ray spectra for α and ^{3}He reactions (27 MeV lab) on Sm isotopes. The thin continuous lines represent the envelope of the experimental yields including error bars reported by Snover[1]. The heavy solid line is the compound nucleus γ-ray contribution result of Snover. The dotted line is the npγ bremsstrahlung result, as in Ref. 1, and the long dashed line is the precompound contribution calculated according to the one body radiative transition model described in this work.

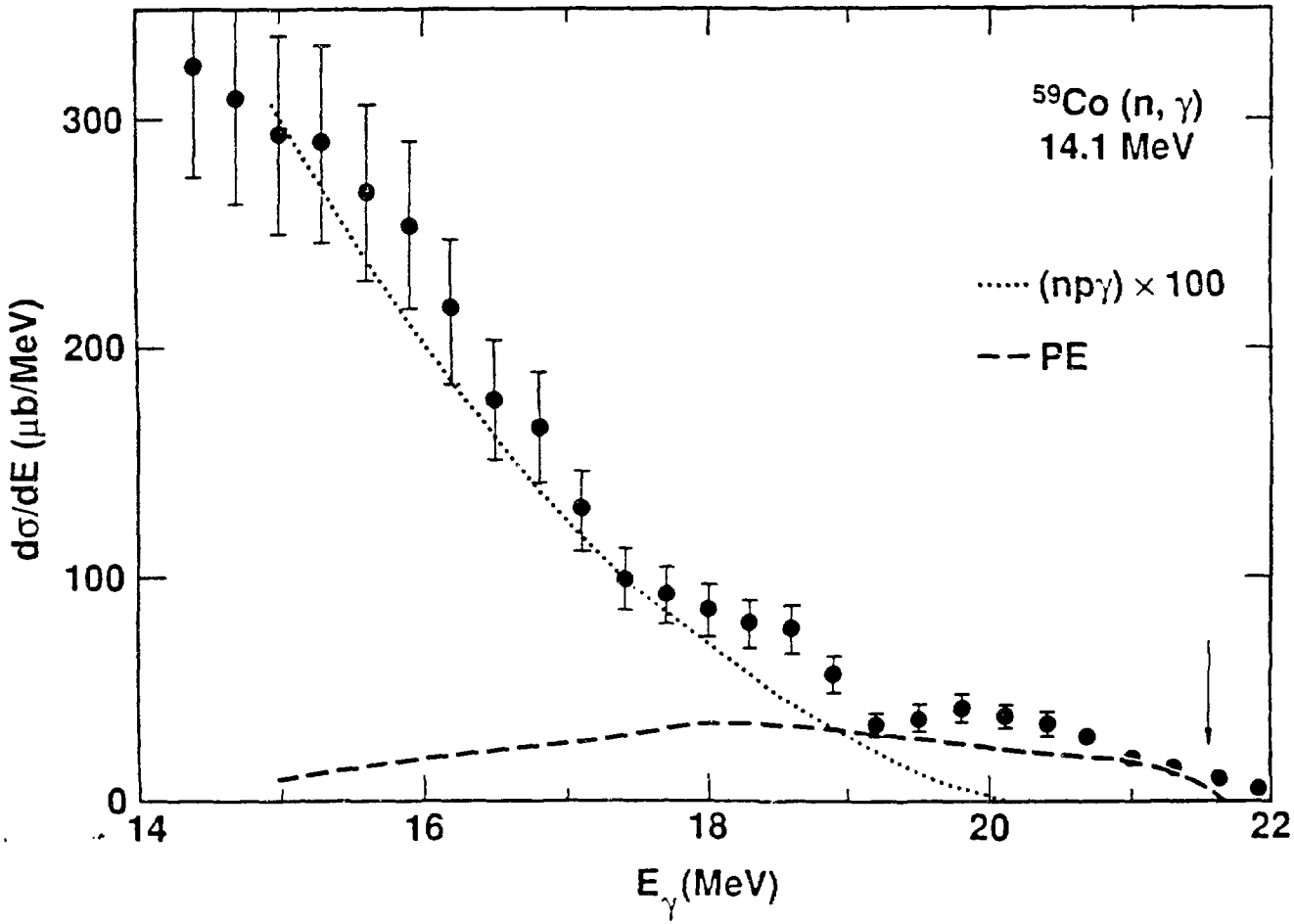
^{59}Co (n, γ)
14.1 MeV
····· (npγ) × 100
– – PE
dσ/dE (μb/MeV)
300
200
100
0
14
16
18
20
22
E_γ(MeV)

Figure 1

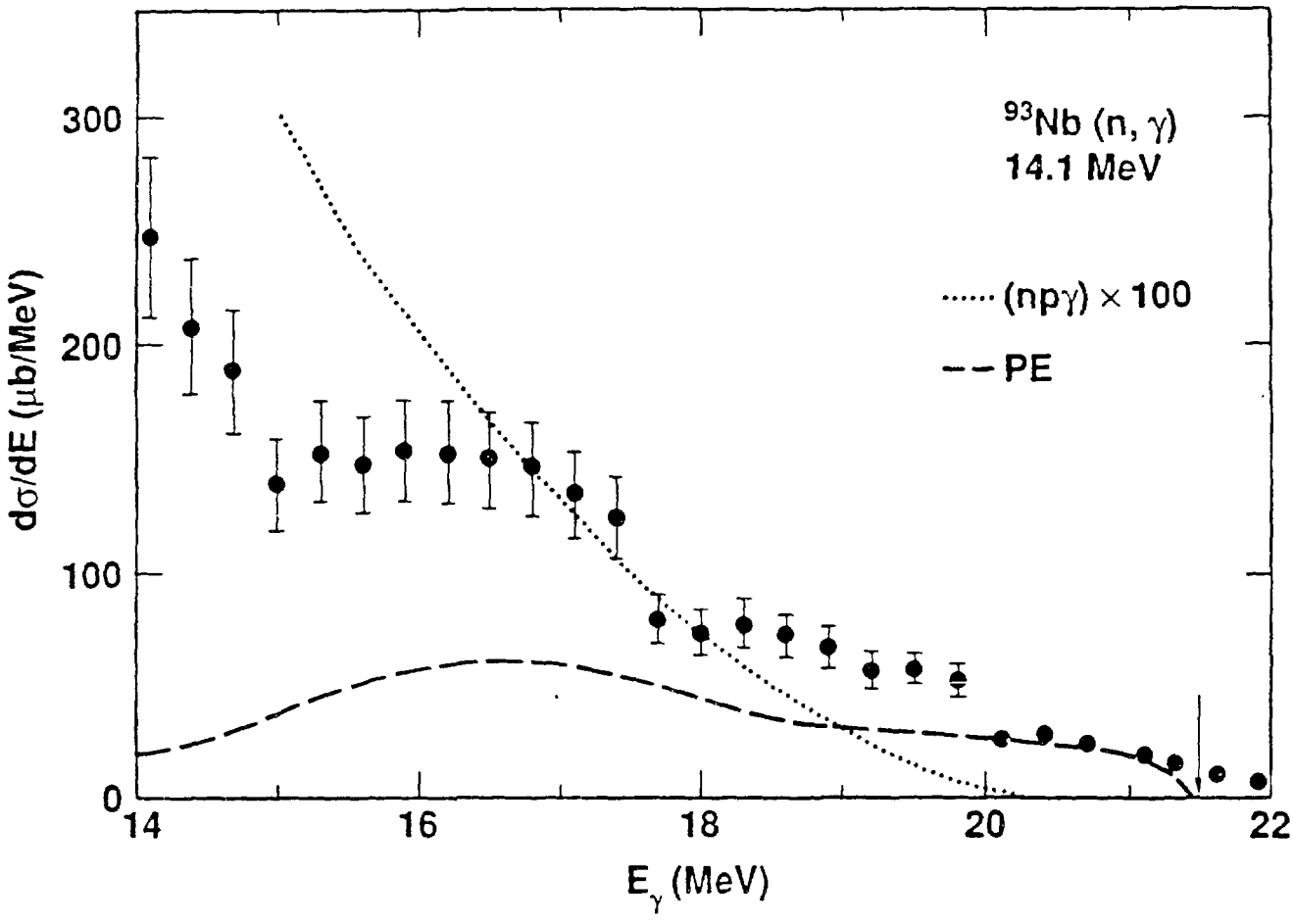
^{93}Nb (n, γ)
14.1 MeV
····· (npγ) × 100
– – PE
dσ/dE (μb/MeV)
300
200
100
0
14
16
18
20
22
E$_γ$ (MeV)

Figure 2

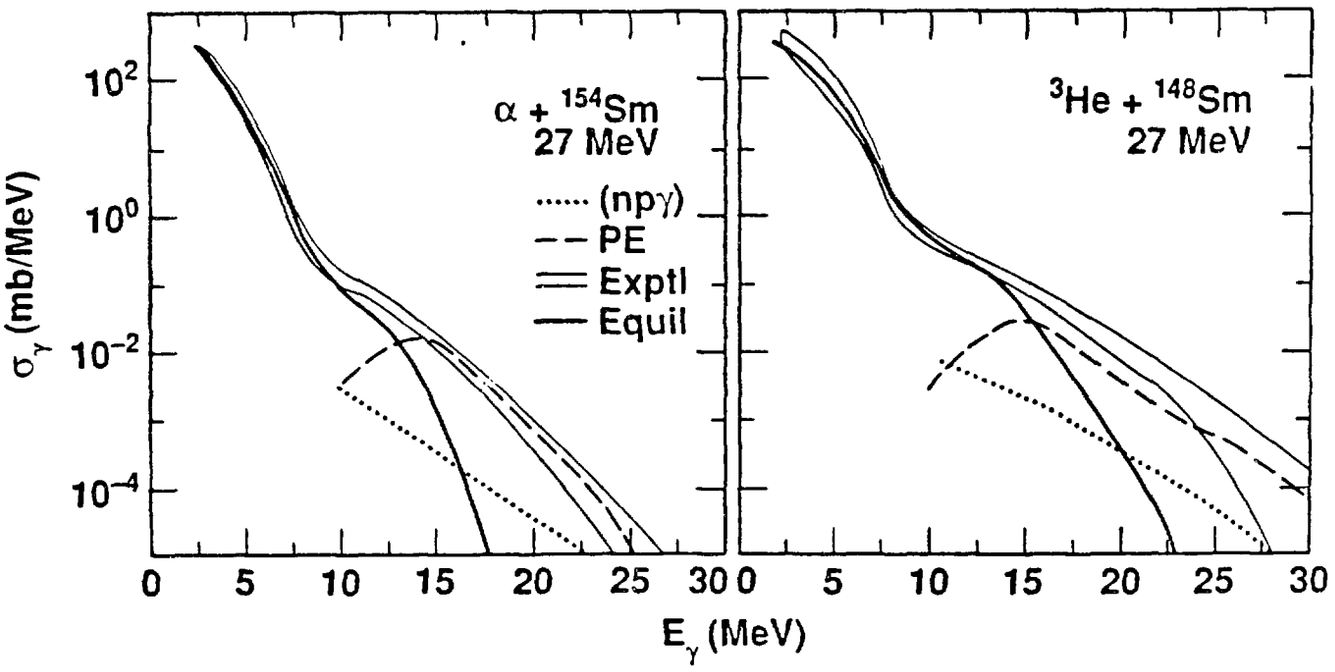

Figure 3

UCRL-95374
PREPRINT

Calculation of γ-ray Cascades in Code ALICE

M. Blann
G. Reffo
F. Fabbri

This paper was prepared for submittal to
Nuclear Instruments and Methods

September 1986

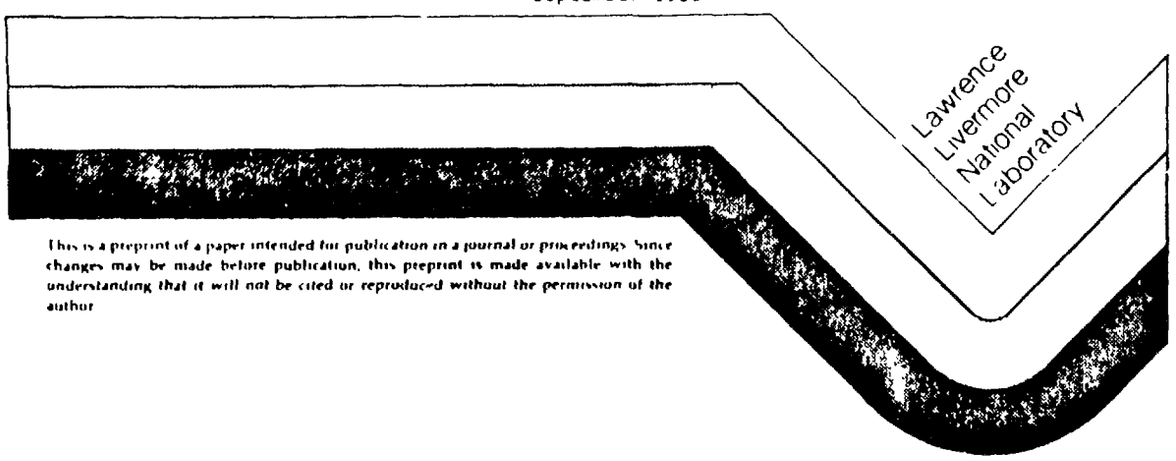

ALICI

^{93}Nb

and

The

ENEA

Calculation of γ-ray Cascades in Code ALICE

M. Blann
Physics Department
Lawrence Livermore National Laboratory
University of California
Livermore, California

G. Reffo and F. Fabbri
ENEA, Bologna, Italy

We describe the methods used to calculate γ-ray cascades in the code ALICE/LIVERMORE 300. Results are compared with experimental spectra for ^{93}Nb (n,xγ), ^{27}Al (n,xγ) and ^{197}Au (n,xγ) at ϵ_n = 9.5, 14 and 18.5 MeV (average bin energies), and for ^{181}Ta (n,xγ) at 14 MeV. The ^{93}Nb and ^{181}Ta γ-ray spectra are also compared with results of the ENEA code PENELOPE.

I. INTRODUCTION

The code ALICE is a nuclear reactions code which was designed for versatility and ease of use in the bombarding energy range of a few MeV to several hundred MeV.[1] The requirement of detailed input parameters was sacrificed to achieve these goals. The minimum input required to run ALICE is the target and projectile charge and mass numbers, projectile energy, and a title card.

Many options exist for types of reactions to be considered, e.g., heavy ion fusion-fission with angular momentum dependent fission barriers, light ion fusion-fission, precompound decay reactions and evaporation reactions. The ALICE code provides yields and spectra for all reactions populated by all combinations of n, p, d and α decay, and can provide all input parameters internally (with the exception of the minimum input parameters listed above). The running time of the code is very short, being typically 0.5 sec on a CDC-7600 computer and 20 sec on a MICRO VAX.

The ALICE code has been successfully used to reproduce data of (HI, xnypzαf) reactions, (n,xnypzαf) reactions, photonuclear reactions for $\epsilon_\gamma \leq 140$ MeV, and stopped pion capture reactions. In this paper, we describe the addition of a routine to calculate γ-ray spectra from de-excitation of the excited nuclei formed during the precompound/compound reaction cascade. Excellent codes exist to accomplish this task with sophisticated physics and with detailed nuclear structure input. Our goal is to see how well we can do within the framework of the ALICE code, requiring no additional input information than required to run earlier code versions.

II. ADOPTED TREATMENT OF γ-RAY CASCADES

A. Equilibrium γ-rays

The primary assumption made in the present treatment is that the preponderance of equilibrium γ-rays come from excited but particle stable nuclei. We therefore assume that where n or p may be emitted (i.e., the excitation energy exceeds the neutron binding energy or the p or α binding plus an increment for an effective coulomb barrier) there is no γ-ray

competition. If this is so, we may sum populations of all residual nuclei as a function only of excitation, since we follow no discrete levels, nor do we keep account of spin and parity population.

This situation is summarized in Fig. 1, where we indicate at the bottom of the figure the summing up of all particle emission stable residual cross-sections as a function of residual excitation. The upper part of the figure pictorially represents the sequence with which the ALICE code considers all de-excitation paths by n, p, and α decay, giving the residual nucleus populations which we sum for the γ-ray cascade calculation. The summed populations $\sigma(u)$ at each excitation energy u are next used to generate the γ-ray cascade.

We replaced the Fermi gas level density of ALICE

$$\rho(u) \propto u^{-5/4}\, e^{2\sqrt{a(u-\delta)}} \qquad \text{(Eq. 1)}$$

by a constant temperature form

$$\rho(u) \propto \frac{1}{T}\, e^{U/T} \qquad \text{Eq. 2)}$$

for residual excitations below the average neutron binding energy of the first two neutrons emitted. The constant temperature density was normalized to the Fermi gas form at the matching excitation U_x. The temperature was defined in the usual way as:

$$T = \sqrt{U_x/a} \qquad \text{(Eq. 3)}$$

where $a = A/9$ and U_x is the average neutron binding energy referred to above. These constant temperature level densities affected both particle emission and γ-ray spectra.

The γ-ray spectra are calculated using a Lorentzian form for the photon absorption cross-section,[2]

$$\sigma_L(\epsilon) = \sum_{R=1}^{2} \sigma_R \frac{\epsilon^2 \Gamma_R^2}{(\epsilon^2 - E_R^2) + \epsilon^2 \Gamma_R^2} \qquad \text{(Eq. 4)}$$

where $\epsilon_0 = 43.4\ A^{-0.215}$, $E1 = E_0(1-\beta/3)^2$, $\sigma_1 = 0.0145\ A/E1$, $\Gamma_1 = 0.232\ E_1$, $E_2 = E_0\ (1-0.16\beta)$, $\sigma_2 = 0.0235\ A/E2$, and $\Gamma_2 = 0.275\ E_2$. While β could be made an input parameter, we have simply set $\beta = 0$ internally.

We assume only E1 radiation, so that the relative γ-ray cross-section from de-excitation of a population at excitation energy U with cross-section σ(U) is given by

$$\sigma_\gamma(\epsilon_\gamma) \propto \epsilon_\gamma^2\ \sigma_L\ (\epsilon)\ \rho(u)\ \sigma(u), \qquad \text{(Eq. 5)}$$

and this expression is normalized to the total emission to give absolute cross-sections.

Results of γ-ray spectra calculated with this formulation were found to be too soft. Prompted by this shortcoming, we made one additional assumption, that the levels accessible for each γ-ray transition were half the total. This may be justified by the argument that generally half the levels are even parity and half are odd parity, and E1 γ-ray transitions can populate only levels of a single parity for a given initial parity. Results of calculations with this modification are shown in Figs. 2-11. The agreement with experimental results is generally satisfactory, and we have adopted this approach for the code.

B. Precompound γ-rays

Some γ-rays of energy 15-22 MeV have been seen in 14 MeV neutron bombardment of several targets.[5,6] We have taken a purely empirical approach to reproduce these results for applications where high energy γ-rays, though in low abundance, may be important (e.g., in shielding calculations).

Our first step was in plotting the log of the experimental cross-sections versus log of residual excitation. This indicated a proportionality of the precompound γ-ray spectra to U and U^3, similar to 3 and 5 exciton state densities. By considering the dimensionality, we parametrized the $\sigma_\gamma(\epsilon)$ as:

$$\sigma_\gamma(\epsilon) = \frac{\sigma_R \epsilon_\gamma^2}{AE^2} [k_1 U + k_2 \frac{U^3}{E^2}] \qquad \text{(Eq. 6)}$$

where a fit to the ^{59}Co (n,xγ) data gave k_1=0.0011 and k_2=0.028. In Eq. 6, σ_R is the projectile + target reaction cross-section, A is the target mass number, U the residual nucleus excitation energy and E the compound nucleus excitation energy. This algorithm is applied only to the compound nucleus. A total calculated ^{93}Nb(n,xγ) spectrum is shown in Fig. 12, including the high energy precompound γ-rays, compared with experimental results.

We should emphasize that the procedure used for these high energy precompound γ-rays is ad-hoc and arbitrary. It is not physics. The method may be useful for reactions induced by neutrons of around 14 MeV. Extrapolation to other regimes is unwarranted and dangerous, until such time as the algorithm may be tested versus experimental results for various projectile energies and target mass numbers.

III. CONCLUSIONS

The Lorentzian line shape has been used for El radiation for equilibrium γ-ray emission in the code ALICE. No spins or parities are followed or retained in the calculation, and no additional input parameters are required with respect to the earlier code version. The results are in quite reasonable agreement with experimental spectra for the wide range of target masses considered.

IV. ACKNOWLEDGEMENTS

One of the authors (MB) wishes to acknowledge the kind hospitality of Dr. Enzo Menapace and ENEA, Bologna where this work was done. The help and support of R. W. Howerton is also very much appreciated.

This work was performed under the auspices of the U.S. Department of Energy by the Lawrence Livermore National Laboratory under contract number W-7405-ENG-48.

1035A-9/8/86

References

1. M. Blann and H. K. Vonach, Phys. Rev. C 28, 1648 (1983); M. Blann, Lawrence Livermore National Laboratory, Report UCID 20169 (1984) unpublished.

2. K. Wisshak, J. Wickenhauser, F. Käppeler, G. Reffo and F. Fabbri, Nucl. Sci. and Eng. 81, 396 (1982).

3. D. M. Drake, E. D. Arthur and M. G. Silbert, Nucl. Sci. and Eng. 65, 49 (1978).

4. J. K. Dickens, T. A. Love and G. L. Morgan, Oak Ridge National Laboratory Report ORNL-TM-4232 (1973) unpublished; G. L. Morgan and E. Newman, ibid. ORNL-TM-4973 (1975) unpublished; G. L. Morgan and F. G. Perey, ibid. ORNL-TM-5241 (1976) unpublished; J. K. Dickens, G. L. Morgan and E. Newman, ibid. ORNL-TM-4972 (1975) unpublished.

5. F. Rigaud, G. Longo and F. Saporetti, Nucl. Phys. A 173, 551 (1971).

6. V. A. Plyuyko and G. A. Prokopets, Phys. Lett. 76B, 253 (1978).

Figure Captions

Figure 1 Diagrammatic representation of the ALICE de-excitation calculation, beginning with a composite nucleus of mass number A and charge Z. Precompound n and p are emitted, followed by equilibrium n,p,d and α. The daughter products in turn decay by evaporation of n,p,d and α. Each nuclide has a population σ_U versus excitation energy U. Following the conclusion of all n,p,d,α emission processes, all particle stable populations are added to give a single population distribution $\sigma(u)$, as shown at the bottom of Fig. 1. This summed buffer is used to calculate the γ-ray cascade.

Figure 2 Experimental ^{27}Al (n,xγ) data with 14.2 MeV neutrons compared with results of the ALICE calculation with $T=\sqrt{E/a}$ below B_n. Data are from Ref. 4.

Figure 3 As in Fig. 2 for ^{93}Nb (n,xγ) with neutrons of average energy 9.5 MeV. Data are from Ref. 4. The dashed histogram represents γ-ray spectra calculated with the ENEA code PENELOPE.

Figure 4 As in Fig. 3 with 14.2 MeV average neutron energy. Data are from Refs. 3 and 4.

Figure 5 As in Fig. 3 for neutrons of average energy 18.5 MeV.

Figure 6 As in Fig. 3 for the ^{181}Ta (n,xγ) reaction with 14.2 MeV incident neutron energy. Data are from Refs. 3 and 4.

Figure 7 As in Fig. 2.

Figure 8 As in Fig. 2.

Figure 9 As in Fig. 2.

Figure 10 As in Fig. 2.

Figure 11 As in Fig. 2.

Figure 12 Comparison of experimental ^{93}Nb (n,xγ) data for 14.2 MeV neutrons and ALICE calculation including the precompound algorithm. Data are from Refs. 3-6.

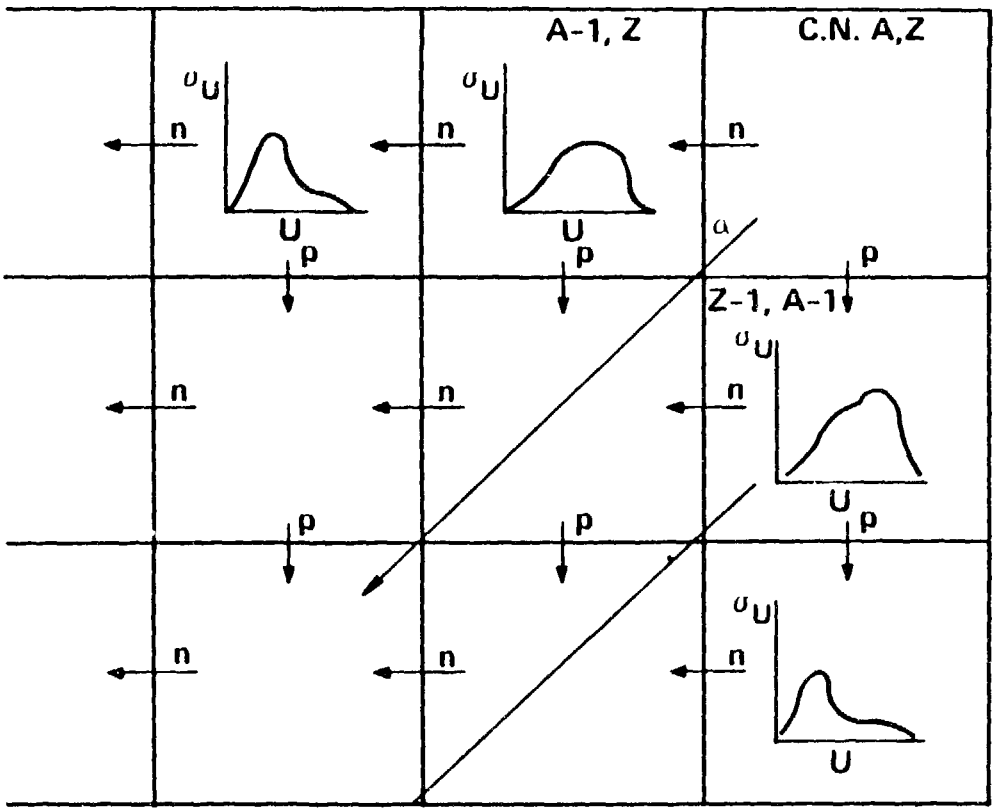

$$\sigma(U) = \sum_{A,Z} \sigma_U(A', Z')$$

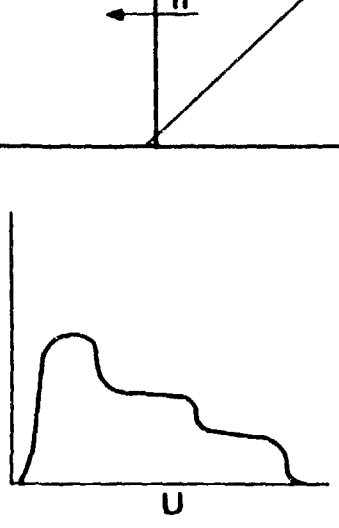

Figure 1

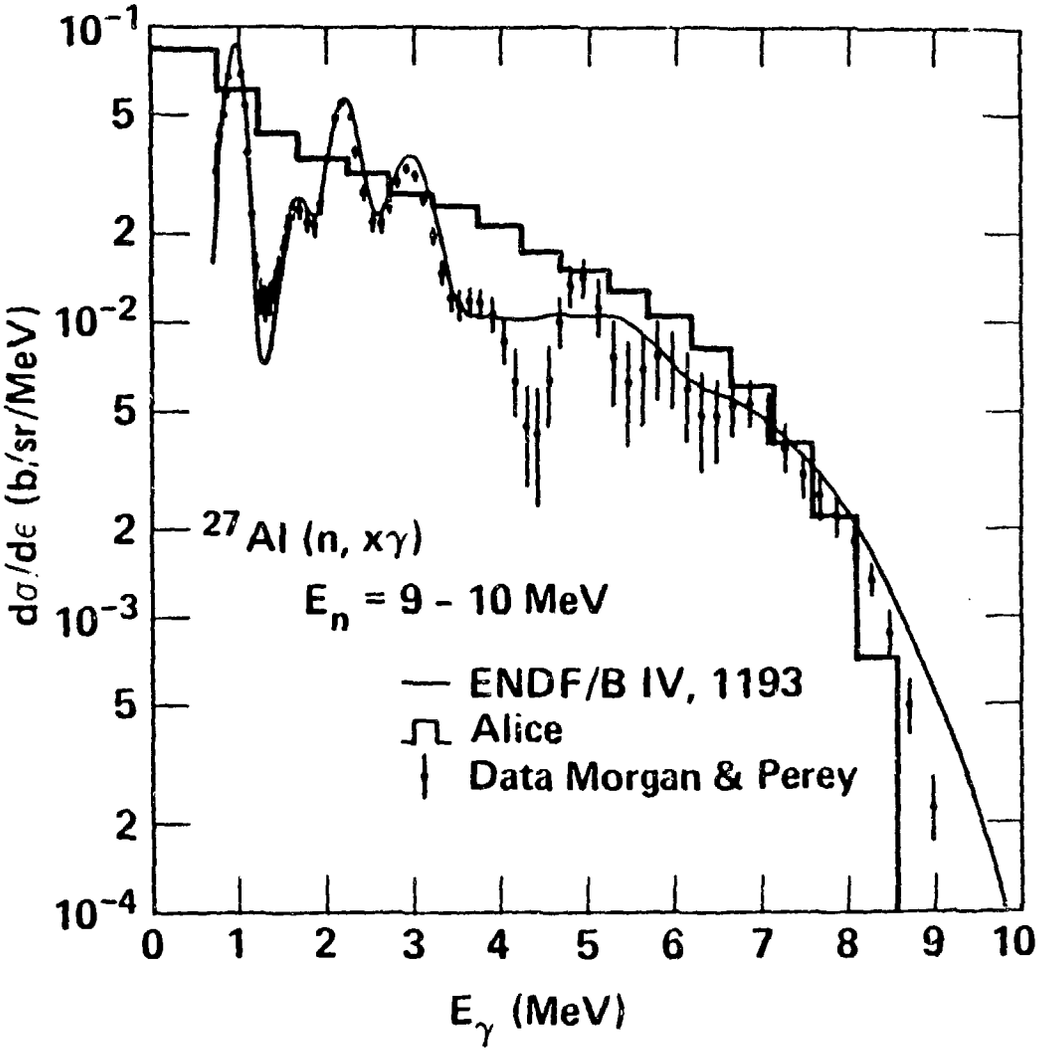
10^{-1}
5
2
10^{-2}
5
2
10^{-3}
5
2
10^{-4}
$d\sigma/d\epsilon$ (b/sr/MeV)
^{27}Al (n, xγ)
E_n = 9 - 10 MeV
ENDF/B IV, 1193
Alice
Data Morgan & Perey
0 1 2 3 4 5 6 7 8 9 10
E_γ (MeV)

Figure 2

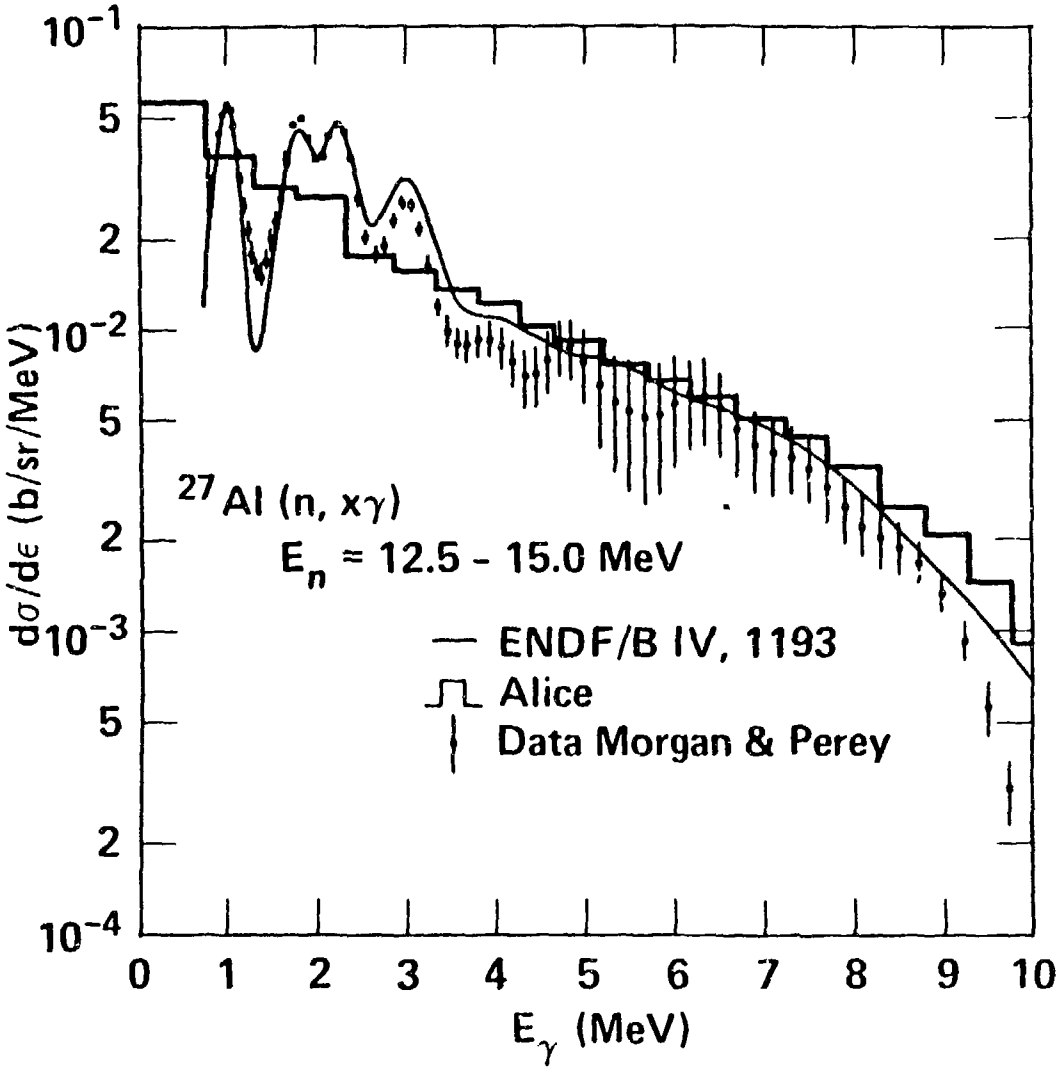
10^{-1}
5
2
10^{-2}
5
2
10^{-3}
5
2
10^{-4}
dσ/dε (b/sr/MeV)
^{27}Al (n, xγ)
E_n ≈ 12.5 - 15.0 MeV
— ENDF/B IV, 1193
Alice
Data Morgan & Perey
0 1 2 3 4 5 6 7 8 9 10
E_γ (MeV)

Figure 3

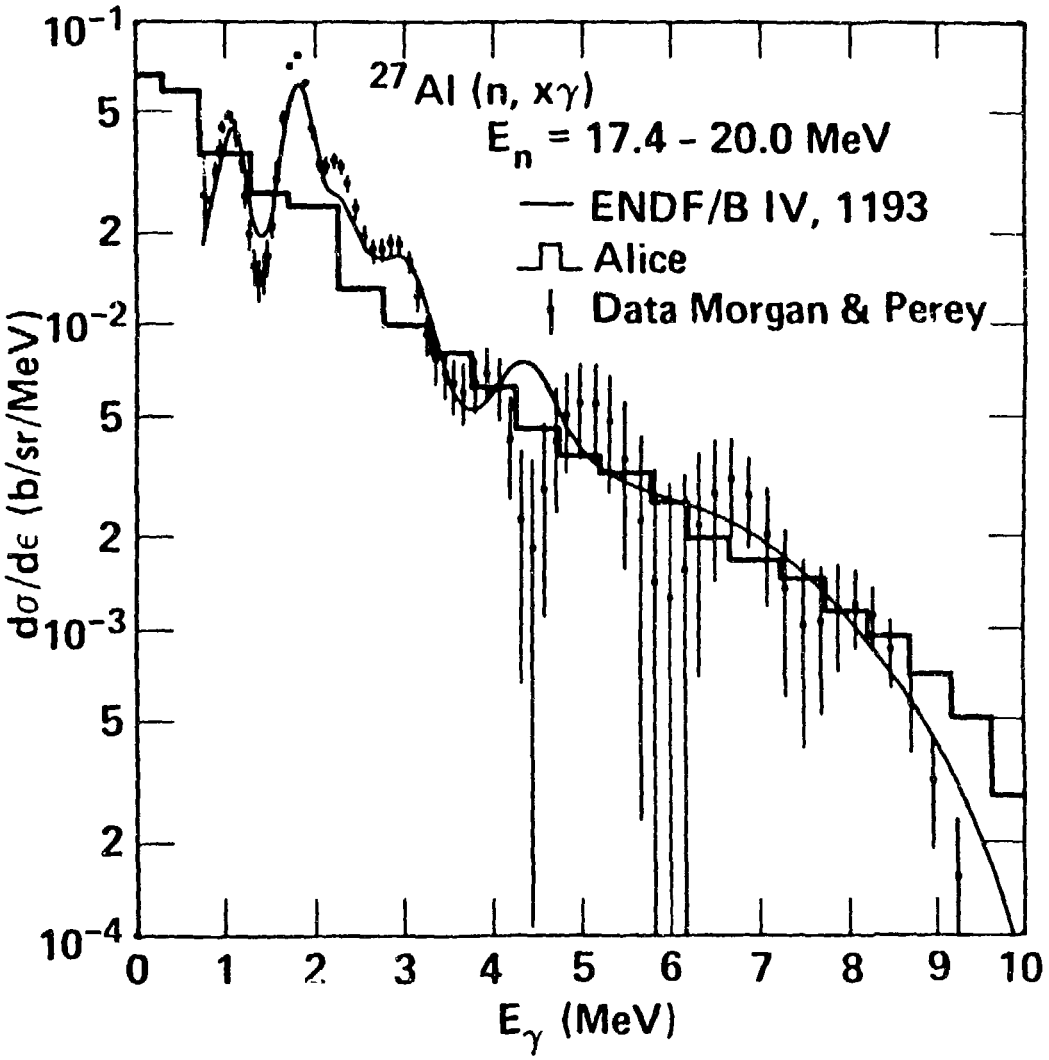
^{27}Al (n, xγ)
E_n = 17.4 - 20.0 MeV
ENDF/B IV, 1193
Alice
Data Morgan & Perey
dσ/dε (b/sr/MeV)
E_γ (MeV)
10^{-1}
5
2
10^{-2}
5
2
10^{-3}
5
2
10^{-4}
0 1 2 3 4 5 6 7 8 9 10

Figure 4

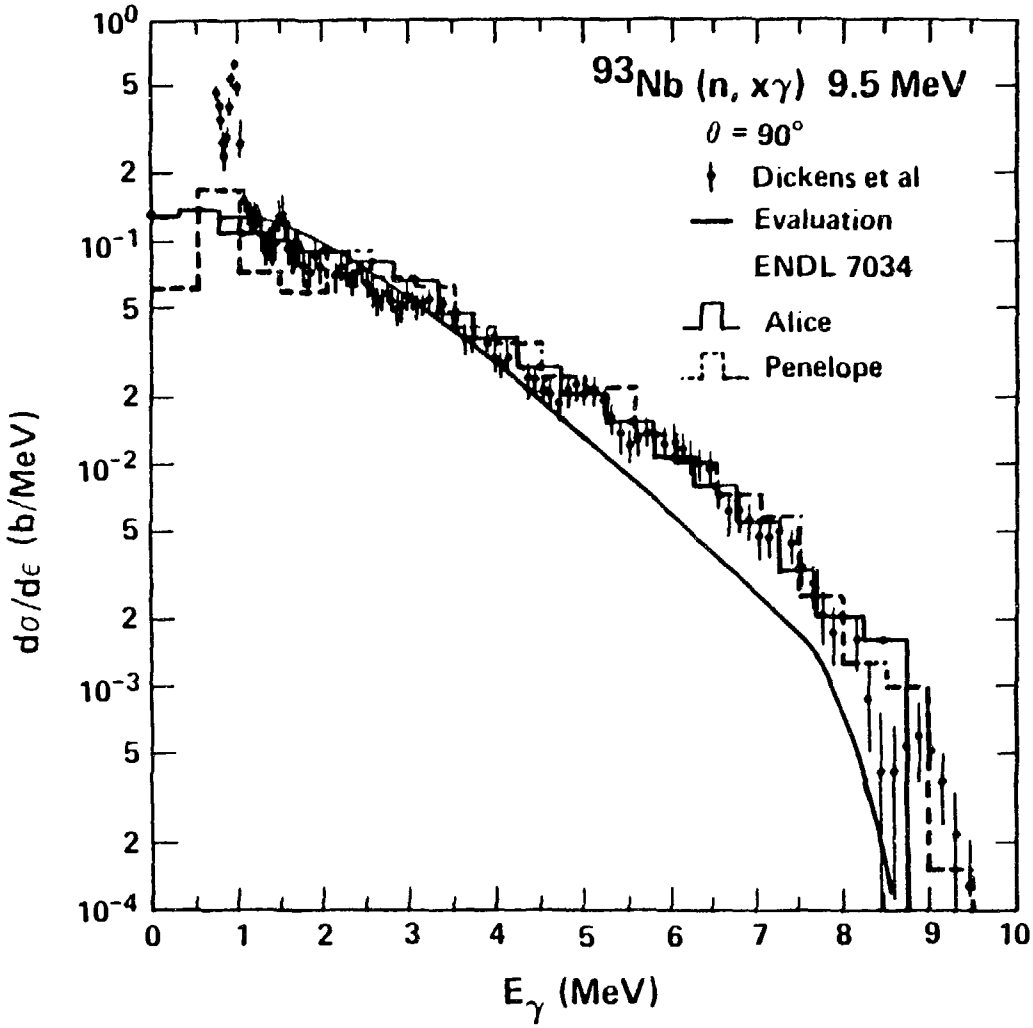
^{93}Nb (n, xγ) 9.5 MeV
θ = 90°
Dickens et al
Evaluation
ENDL 7034
Alice
Penelope
dσ/dε (b/MeV)
E$_\gamma$ (MeV)
10^0
5
2
10^{-1}
5
2
10^{-2}
5
2
10^{-3}
5
2
10^{-4}
0 1 2 3 4 5 6 7 8 9 10

Figure 5

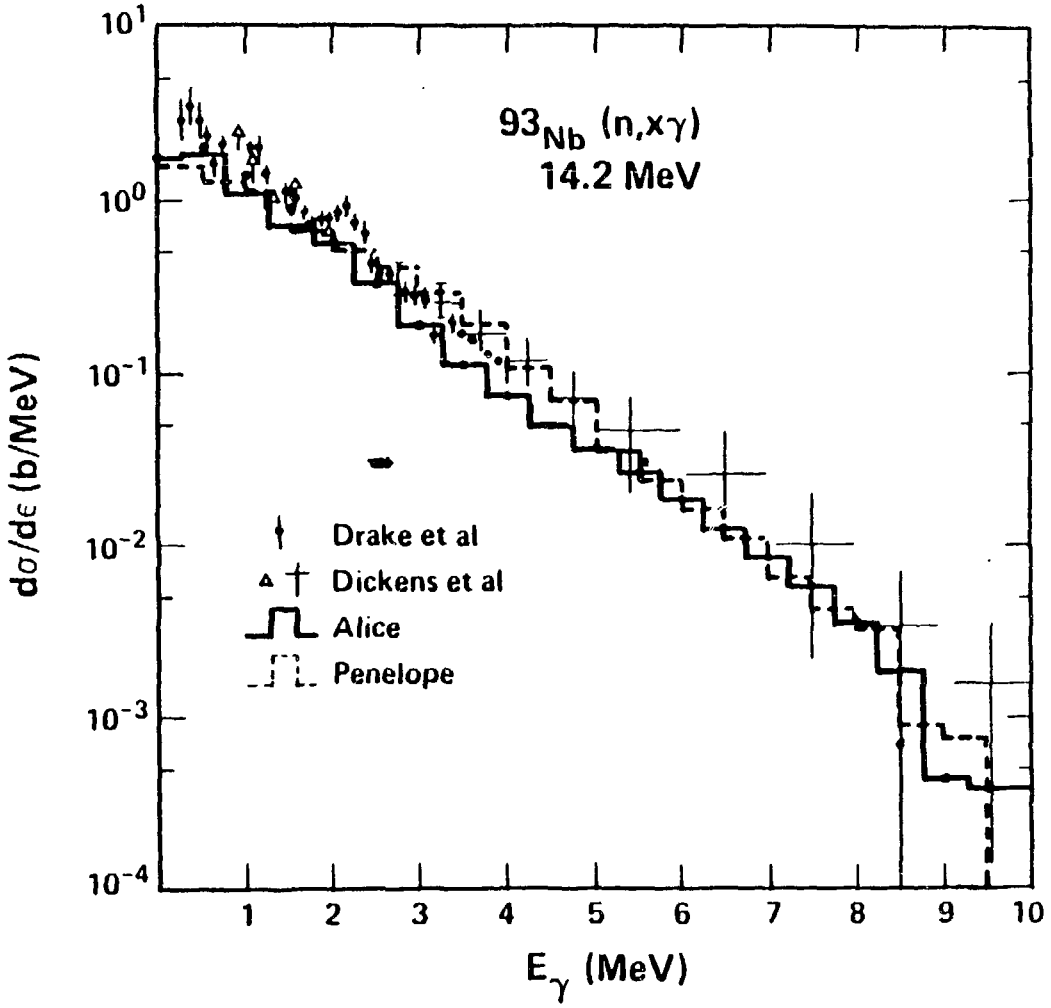
93_{Nb} (n,xγ)
14.2 MeV
Drake et al
Dickens et al
Alice
Penelope
dσ/dε (b/MeV)
E_γ (MeV)
10^1
10^0
10^{-1}
10^{-2}
10^{-3}
10^{-4}
1
2
3
4
5
6
7
8
9
10

Figure 6

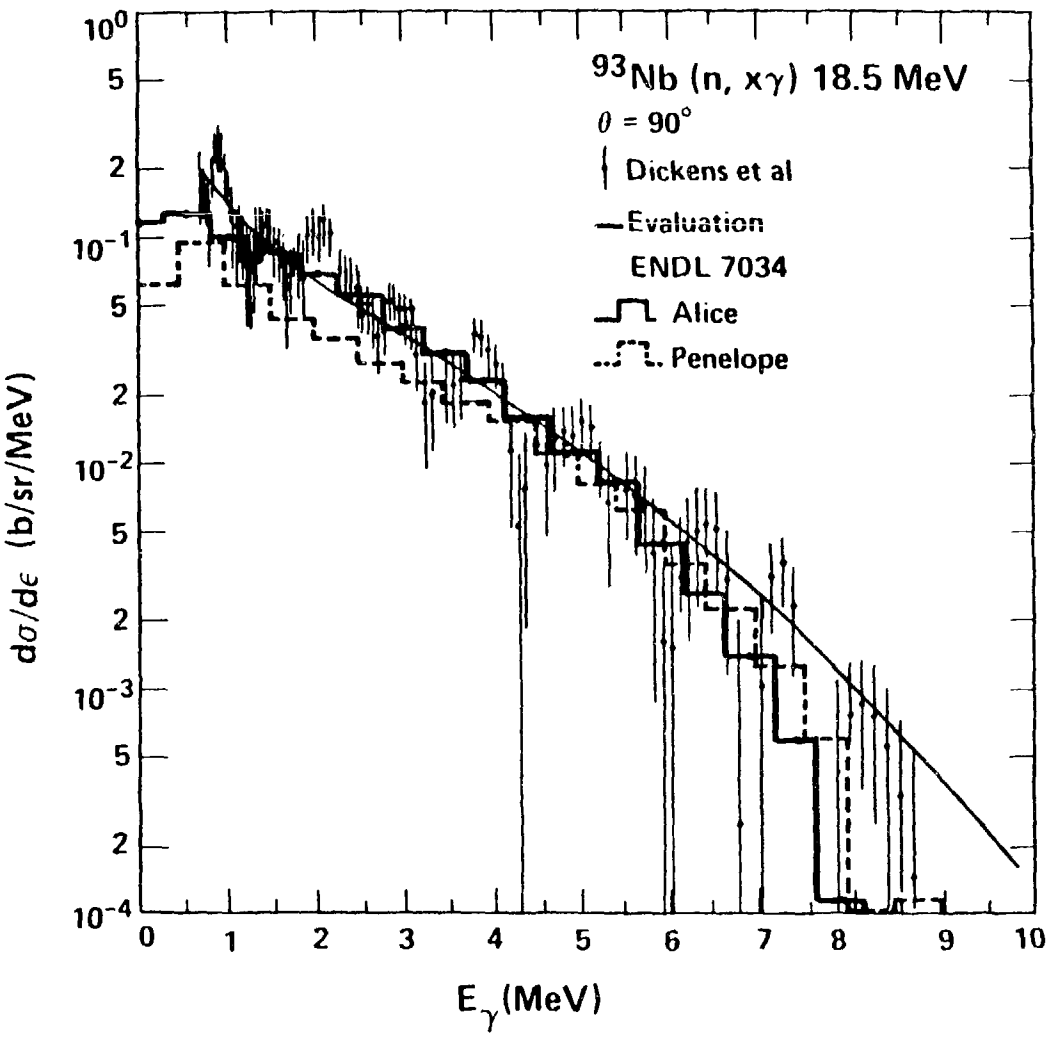
^{93}Nb (n, xγ) 18.5 MeV
θ = 90°
Dickens et al
Evaluation
ENDL 7034
Alice
Penelope
dσ/dε (b/sr/MeV)
dσ/dε (b/MeV)
E$_\gamma$(MeV)
10^0
5
2
10^{-1}
5
2
10^{-2}
5
2
10^{-3}
5
2
10^{-4}
0
1
2
3
4
5
6
7
8
9
10

Figure 7

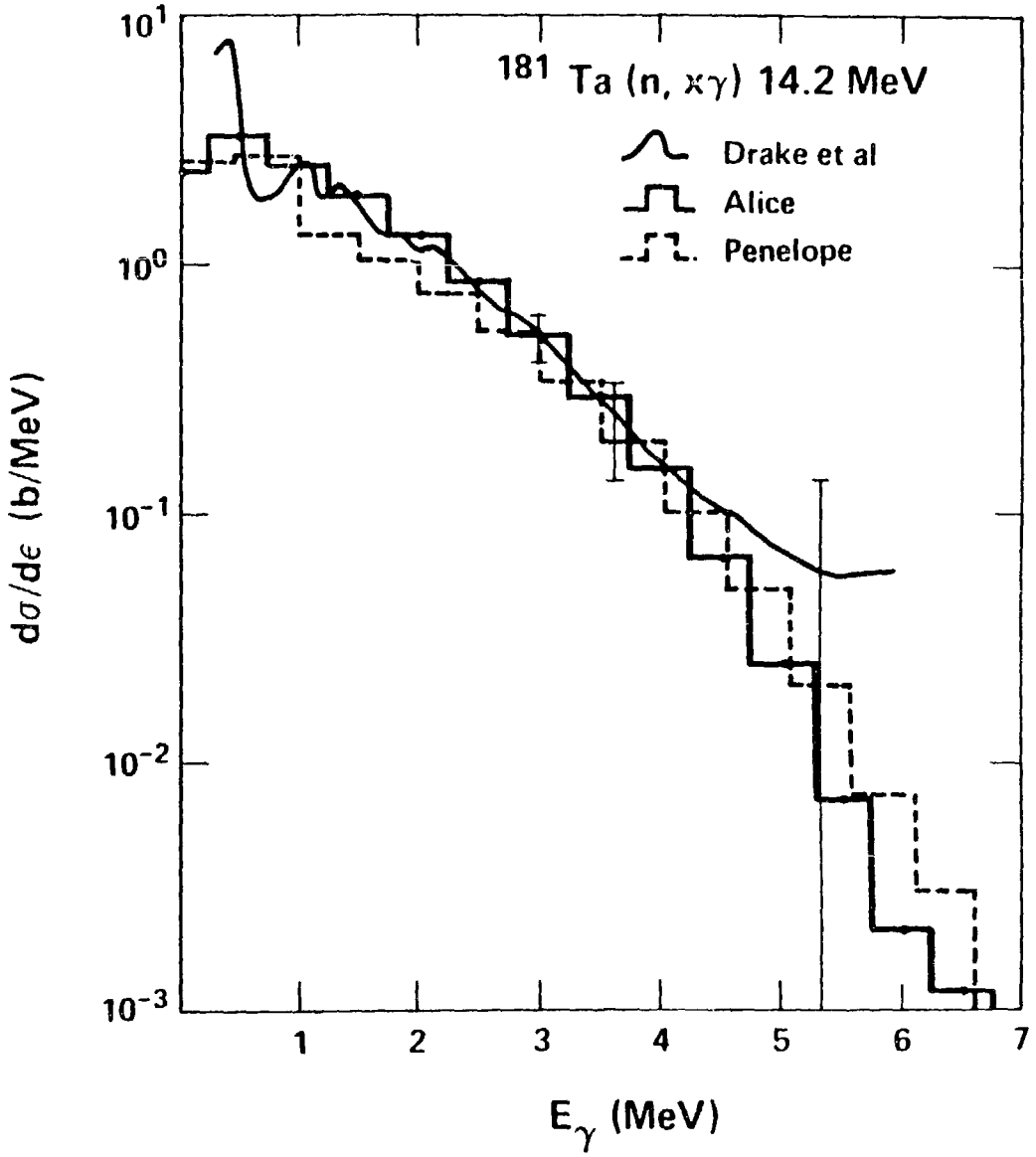
181 Ta (n, xγ) 14.2 MeV
Drake et al
Alice
Penelope
dσ/dε (b/MeV)
Eγ (MeV)
10^1
10^0
10^-1
10^-2
10^-3
1
2
3
4
5
6
7

Figure 8

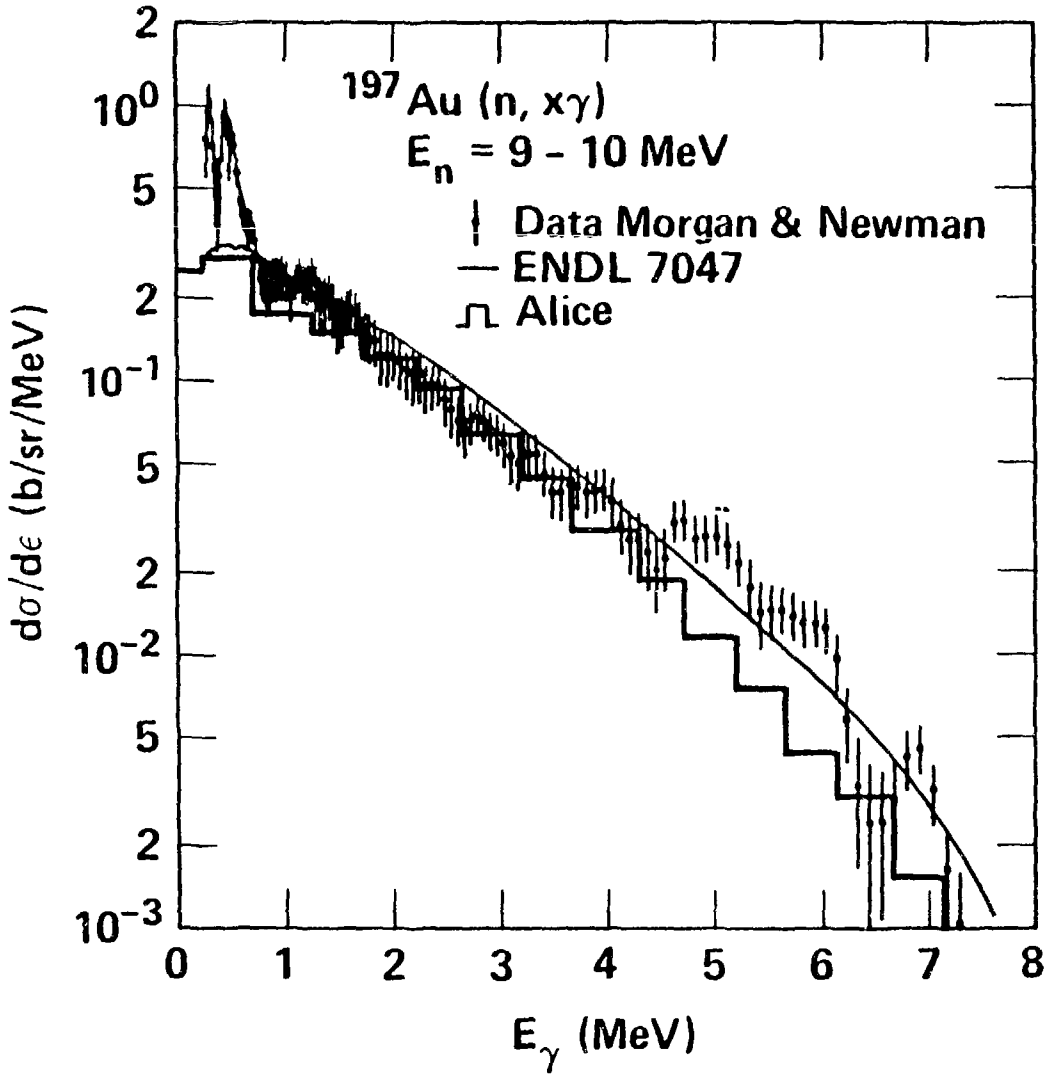
^{197}Au (n, xγ)
E_n = 9 - 10 MeV
Data Morgan & Newman
ENDL 7047
Alice
dσ/dε (b/sr/MeV)
E_γ (MeV)
2
10^0
5
2
10^{-1}
5
2
10^{-2}
5
2
10^{-3}
0 1 2 3 4 5 6 7 8

Figure 9

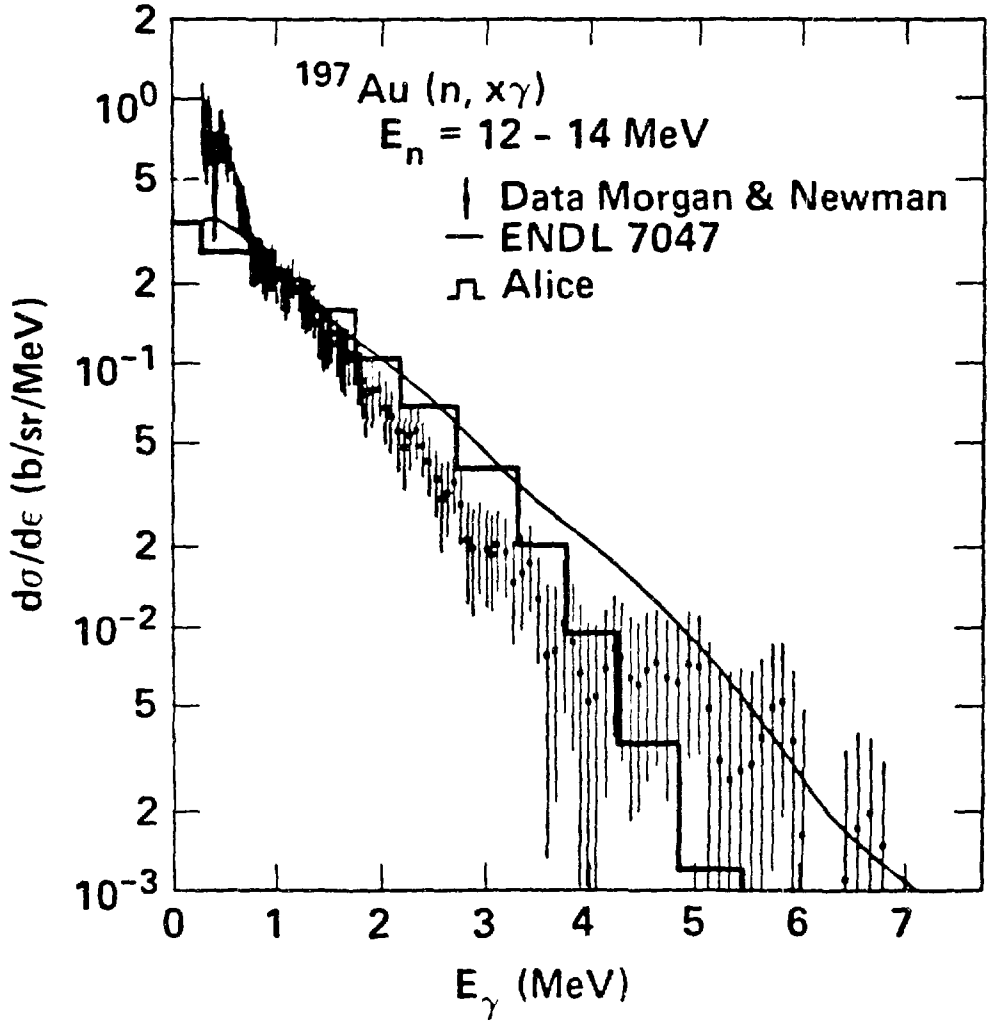

Figure 10

dσ/dϵ (b/sr/MeV)

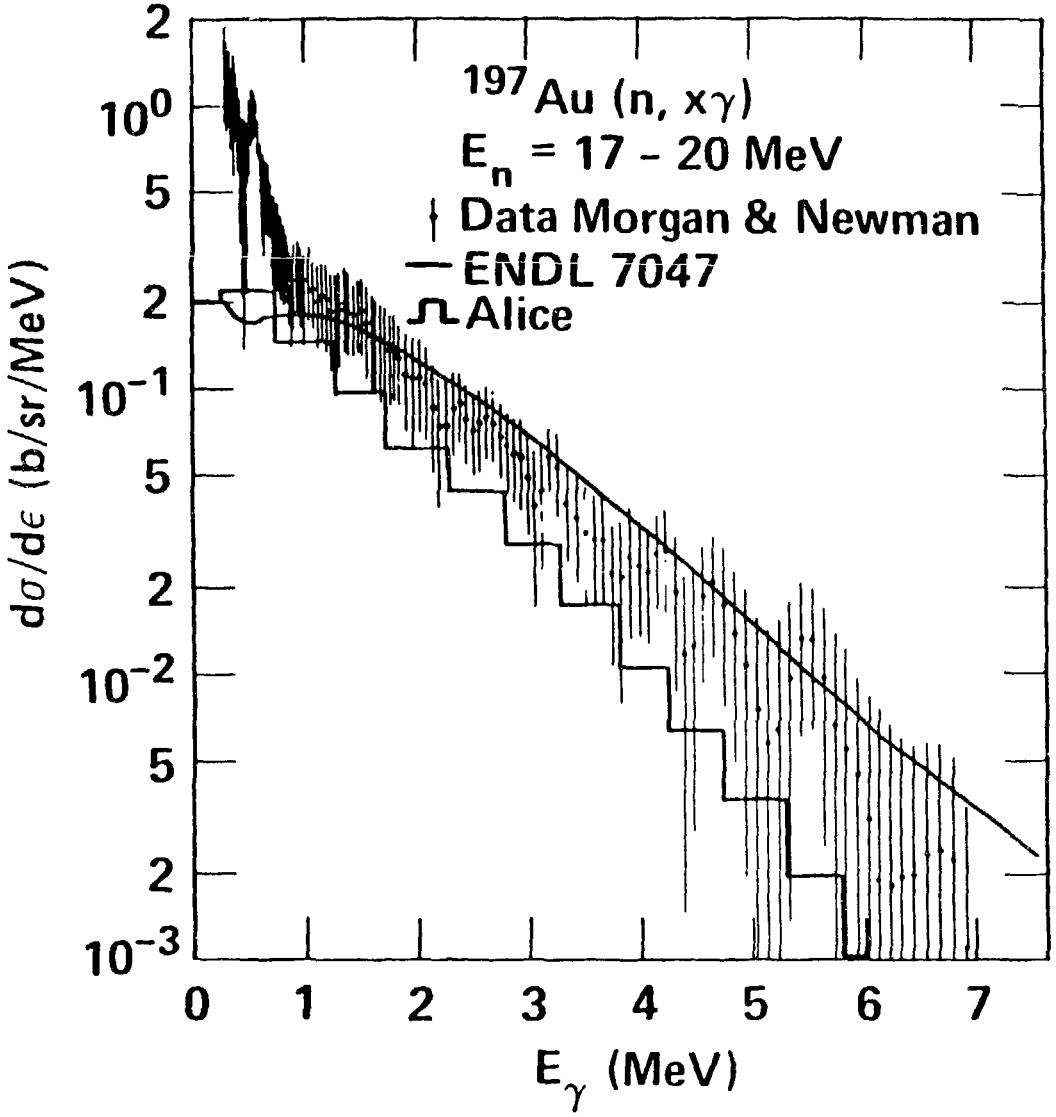
^{197}Au (n, xγ)
E_n = 17 - 20 MeV
Data Morgan & Newman
ENDL 7047
Alice
dσ/dε (b/sr/MeV)
E_γ (MeV)
2
10^0
5
2
10^{-1}
5
2
10^{-2}
5
2
10^{-3}
0 1 2 3 4 5 6 7

Figure 11

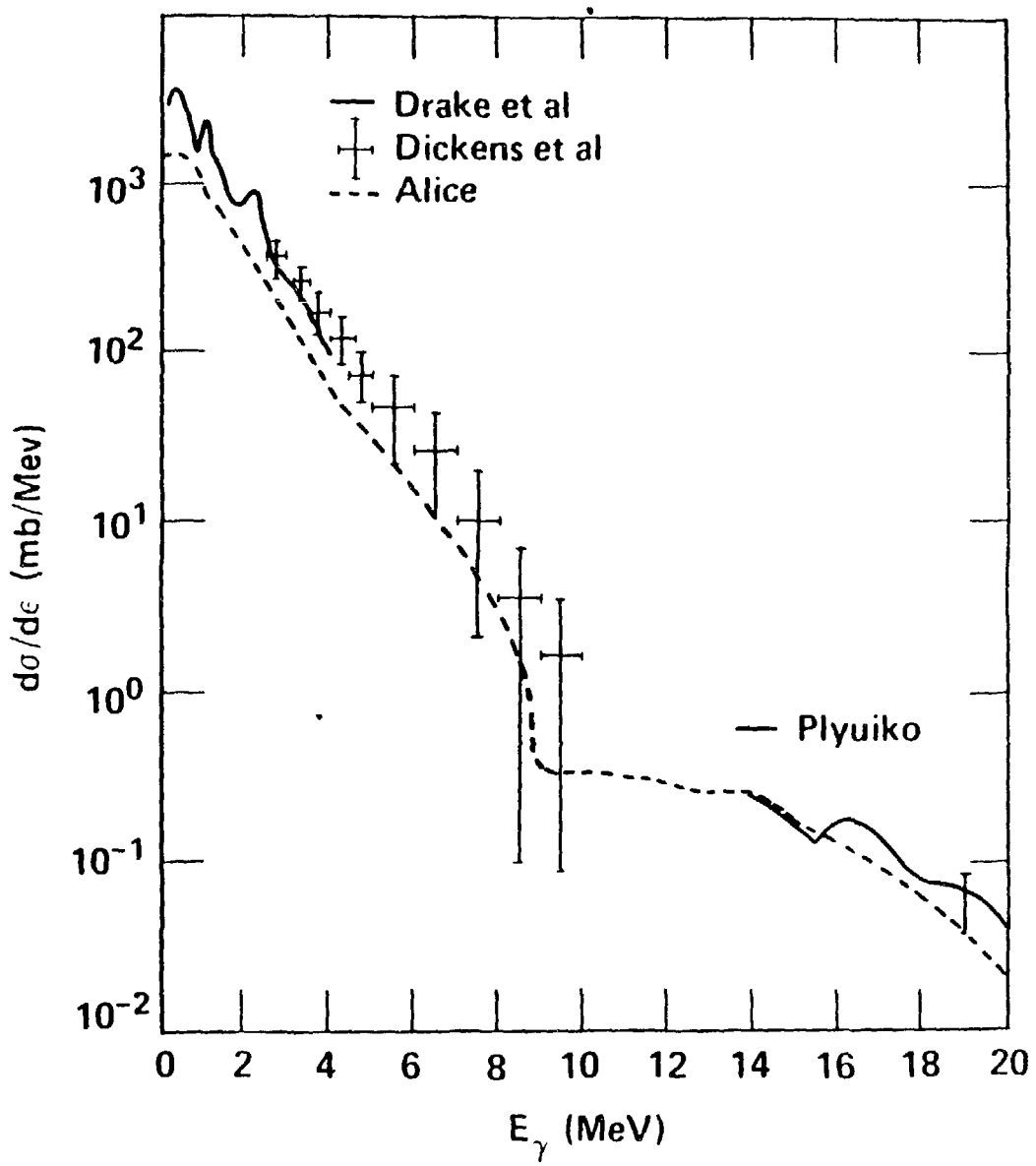
Drake et al
Dickens et al
Alice
Plyuiko
10^3
10^2
10^1
10^0
10^{-1}
10^{-2}
dσ/dε (mb/Mev)
0 2 4 6 8 10 12 14 16 18 20
E_γ (MeV)

Figure 12

Attachments

J. Bisplinghoff "Configuration mixing in preequilibrium reactions: A new look at the hybrid-exciton controversy". Phys. Rev. C 33(5) p. 1569-1580 (May 1986). (Not microfiched)

M. Blann, J. Bisplinghoff "Numerical test of approximations in the hybrid precomound decay model". Z.Phys. A - At Nuclei 326 p. 429-434 (1987). (Not microfiched)

M. Blann, T.T. Komoto "Precompound evaporation analyses of excitation functions for (alpha,xn) reactions". Phys. Rev. C 29(5) p. 1678-1683 (May 1984). (Not microfiched)

M. Blann, W. Scobel, E. Plechaty "Precompound nucleon angular distributions in the continuum". Phys. Rev. C 30(5) p. 1493-1508 (Nov 1984). (Not microfiched)